GLIA RESPONSIVITY IN NICOTINE DEPENDENCE

by

Adewale Oluwamuyiwa Adeluyi

Bachelor of Pharmacy
University of Ibadan, 2008

Master of Public Health
University of South Carolina, 2014

Submitted in Partial Fulfilment of the Requirements

For the Degree of Doctor of Philosophy in

Pharmaceutical Sciences

College of Pharmacy

University of South Carolina

2019

Accepted by:

Jill Turner, Major Professor

Michael Wyatt, Chair, Examining Committee

Lorne Hofseth, Committee Member

Jeff Twiss, Committee Member

Pavel Ortinski, Committee Member

James Chou, Committee Member

Cheryl L. Addy, Vice Provost and Dean of the Graduate School

DEDICATION

I dedicate this work to Almighty God that has brought me this far. To the memory of my late parents, Emmanuel Adeluyi and Grace Adeluyi, who besides their numerous sacrifices, taught me to never give up, keep my eye on the prize, and work hard. Together, they left me a legacy that is the bedrock of my success.

To my siblings – Adekemi Adeluyi, Aderonke Adeluyi, Adeola Adeluyi (late), Adenike Adeluyi, and Adedotun Adeluyi, who are always there for me. We are knit together, and I cannot ask for a better five.

To my wife, Mayomi, for being part of this journey. Finally, to my adorable son, Tobiah Adeluyi, for bringing one of the best moments in my life and supporting me by seeking attention.

ACKNOWLEDGEMENTS

First, I would like to thank my advisor, Dr. Jill Turner for her guidance, training, and immense support during the course of my graduate work. Her mentorship is so invaluable, I cannot ask for anything better. Her readiness to allow me to explore and apply data science to my research represents a defining moment in my graduate program. She also gave me an amazing opportunity to be part of a fabulous lab and I am extremely happy and grateful to have learnt a lot from one of the best.

I would also like to thank my committee members, Dr. Michael Wyatt (Chair), Dr. Lorne Hofseth, Dr. Jeff Twiss, Dr. Pavel Ortinski, and Dr. James Chou, for their extremely helpful insight and suggestions, in addition to their encouragement throughout the course of this project. Together, you have all shaped me into a better scientist.

I would also like to acknowledge my amazing lab colleagues, Dr. Miranda Fisher and Erin Anderson for their help with science-related issues and encouragement during the course of this work. I would not forget to mention the past members of our lab, Dr. Luyi Zhou and Lindsey Guerin, for their help in lab-related matters.

Further, I would like to thank people who have collaborated with me on different projects or assisted me at some points during the course of my program. Particularly, Dr. Shannon Davis, Dr. Linnea Freeman, Dr. Sherine Chan, Ashley

Galloway, Dr. Bernadette O' Donovan, Dr. Rob Cole. I would also like to appreciate Dr. Seung Joon Lee and Dr. Changlong Liu, who both helped me at different points in my project.

Finally, I would like to thank my friends who have more or less become a family, Babatunde Oyelowo, Eniola Olatunji, Ada Obi and Nefe Omofuma. Thank you all for your unflinching support all through the years.

ABSTRACT

Neurons are the primary research target in the exploration and development of novel smoking cessation pharmacotherapies over the years. These research efforts have led to the discovery and development of three FDA-approved smoking cessation aids – nicotine replacement therapy, varenicline, and bupropion, each of which have quantifiable success as smoking cessation aids. However, relapse is still very common and smoking cessation is successful in less than 5% of quit attempts, making paramount the development of novel therapeutics. One untapped therapeutic target are glia, particularly, astrocytes and microglia, which are active participants in the neuroplastic events underlying drug addiction.

First, we examined microglial changes in the striatum – a mesolimbic brain region implicated in both the rewarding effects of drugs and the affective disruptions occurring during drug withdrawal. We show that chronic nicotine and withdrawal induce microglial activation accompanied with distinct expression of pro-inflammatory cytokines in the nucleus accumbens. Nicotine withdrawal-related pro-inflammatory effects accompany activation of microglia-related NADPH Oxidase 2 (Nox2) and induction of reactive oxygen species (ROS). Both cellular correlates of inflammation and increased anxiety-like behaviors occurring during nicotine withdrawal are absent following microglial depletion with colony stimulating factor 1 receptor inhibitor, PLX5622.

Based on these findings, we extended our study to capture tissue-level transcriptome-wide responses in the nucleus accumbens during chronic nicotine and withdrawal (24 h and 48 h). We show temporally-dependent activation of distinct gene programs in the nucleus accumbens during nicotine withdrawal. Differential gene expression analysis suggests that chronic nicotine treatment activates subset of genes that are neuroprotective while withdrawal from nicotine provokes neuroinflammation and oxidative stress-related transcriptional programs in the nucleus accumbens

To have a finer resolution that aid better characterization of transcriptomic changes, we performed cell type-specific RNA sequencing and evaluated astrocyte- and microglia-specific transcriptome changes during nicotine treatment and 48 h withdrawal. We show that gene programs associated with neuroinflammation were suppressed in microglia following chronic nicotine treatment while nicotine withdrawal triggers microglial pro-inflammatory networks. Further, whole transcriptome data suggest astrocytes assume a reactive phenotype during nicotine withdrawal.

Taken together, this work provides the first evidence of microglia involvement in nicotine dependence. In addition, our transcriptomic studies offer a less complex insight into the role of nucleus accumbal glia in nicotine dependency, pioneering future exploration of glia modulators as potential therapeutic targets for the development of smoking cessation therapeutics.

TABLE OF CONTENTS

LIST OF FIGURES

CHAPTER 1

GENERAL INTRODUCTION

---

[1] Adewale Adeluyi, Jill R. Turner. To be submitted to Nicotine and Tobacco Research.

1.1 GENERAL OVERVIEW OF NICOTINE DEPENDENCE

Tobacco smoking is the principal cause of preventable disease and premature death in the world. Globally, over 5 million premature deaths are attributable to tobacco smoking every single year, and nearly one-tenth – about 480,000, of these deaths occur in the United States (Changeux 2010, Reitsma et al 2017). Despite decreased smoking prevalence in the United States over the last decade, the disease burden attributable to tobacco smoking continues to rise. This is due in part to population growth, but also the high failure rate in quit attempts made by current smokers (Ng et al 2014).

Currently, over 42 million Americans still smoke, and nearly 80% of these smokers have made serious attempts to quit without success (Benowitz 2010). While quitting smoking significantly reduces the risk of smoking-related disease and death, successful smoking cessation remains a major challenge in the United States with only 3% success rate in quit attempts each year (Benowitz 2010, Changeux 2010). Today, it has become clearer that effects of nicotine and its withdrawal (during smoking cessation) on neural circuits relevant in nicotine dependence are more complex than initially thought. Therefore, in this chapter, I will discuss the molecular effects of nicotine, highlighting some of these effects in a well-defined neurocircuitry of addiction. Further, I will review the symptomology of nicotine withdrawal and the potential role of non-neuronal cell types in nicotine dependence.

1.2 NEUROBIOLOGY OF NICOTINE DEPENDENCE

Nicotine and Neuronal Nicotinic Acetylcholine Receptors (nAChRs) – Acute Effects

Nicotine is the major psychoactive component in tobacco that drives the neurobiological effects underlying the sustainment and reinforcement of tobacco smoking (Balfour 2008, Benowitz 2010, Grunberg 2007). Smoke particles containing nicotine are inhaled into the lungs, where about 90% of nicotine present in the inhaled smoke is immediately absorbed into the pulmonary venous circulation (Jiloha 2014). Following absorption, it takes seven seconds for nicotine to reach the brain (Jiloha 2010), where it binds and activates nicotinic acetylcholine receptors (nAChRs). These receptors are ionotropic and are comprised of 5 subunits. There are 12 nAChR subunits expressed in the mammalian brain, including α2 - α10 and β2 - β4. Neuronal nAChRs can exist as either homomeric nAChR subtypes, in which all subunits are the same (i.e., α7 nAChRs), or as heteromeric nAChR subtypes, which are a mix of different subunits (i.e., α4β2 nAChRs). This varying subunit composition influences the pharmacological features of nAChRs, and ultimately their responses to nicotine stimulation (D'Souza & Markou 2011, Govind et al 2009). For example, evidences from preclinical studies have indicated that α4-, α5-, α6-, α7-, and β2-containing nAChRs mediate the reinforcing and behavioral effects of nicotine (Fowler et al 2008).

Activation of nAChRs opens the cationic channel, allowing passage of potassium, sodium and calcium ions. Because nAChRs are preferentially located

at the presynaptic terminal, their effects are primarily modulatory and result in the release of nearly every major neurotransmitter (Benowitz 2010, Markou 2008). This results in a diverse array of effects. For example, dopamine, one of the several neurotransmitters released following nAChR activation, is highly linked to nicotine's reinforcing and rewarding properties (Jiloha 2010, Volkow & Li 2004). Other neurotransmitters modulated by nAChRs include γ-aminobutyric acid (GABA), β-endorphin, glutamate, serotonin, acetylcholine, and norepinephrine (Jiloha 2010). The release of GABA or β-endorphins results in attenuation of anxiety and tension (Benowitz 1999). Increased levels of glutamate enhance learning and memory, while serotonin release is connected to mood modulation and appetite suppression (Benowitz 1999). Both acetylcholine and norepinephrine modulate arousal but in addition, the release of acetylcholine enhances cognition while increased norepinephrine levels suppress appetite (Benowitz 1999). nAChRs' propensity to promote release of myriad neurotransmitters following their activation provides a functional basis for nicotine's modulation of various behaviors (Benowitz 2008a).

Nicotine and Neuronal Nicotinic Acetylcholine Receptors (nAChRs) – Chronic Effects

Chronic nicotine exposure results in numerous neuroadaptations within the brain. One prime example is the canonical subtype-specific upregulation of nAChRs (Buisson & Bertrand 2001, Changeux et al 1984). The term "upregulation" describes the persistent increase in nAChR radio-ligand binding sites in the brain

following long-term nicotine exposure. It is noteworthy that the receptor binding affinity of nicotine depends on nAChR subunit composition, which ultimately influence Ca^{2+} permeability as well as the tendency and extent of nicotine-induced upregulation. For example, a large percentage (~90%) of high affinity nicotine binding sites in the brain are made up of α4 and β2 subunits (Whiting & Lindstrom 1988). In addition, studies have shown that incorporation of β4 into α6- or α3-containing nAChRs leads to a remarkable degree of upregulation by nicotine, while the presence of α5- or α3-subunits in β2-contatining nAChRs seems to block upregulation by nicotine (Govind et al 2009). Several molecular mechanisms have been proposed for nicotine-induced upregulation of nAChR subtypes. First, unlike acetylcholine, nicotine is not a substrate for acetylcholine esterase hydrolytic degradation. As a result, nicotine's presence and activity are prolonged, which consequently leads to nAChRs desensitization. The suggested neuronal adaptive response to long-term desensitization of nAChRs is upregulation (Picciotto et al 2008, Wonnacott 1990). In contrast, another study demonstrated that nicotine-induced nAChR upregulation is an intrinsic attribute of the nAChR protein rather than the suggested adaptive response of neurons expressing these receptors (Peng et al 1994). In support, they showed that upregulation results from decreased surface nAChR turnover, which is associated with nicotine-induced changes in nAChR conformation (Peng et al 1994). Another proposed mechanism for nicotine-induced upregulation is nicotine's blockade of nAChR degradation through modulation of proteasomal activity (Ficklin et al 2005, Rezvani et al 2007). Other processes that may contribute to nAChR upregulation include increased

nAChR trafficking to the cell surface (Darsow et al 2005) and increased nAChR subunit maturation and assemblage (Harkness & Millar 2002, Sallette et al 2005). Another critical aspect of nicotine-induced neuroadaptation is that upregulation of nAChRs occur in a subtype-specific manner, and each of these receptor subtypes are differentially expressed across brain regions. These regional dissimilarities in nAChR subtype expression and upregulation following chronic nicotine use may influence nicotine-induced neuroadaptation in various neural circuitry (De Biasi & Dani 2011). Evidence of such diversity in nAChR subtype expression and upregulation have been shown in the mesolimbic dopamine reward circuit. For example, striatal dopaminergic neurons primarily express five nAChR subtypes – α4α5β2, α4α6β2β3, α4β2, α6β2β3, α6β2; however, the expression density of the α4* subtypes is higher compared to the α6* subtypes across the striatum (Grady et al 2007). α4β2 nAChR is one of the most abundant and widely distributed nAChR subtypes in the brain. It is well expressed by both dopaminergic and non-dopaminergic neurons in the striatum, but a subpopulation also containing α5 (α4α5β2 subtype) is only expressed on the striatal dopaminergic terminals (Zoli et al 2002). Amongst many other nAChR subtypes, α4β2 nAChRs are the most implicated in nicotine-induced neuroadaptation and nicotine dependency (Benowitz 2008b). For example, evidence from previous studies examining functional upregulation of nAChR, a direct and important nicotine-induced neuroadaptation, have demonstrated that α4β2 subtype is the most upregulated in the brain compared to other nAChR subtypes (Buisson & Bertrand 2002). Another study also reported that chronic nicotine administration selectively increases the

expression of α4β2 nAChR on dopaminergic terminals in the striatum, and more importantly, this receptor remains functional in contrast to the general idea that upregulated receptors are desensitized (Xiao et al 2009). Further studies also implicated selective upregulation of α4β2 nAChR in presynaptic modulation of dopamine release in the striatum (Sharples et al 2000), even though, another study showed that α6β2β3 nAChR can partly contribute to this nAChR-related function in the striatum (Cao et al 2005). However, it is noteworthy to mention that there is ambiguity in findings related to nicotine-induced upregulation of α6β2 receptors. While a study that utilized mammalian cell lines showed that co-expression of β3-subunits increase in α6β2 and α6β4 receptor levels (Tumkosit et al 2006), another study in brain tissue showed that striatal α6-containing receptors without β3 are downregulated by nicotine and those containing β3 are unaltered.

1.3 MAJOR NEURAL PATHWAYS INVOLVED IN NICOTINE DEPENDENCE

Following nAChR activation in the brain, nicotine engages multiple neurotransmitter systems, usurping their neural elements to precipitate its effects. One of these neurotransmitter systems is the brain's dopaminergic system, which is the primary neural framework mediating the reinforcing and rewarding effects of nicotine. Other key neurotransmitter systems are the major excitatory and inhibitory neurotransmitters in the brain, namely glutamate and GABA, respectively. Both neurotransmitters can modulate nicotine's reinforcing and rewarding effect by enhancing (glutamate) or inhibiting (GABA) dopamine release in the mesocorticolimbic circuits. Excitatory and inhibitory control of nicotine-

induced dopamine effects is possible because of complex interactions existing between mesocorticolimbic dopaminergic neurons and the glutamatergic inputs from the cortical and limbic nuclei, and GABAergic inputs from the local interneurons as well as interneurons from distant nuclei (D'Souza & Markou 2013, Yager et al 2015). Studies investigating how these interactions impact nicotine dependence have shown that inhibition of glutamatergic neurotransmission or stimulation of GABAergic neurotransmission attenuates nicotine intake and nicotine-seeking behavior in rodents (D'Souza & Markou 2013).

Mesocorticolimbic pathway

The mesocorticolimbic pathway, also known as the reward pathway, is the critical neural pathway for reinforcing rewarding behaviors, including those behaviors underlying drug addiction. All drugs of abuse including nicotine are believed to enhance the effect of dopaminergic function in the mesocorticolimbic pathway, particularly, at the dopaminergic nerve terminals in the nucleus accumbens (NAc) – a key neural substrate of motivation and reward (D'Souza & Markou 2011, Dani & De Biasi 2013, Hyman et al 2006, Volkow & Li 2004). Apart from the NAc, other major brain structures in the dopaminergic pathway includes ventral tegmental area (VTA), prefrontal cortex (PFC), substantia nigra (SNr), and caudate-putamen (CPu). Although dopaminergic neurons originate from both SNr and VTA, these structures project to different brain regions. Dopaminergic axons from the SNr project to the caudate putamen in the nigrostriatal pathway, while the axons of dopaminergic neurons in the VTA project primarily to the NAc and PFC in the

mesocorticolimbic circuit (Figure 1). In drug addiction, the role of dopaminergic axon projection from SNr to its targets is not really well-defined (Dani & De Biasi 2013), even though it is a well-described motor circuit. However, VTA dopaminergic projections to the NAc have been identified as the principal neural

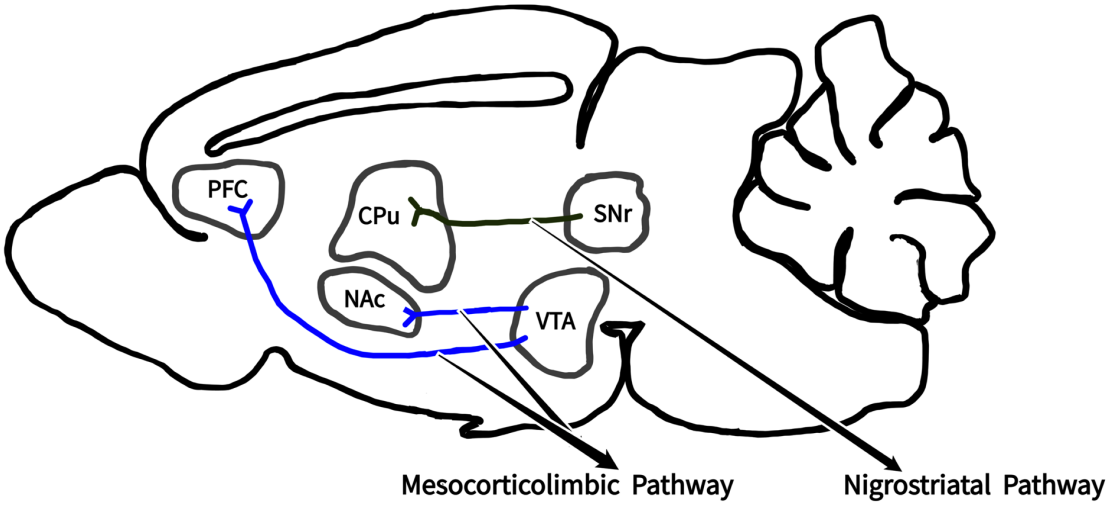

Figure 1.1: Simplified mesocorticolimbic and nigrostriatal pathways

framework shaping reward-related behaviors. In fact, in the context of drug addiction, this pathway is the most crucial neural substrate for acute rewarding effects of all drugs of abuse, regardless of their dissimilar mechanism of action (Markou 2008, Volkow & Li 2004, Volkow & Morales 2015). Nicotine's activation of the VTA-NAc pathway can occur either directly via stimulation of nAChRs on VTA-NAc dopaminergic terminals in the VTA or indirectly through stimulation of nAChRs on glutamatergic nerve terminals innervating dopaminergic neurons in the VTA (D'Souza & Markou 2011). Regardless, both activation pathways lead to dopamine release in the NAc.

Striatum Neuroanatomy

The striatum is a critical component of the mesocorticolimbic system, and it is a heterogeneous structure with two distinct subregions – the dorsal striatum (mainly the CPu) and the ventral striatum (mainly the NAc). These striatal subregions are the main input structures in the mesocorticolimbic pathway, functioning as hubs coordinating various neuronal activities. Major inputs received by these subregions includes the dopaminergic inputs from VTA and SNr, and the glutamatergic projections from the PFC. Both inputs physically interact at different sites on the dendritic spines of striatal GABAergic medium spiny neurons (MSN), which account for ~95% of the striatal neuronal population (Yager et al 2015). This complex interaction controls MSN activity within the striatum (Yager et al 2015). Striatal MSNs relay information to neighboring structures such as SNr via the direct pathway (dMSNs) and to the subthalamic nuclei (STN) via the indirect pathway (iMSNs). While these striatal output pathways are found in both the CPu and NAc, their target structures are different. In the NAc, the iMSNs, which primarily express dopamine D2 receptors, specifically project to the ventral pallidum (VP), and the dMSNs, which generally express dopamine D1 receptors, project mainly to the VTA and SNr. In contrast, iMSNs in the CPu project largely to the globus pallidus external (GPe) and STN, while its dMSNs extend particularly to the globus pallidus internal (GPi) and SNr. Of note, these striatal output pathways are not absolutely separated as there can still be overlapping projections such as the extension of dMSNs axon collaterals to the GPe/VP (Fujiyama et al 2011). In drug addiction, the CPu and the NAc have differing functional roles, even though in a simplistic

view they both receive similar neuronal inputs. For instance, as drug addiction progresses from occasional recreational use to compulsive use, drug-seeking behavior is thought to switch from reward-driven to habit-driven – drug-seeking behaviors that are controlled by NAc and CPu respectively (Clarke & Adermark 2015). This differential role is supported by several studies such as that which previously demonstrated dissimilar dopamine signaling in the CPu and NAc following chronic nicotine use (Zhang et al 2009). Overall, these differences in the neuroanatomical organization of caudate-putamen and nucleus accumbal afferents and efferents contribute to their differential roles in motivation and motor function.

1.4 ROLE OF WITHDRAWAL SYMPTOMS IN NICOTINE DEPENDENCE

Nicotine withdrawal symptoms manifest a few hours after discontinuation of nicotine use, and the collection of these negative symptoms during abstinence from nicotine is the major determinant preventing smokers from successful quitting (McLaughlin et al 2015). Symptoms of nicotine withdrawal encompass affective, cognitive, and somatic domains. Affective symptoms include anxiety, depression, irritability, anhedonia, hyperalgesia, and dysphoria, while memory impairment and difficulty concentrating are cognitive manifestations (McLaughlin et al 2015). Together, the biological basis of nicotine addiction can be regarded as a mix of positive reinforcement, such as mood enhancement, and avoidance of negative effects associated with nicotine withdrawal (Benowitz 2010, Cosci 2011, Markou 2008).

Anxiety-Related Withdrawal Phenotypes

Affective nicotine withdrawal symptoms are critical determinants of smoking motivation (Leventhal et al 2013) and individuals who quit smoking often experience symptoms of anxiety. A randomized placebo-controlled clinical trial has shown that anxiety is a discrete, quantifiable affective manifestation of nicotine withdrawal, which directly impacts relapse to smoking (Piper et al 2011). To advance the current understanding of anxiety-like behaviors during withdrawal from nicotine, better insight into the neurocircuitry and neuroadaptations associated with withdrawal-induced anxiety is critical.

There is mounting evidence implicating the mesolimbic dopamine signaling in the neurobiology of mood and anxiety (Russo & Nestler 2013). One of the critical neural substrates of anxiety-like behaviors in the mesolimbic pathway is the nucleus accumbens. The nucleus accumbens plays an important role in anxiety disorders (Levita et al 2012, Russo & Nestler 2013) and nicotine withdrawal-related anxiety (Morud et al 2018, Torres et al 2015). Besides the nucleus accumbens, studies have also demonstrated the role of ventral hippocampus (Fisher et al 2017) and medial habenula (McLaughlin et al 2015, Pang et al 2016) in nicotine withdrawal-related anxiety. This indicates that withdrawal-related anxiety may be a function of molecular disruptions or neuroadaptive changes in multiple neuroanatomical structures or neurocircuitry. Withdrawal from nicotine during smoking cessation alters nAChR number or function in widely distributed neural circuits such as the mesocorticolimbic circuitry, and these changes have been shown to coincide with anxiety (Grady et al 2007, Yohn et al 2014). Studies have

also shown that withdrawal-induced anxiety can be influenced by the subunit composition of nAChRs. For instance, α6- and β2-containing nAChR subunits are required for increased anxiety during nicotine withdrawal (Jackson et al 2008, Jackson et al 2009), while α5 and α7 may not be necessary (Jackson et al 2008).

Generally, quantification of anxiety and other affective symptoms in rodents are relatively subtler than somatic signs, which are the most often evaluated withdrawal symptoms in rodent models. One of the well-validated behavioral paradigms commonly used in assessing anxiety-like behavior in chronic nicotine studies is the novelty-induced hypophagia (NIH), which is very sensitive to acute treatment with anxiolytic drugs. The NIH test is a hyponeophagia-based paradigm that quantifies anxiety based on animals' latency to feed in a novel environment (Dulawa & Hen 2005, Fisher et al 2017). Open field (Cohen et al 2009) and marble-burying (Turner et al 2014, Turner et al 2013b) tests are also frequently used in evaluating anxiogenic behavior in mice. Both behavioral paradigms, similar to NIH, are well-validated models with high predictive validity for anxiolytics and antidepressants.

Cognition-Related WD Phenotypes

Cognition is a brain-related function that is negatively impacted by nicotine withdrawal. Impaired neurocognitive control during nicotine withdrawal often manifest as inability to change nicotine-seeking and -taking responses that are provoked by stimuli related to previous nicotine's rewarding effects. This symptom is basically characterized with attention deficits and memory impairment, and

together with affective nicotine withdrawal symptoms, are thought to predict relapse (Ashare et al 2014). Previous studies in mice and humans have shown that re-exposure to nicotine can reverse nicotine withdrawal-related cognitive deficits (Davis et al 2005, Ernst et al 2001, Patterson et al 2009, Portugal & Gould 2007).

An important neural substrate of cognitive control processes is the frontostriatal circuits, which include discrete regions of the prefrontal cortex and the striatum. The frontostriatal circuits are critical neural pathways for executive functions, which include adaptation to changes, decision making, working memory, planning and organization. These cognitive functions are normally disrupted during nicotine withdrawal (Parikh et al 2016). However, while the neural mechanism altered during nicotine withdrawal is still not completely understood, changes in nAChR numbers and function may contribute to the disruption and impairment of cognitive control processes during nicotine withdrawal. For example, studies have indicated that β2-containing nAChRs, including α4β2 receptors, mediate nicotine withdrawal-related deficits in contextual fear conditioning (Gould et al 2012, Portugal et al 2008), which is a form of associative learning. Evaluation of associative learning can be performed in rodents by utilizing contextual and cued fear conditioning test, which are behavioral models that assess the ability of a mice to learn and recall an association between environmental cues (context such as a location or stimulus such as a tone) and aversive experiences (aversive stimuli such as an electric shock) (Ashare et al 2014). Another relevant behavioral paradigm of cognition is the novel object recognition test. This test is frequently

utilized in evaluating memory-related cognitive deficits. It assesses rodents based on their tendency to spend more time exploring a novel object rather than a familiar one. One more cognitive control process that may be impaired during nicotine withdrawal is attention. Attention-related cognitive deficits are evaluated in rodents by performing operant signal detection task (Ashare et al 2014).

1.5 NOVEL TARGETS FOR SMOKING CESSATION: NON-NEURONAL CELLS IN NICOTINE DEPENDENCE

Over the years, exploration of neuronal targets has been the primary research focus of nicotine dependency; however, it is becoming evident that non-neuronal cell-types such as astrocytes and microglia, are actively involved in the functional organization of the brain (Allen & Barres 2009, Cerbai et al 2012). Both neuronal and non-neuronal cell-types constantly interact in their local microenvironment to maintain the integrity of brain structures (Allen & Barres 2009). However, impaired interplay amongst these brain cell-types as a consequence of chronic exposure to nicotine may be a major determinant underlying high relapse rates among smokers.

Astrocytes

Astrocytes are the most abundant glial cells in the mammalian brain. They are morphologically complex cells with numerous processes, which are typically bushy. However, with their finest branching processes, they physically interact with blood vessels, other glial cells, and synapses (main elements are presynaptic and

postsynaptic terminals) in a structure known as the tripartite synapses. It is considered that finely branching processes from a single astrocyte physically interact with several hundreds of multiple neuronal dendrites and wraps over 100,000 synapses in the hippocampus or cortex (Sofroniew & Vinters 2010). Similar studies in the hippocampus demonstrated that ~57% of synapses are in physical contact with astrocytes (Harada et al 2015).

Furthermore, astrocytes can exhibit regional heterogeneity with respect to their ratio to that of neurons (astrocyte-to-neuron ratio). They exist in high density in some neural circuits such as the cerebral cortex, where the astrocyte-to-neuron ratio is high, and low density in some regions like the cerebellum, where the astrocyte-to-neuron ratio is low (Khakh & Sofroniew 2015). The functional relevance of this regional diversity is still unclear.

The role of astrocytes in the brain were once thought to be limited to metabolic and trophic support for neurons, ionic and pH homeostasis, and the formation and maintenance of the blood-brain barrier; however, it is now becoming more evident that astrocytes are active participants in the modulation of neuronal activity in the brain. Drugs of abuse such as nicotine can disrupt the interplay between astrocyte and neuron in the brain by direct or indirect modulation. For direct modulation, nicotine can directly bind to nAChRs on astrocytes. Studies have demonstrated that astrocytes express α3, α4, α7, β3, β4 subunits of nAChR, with the α7 subunit being the most predominantly expressed (Gotti & Clementi 2004). In addition, α3β4 and α4β2 nAChR expression have also been reported in the soma and processes of astrocytes (Graham et al 2003). Several studies have

linked astrocyte nAChRs, especially the α7-subtype, to neuroinflammatory processes in Alzheimer's (Teaktong et al 2003) and Parkinson's disease (Liu et al 2015, Quik et al 2009), both neurodegenerative disorders in which nicotine use has been reported as beneficial (Newhouse et al 2012, Villafane et al 2007). Nicotine's interaction with astrocyte nAChRs may further result in an increase in the intracellular Ca^{2+} concentration (Sharma & Vijayaraghavan 2001) and subsequent release of gliotransmitters. Gliotransmitters can alter synaptic activity and function in neural circuits. For example, a study examining nicotine's modulation of neuron-glial interaction showed that the release of astrocyte D-serine following nicotine stimulation is necessary for nicotine's enhancement of synaptic transmission and long-term memory (Lopez-Hidalgo et al 2012). However, for indirect modulation, nicotine can regulate astrocyte activity and function by releasing neuromodulators such as dopamine. For instance, a recently published study demonstrated that extracellular dopamine can modulate astrocyte morphology and function (Galloway et al 2018).

One other mechanism through which astrocytes actively participate in synaptic transmission is the clearance of small molecule neurotransmitters, such as glutamate. Excitatory amino acid transporter (EAAT2), which is primarily expressed on astrocytes, plays a major role in glutamate clearance – responsible for >90% glutamate uptake (Kim et al 2011). Elevated glutamate levels in the brain underlies many neurodegenerative and neurological disorders, and dysfunctional EAAT2 have been linked with the initiation of a number of these brain disorders (Kim et al 2011). Similarly, in nicotine addiction studies, rats undergoing withdrawal

from chronic nicotine were found to have decreased EAAT2 expression (Knackstedt et al 2009), indicating a role for this astrocyte glutamate transporter in nicotine seeking behaviors (Spencer & Kalivas 2017). Together, astrocytes may be active participants in the regulation of neuronal activities that are key for nicotine dependency.

Microglia

Microglia are the resident innate immune cells in the brain and account for ~10% of the CNS cell population in the healthy brain (Salter & Stevens 2017). In terms of their developmental origin and functions, microglia are a unique population among the other brain cell-types. Like peripheral myeloid cells, microglia are derived from mesoderm lineage, and are unlike other brain cell-types, which are derived from neuroectodermal progenitors. Recent lineage-tracing studies provided additional characterization of microglia origin, showing that they are derived from the yolk-sac progenitors – an embryonic origin distinct from that of the peripheral myeloid populations (Madore et al 2017).

Microglia are highly branched, dynamic cells with relatively rapid movement compared to other brain cell-types. These features, in addition to their fine motile processes, allows them to constantly scan the brain parenchyma to maintain homeostasis. Further, as CNS surveillance elements, microglia can sense and respond accordingly to extracellular signals. Based on the signal pattern, microglia can assume diverse morphological phenotypes that have been previously classified into M1 microglia – the pro-inflammatory activation phenotype, or M2

microglia - the anti-inflammatory activation phenotype. This simplistic characterization of microglia activation phenotypes is based on the presence of particular cell surface molecules and the expression of specific sets of cytokines (Butovsky & Weiner 2018). For example, M1 microglia were associated with factors such as tumor necrosis factor alpha (Tnfα), interleukin-1-beta (Il1β), and reactive oxygen species (ROS), while M2 microglia were typified by interleukin-10 (Il10) and transforming growth factor beta (TGF-β) (Butovsky & Weiner 2018, Tang & Le 2016). However, evidence from more recent studies that re-characterize microglial diversity (Butovsky et al 2014) have shown that the simplistic view of microglial phenotype does not sufficiently represent the intricate physiology of microglial cells (Ransohoff 2016). In addition to the phenotypic complexities of microglia, they are also largely heterogeneous across diverse neural circuits and brain regions. For example, a recent study that examined microglial phenotypes among a group of subcortical nuclei revealed that microglia across the basal ganglia are very diverse in terms of their density and morphology, metabolic and activational state, and transcriptome (De Biase et al 2017). This implicates local cues as a critical mediator of microglia phenotype across neural circuit (McCarthy 2017). Further, regional microglial heterogeneity may also reflect diverse functional phenotypes required for the integrity of the various CNS environment in which the microglia lives.

Microglia were once considered only as support cells in the brain (Streit 2002), but recent evidences suggest they are active players in brain function and dysfunction (Salter & Stevens 2017). In addition to their immune functions,

microglia are critical elements in synaptic remodeling and plasticity (Miyamoto et al 2016, Torres et al 2016), placing them as a potential participant in neuroplasticity underlying drug addiction. Similar to astrocytes, nicotine and many other drugs of abuse can directly modulate microglial morphology and function via interaction with nAChR on microglia. However, to date, α7-nAChR is the only nAChR subtype reportedly found on microglia. It is noteworthy to mention that most studies, except one (Shytle et al 2004), that have reported α7-nAChR expression on microglia were done in immortalized microglial cell lines or primary microglial cultures (De Simone et al 2005, King et al 2017, Mencel et al 2013, Shytle et al 2004, Suzuki et al 2006), which both have their own drawbacks (Stansley et al 2012). Microglia may also be indirectly modulated by nicotine via neurotransmitter release. Human induced pluripotent stem cells, human postmortem tissues, or rodents may be more suitable models for investigating nicotine's interaction with microglia. At the present time, nicotine's modulatory mechanism of microglial function and how these may impact behavior are still unclear. However, a recent study demonstrated that microglial activation and impaired neurogenesis are associated with cognitive deficits during nicotine withdrawal (Saravia et al 2019). While microglia may actively contribute to nicotine dependency, research studies investigating the role of microglia in nicotine dependence is still in the early stages.

1.6 CONCLUSION

This chapter extensively covered acute and chronic effects of nicotine, as well as the neural substrate of motivation and reward-related behaviors. We discussed

functional upregulation of nAChRs, a nicotine-induced neuroadaptation, and highlighted its potential role in nicotine withdrawal-related behaviors. Finally, rather than the conventional research focus on neuronal targets, we explored the possibilities of non-neuronal cell types as novel targets in the development of new smoking cessation aids.

Future of pharmacotherapy development and potential role of glial targets

There are presently three FDA-approved first-line smoking cessation medications: Nicotine Replacement Therapy (NRT), bupropion, and varenicline (Jiloha 2014, Prochaska & Benowitz 2016). However, despite years of innovation and advancement in the development of smoking cessation medications, a large population of smokers attempting to quit still fail. This may be largely attributable to the inability of current smoking cessation therapies to address some critical aspects of nicotine dependency. For instance, all the three FDA-approved smoking cessation medications were developed to mechanistically target neuronal nAChRs, neglecting the possible contributions of targets on non-neuronal cells like astrocytes and microglia.

To advance nicotine addiction research, novel studies exploring astrocytes and microglia function in nicotine dependence should be prioritized. Long-term, this may represent an untapped therapeutic avenue for smoking cessation.

CHAPTER 2

MICROGLIAL MORPHOLOGY AND PROINFLAMMATORY SIGNALING IN THE NUCLEUS ACCUMBENS DURING NICOTINE WITHDRAWAL[1]

[1] Adewale Adeluyi, Lindsey Guerin, Miranda L. Fisher, Ashley Galloway, Robert D. Cole, Sherine S. L. Chan, Michael D. Wyatt, Shannon W. Davis, Linnea R. Freeman, Pavel I. Ortinski, Jill R. Turner. Submitted to Science Advance, 4/15/2019.

2.1 ABSTRACT

Microglia are active participants in the pathogenesis of several neurodegenerative diseases; however, their role in nicotine withdrawal-related anxiety, which directly impacts relapse to smoking in humans, is unknown. This study outlines a series of novel findings that demonstrate alteration in microglial morphology and function underlies nicotine withdrawal-related anxiety. Here, we examined the striatum – a key brain region implicated in reward-related processes and affective behavioral symptoms such as anxiety. First, we show that both chronic nicotine and withdrawal provoke microglial activation in the nucleus accumbens but not the caudate putamen. Further, in the nucleus accumbens, nicotine withdrawal induces proinflammatory responses, which was muted during chronic nicotine treatment. Similarly, microglia-related NADPH oxidase 2 (Nox2) induction and aberrant reactive oxygen species (ROS) production occurred during nicotine withdrawal, but not during chronic nicotine treatment, in the nucleus accumbens. We utilized a well-described antioxidant, N-acetylcysteine (NAC), and show that aberrant ROS production significantly contributes to nicotine withdrawal-related anxiety. Further, depletion of microglia with PLX5622 attenuates both nucleus accumbal Nox2 and ROS, as well as nicotine withdrawal-related anxiety. More directly, our microglia depletion studies reveal a strong link between microglial function and nicotine withdrawal-related anxiety. Taken together, we provide the first evidence that nicotine withdrawal alters microglial morphology and function, which underlies nicotine withdrawal-related anxiety. Long-term, further investigation into

modulators of microglial function during nicotine withdrawal represents an untapped therapeutic avenue for smoking cessation.

2.2 INTRODUCTION

While smoking cessation significantly reduces the risk of smoking-related diseases such as cancer, stroke, respiratory and heart diseases (Babizhayev 2014, Samet 2013), nearly 80% of smokers attempting to quit still fail (Polosa & Benowitz 2011). Currently, tobacco smoking is the leading cause of preventable morbidity and mortality globally (World Health Organization 2012), which underscores the need for better therapeutics for nicotine dependence. Pharmacotherapies for nicotine dependence have largely targeted nicotinic acetylcholine receptors (nAChRs), as activation of these receptors by nicotine mediates the rewarding effects of tobacco (Coe et al 2005, Polosa & Benowitz 2011, Rollema et al 2007, Xiao et al 2006). However, the molecular mechanism underlying vulnerability to smoking relapse is multifaceted (Polosa & Benowitz 2011). One avenue for development of new therapeutics is reassessing the symptomology of individuals undergoing nicotine withdrawal. For example, patients with smoking-related disease, such as chronic obstructive pulmonary disease, often present with increased cellular oxidative stress levels. These observed effects may be the result of inhaled oxidants present in cigarette smoke (Babizhayev 2014). However, individuals attempting to quit smoking may also lose nicotine's neuroprotective effects (Barreto et al 2014, Lu et al 2017, Ross & Petrovitch 2001, Tariq et al 2005) . For example, clinical studies have shown nicotine transdermal patches to be neuroprotective in

neurodegenerative diseases such as Alzheimer's (Newhouse et al 2012, Wilson et al 1995) and Parkinson's (Villafane et al 2007), two diseases with extensive ties to inflammatory responses (Amor et al 2010). This would suggest that smoking cessation, while reducing the inhaled level of oxidants, may also remove the potential anti-inflammatory benefits of nicotine in the brain.

Microglia are highly specialized resident immune cells, which act as the brain's homeostatic sensor. Their constant surveillance of the brain microenvironment enables them to detect and respond to homeostatic perturbations by altering their own morphology in diverse ways depending on the type of stimuli they sense. Such changes in microglial morphology are more indicative of an imbalance in CNS homeostasis following an insult or injury and not a particular activation phenotype (M1 pro-inflammatory phenotype or M2 anti-inflammatory phenotype) as initially conceptualized (Ransohoff 2016, Salter & Stevens 2017). Furthermore, studies have described microglia as critical elements in synaptic remodeling (Miyamoto et al 2016, Weinhard et al 2018), as well as learning and memory (Torres et al 2016) – processes prominently affected during development of drug dependence (Kutlu & Gould 2016, Torregrossa et al 2011). In addition to neuroplasticity-related events, microglia actively participate in reactive oxygen species (ROS) generation (Lull & Block 2010). While ROS are key intracellular signaling molecules for normal cell function, they can become toxic when there is a chronic imbalance between oxidant and antioxidant signaling within the cell, termed oxidative stress (Schieber & Chandel 2014). Since neurons are particularly susceptible to oxidative insult, aberrant ROS production and

signaling can significantly impact brain function and behavior (Li et al 2016, Seo et al 2012). For example, correlative studies examining patients diagnosed with Parkinson's disease found a strong relationship between oxidative stress and striatal neurodegeneration (Ikawa et al 2011). However, while the striatal neurocircuit is a major site for neuroadaptive events underlying addictive processes (Yager et al 2015), the effects of nicotine withdrawal on microglia phenotype and related ROS homeostasis in this region are unknown.

The striatum is a heterogeneous structure with two distinct sub-regions – the caudate-putamen, which contributes to motor functions and movement, and the nucleus accumbens, which is key for motivation and reward processes (Yager et al 2015). Our lab (Fisher et al 2017, Turner et al 2014) and others (Lee et al 2015, Manhaes et al 2008) have shown that anxiety is a discrete, quantifiable symptom of nicotine withdrawal, which has been shown to directly impact smoking relapse in humans (Piper et al 2011). Previous studies in humans have demonstrated the contribution of mesolimbic dopamine signaling in the nucleus accumbens to anxiety-related processes (Kim et al 2008, Levita et al 2012, Lorberbaum et al 2004). Further, chronic stress studies have reported increased levels of oxidative stress markers in other parts of the mesolimbic circuitry to coincide with increased anxiety-like behavior (Patki et al 2013, Salim et al 2010). However, it is unknown whether nicotine withdrawal elicits changes in microglial morphology and function, and whether these changes directly impact anxiety. Our studies are the first to report nucleus accumbens-specific alterations in microglial morphology and ROS homeostasis. Further, we demonstrate compelling evidence that these microglia-

related effects are critical mediators of anxiety-like behaviors in mice during nicotine withdrawal.

2.3 MATERIALS AND METHODS

Animals

For the majority of the experiments described, male B6/129SF1 and B6/129PF1 mice were purchased from Jackson Laboratories (Bar Harbor, ME, USA; 8 -10 weeks of age; 20 - 31 g). Magnetic activated cell sorting (MACS) experiments examining cell-type specific mRNA expression utilized male B6/129 mice bred in house (8 -10 weeks of age; 20 - 31 g). All mice were housed in groups of two to four, and randomly assigned to treatment conditions. They were maintained on a 12-h light/dark cycle with food and water *ad libitum* in accordance to the University of South Carolina Animal Care and Use Committee. All behavioral testing sessions were conducted between the 0900 and 1300 hours.

Osmotic drug delivery and treatment

(-)-Nicotine tartrate (MP Biomedicals, Solon, OH, USA) was dissolved in sterile 0.9% sodium chloride solution, and then infused subcutaneously via osmotic minipumps (Alzet model 2002; DURECT Corporation, Cupertino, CA, USA) at a dose of 18 mg/kg/day for 15 days. The control group was infused with saline for the same period of time. Chronic treatment with nicotine at this dose yields a plasma level of approximately 0.3 μM in mice (reported as nicotine free base molecular weight), a concentration comparable to that observed in human smokers

consuming an average of 17 cigarettes a day (plasma levels between 0.06 - 0.31 μM) (Matta et al 2007). Prior to the start of surgery, mice were anesthetized with isoflurane/ oxygen mixture (1 - 3%), and minipumps were inserted using aseptic techniques. Surgical wounds were closed with 7 mm stainless steel wound clips (Reflex, Cellpoint Scientific, Gaithersburg, MD, USA), after which mice were left to recover on the recovery pad before they were returned to their individual cages. After 14 days of chronic administration of either saline or nicotine via osmotic minipumps, mice earmarked for withdrawal from chronic nicotine and their assigned saline controls were subjected to spontaneous withdrawal by the removal of their osmotic minipumps using a similar aseptic surgical approach as above. Tissues were collected from mice after 48 h withdrawal.

Injection drug delivery and treatment

N-acetylcysteine (NAC) (A7250, Sigma-Aldrich, St Louis, MO, USA) was dissolved in sterile 0.9% sodium chloride solution, adjusted to pH 7, and administered intraperitoneally (IP) at a dose of 150 mg/kg per day for 4 days (24 h prior to withdrawal, and each morning for the next 3 days). The administered NAC dose was selected based on previously published studies (Cao et al 2012, Victor et al 2003). Post-withdrawal NAC injections were given 30 minutes before behavioral testing. Mice not receiving NAC were injected with vehicle (sterile 0.9% sodium chloride solution) during this treatment period.

Microglia depletion via chow treatment

Plexxikon Inc. (Berkeley, CA) provided colony stimulating factor-1 receptor (CSF1R) inhibitor, PLX5622, which was formulated in AIN-76A chow at a dose of 1200 ppm by Research Diets (New Brunswick, NJ). Control chow was also provided. Male B6/129SF1 mice (8 weeks old) received either control chow or PLX5622 chow for 7 days prior to withdrawal and all through 48 h withdrawal period.

Open field test and locomotor activity

The open field test is an anxiety-related behavioral model, which also allows simultaneous assay of overall locomotor activity levels in mice. All mice were tested in this model at 24 h withdrawal timepoint. Test chambers were wiped with 70% ethanol in between tests to remove any scent cues left by the previous mouse. The ethanol was allowed to dry completely before each testing, and every testing session lasted for 15 minutes. For the analysis, Top Scan (Clever Sys Inc., Reston, Virginia, USA) software was utilized to track and evaluate mouse movement. Prior to tracking analysis for each mouse, a background profile was generated, and the testing chamber was calibrated in arena design mode according to manufacturer's instructions. Software output for each individual test includes total distance moved (in mm) and the time spent in the center (in %). These data were then normalized to the saline/vehicle control group.

Marble-burying test

The marble-burying test is an animal behavioral model of anxiety that has high predictive value in detecting anxiolytic drugs. All mice were tested in this model at 48 h withdrawal timepoint. Mice were placed individually in small cages (29.0 cm x 17.5 cm), in which 20 marbles had been equally distributed on top of mouse bedding (5 cm deep). A lid was placed on top of the cage to prevent the mouse from jumping out of the cage during the test. Mice were left undisturbed for 15 minutes, after which the number of buried marbles (those covered by bedding three-quarters or more) was counted by an observer blinded to experimental conditions.

Quantitative PCR

Quantitative reverse transcriptase PCR was performed as previously described (Cleck et al 2008) on caudate putamen or nucleus accumbens samples across all treatment groups. Briefly, RNA was isolated using the RNeasy Mini Kit (Qiagen, Venlo, The Netherlands), and qPCR reactions were assembled using synthesized complementary DNA, Thermo Scientific Maxima SYBR Green master mix along with 100 nM primers (Integrated DNA Technologies, Inc., Coralville, Iowa, USA) diluted to 4.3 nM final concentration. The mRNA levels were determined using the $2^{-\Delta\Delta CT}$ method (Livak & Schmittgen 2001) and target genes were normalized to the housekeeping gene, hypoxanthine phosphoribosyltransferase (HPRT). All gene expression values were normalized to their respective saline controls. Primer sequences are available upon request.

Western blot

Protein analysis was performed as described previously (Portugal et al 2012) on nucleus accumbens samples of all treatment groups. Briefly, 20 µg of protein were resolved in Any KD precast polyacrylamide gel (Bio-Rad Laboratories Inc., Hercules, CA, USA) and transferred to nitrocellulose membranes. Membranes were incubated with LI-COR blocking buffer (LI-COR, Lincoln, NE, USA) for 1 h at room temperature before reacting overnight at 4 ^{o}C with primary antibodies (Nox2 (1:1000, ab129068, Abcam Biotechnology, Cambridge, UK) and GAPDH (1:1000, sc-32233, Santa Cruz Biotechnology, Santa Cruz, CA, USA)). After washing in phosphate buffered saline-Tween-20, the blots were incubated in fluorescent secondary antibodies (1:20000, LI-COR) in LI-COR blocking buffer for 1 h at room temperature. Membranes were then washed, and immunolabeling detection and densitometry measurements were performed using the LICOR Odyssey System (LI-COR). Ratios of Nox2 (60 kD band) to GAPDH densities were calculated for each sample and analyzed across conditions.

Protein carbonylation assay

Protein carbonyl derivatives were determined in caudate putamen and nucleus accumbens samples of all treatment groups using OxiSelect Protein Carbonyl Immunoblot Kit (Cell Biolabs, Inc., San Diego, CA, USA) following the manufacturers details. Briefly, 20 µg of protein were resolved in Any KD mini-protean precast polyacrylamide gel (Bio-Rad Laboratories Inc., Hercules, CA, USA) and transferred to nitrocellulose membranes. Membranes were processed

for 2,4-dinitrophenylhydrazine (DNPH) derivatization by equilibrating them in Tris buffered saline (TBS) containing 20% methanol, followed by washes in 2 N HCL, incubation in 1X DNPH, and final washes in 2 N HCL and 50% methanol. DNPH-treated membranes were then incubated with LI-COR blocking buffer (LI-COR, Lincoln, NE, USA) for 1 h at room temperature before reacting overnight at 4 ^{o}C with primary antibodies (Anti-DNP (1:1000, Cell Biolabs, Inc.) and GAPDH (1:1000, sc-32233, Santa Cruz Biotechnology, Santa Cruz, CA, USA)). After washing in Tris buffered saline-Tween-20 (TBST), the blots were incubated with fluorescent secondary antibodies (1:20000, LI-COR) in LI-COR blocking buffer for 1 h at room temperature. Membranes were then washed, and immunolabeling detection and densitometry measurements were performed using the LICOR Odyssey System (LI-COR). DNP signals were normalized to GAPDH densities for each sample.

Immunohistochemistry and microglia morphological analysis

One brain hemisphere from each mouse was collected and fixed overnight in 4% paraformaldehyde in PBS. Fixed brains were cryoprotected by leaving them overnight in 15% sucrose, and then in 30% sucrose for 48 h. Cryoprotected brain hemispheres were sectioned through the striatum at 45 microns and processed for IBA1 immunohistochemistry. Briefly, cryosections were incubated in a rabbit anti-IBA1 primary antibody overnight (1: 1,000; Wako Catalog No. 019-19741), followed by a 2-h incubation in a goat anti-rabbit secondary (1:500, Jackson ImmunoResearch Laboratories, West Grove, PA, USA). The signal was amplified

with the avidin biotin complex (ABC; Vector Labs) method (1:500) and visualized with Vector ® VIP peroxidase substrate to yield a purple reaction product. Images were generated at 200X magnification using Leica DMI 3000B microscope (Leica Microsystems Inc., Buffalo Groove, IL, USA) fitted with Leica DFC 290HD digital camera. Leica LAS core software was used for image acquisition. Morphological analyses were conducted with National Institutes of Health ImageJ software. For IBA1-positive cell count/ density, cell area, and cell perimeter measurements, images were converted from RGB to 16-bit format before applying a threshold and subsequent binary mask. Objects within each masked image were then scanned, counted, and measured using the "Analyze Particles" command. Parameters for analysis of IBA1-positive cells were set in pixel units excluding any object under 400±100 or above 4500±1000 square pixel units. Objects positioned at the edge of the image field were excluded. For analysis of cell process count and length, primary processes extending directly from the cell body and no shorter than 5 microns in length were counted and measured. 5-6 IBA1-positive cells per image field were analyzed for average process count and length measurements. For all morphological analyses, final measurements were reported in microns (resolution of 6.2 pixels per micron).

Isolation of nucleus accumbal microglia and astrocytes by magnetic activated cell sorting (MACS)

Nucleus accumbal tissues were diced with a sterile scalpel into small pieces in a sterile petri dish containing 2 ml of cold Hank's buffered saline solution (HBSS,

minus Ca^{2+}, Mg^{2+}; Life Technologies Corporation, Grand Island, NY, USA). This suspension was transferred into a 15 ml centrifuge tube, and then, spun at 300Xg for 2 minutes at 4 ^{o}C. Supernatant was discarded, and tissue was processed into single-cell suspension by enzyme dissociation using Miltenyl's adult brain dissociation kit (Miltenyl Biotec Inc., Auburn, CA, USA) according to the manufacturer's instructions. Following complete dissociation, cell suspension was applied to pre-wet MACS Smart Strainer (70 µm; Miltenyl Biotec Inc., Auburn, CA, USA), and the flow through was processed for microglia labeling with $CD11b^{+}$ microbeads (Miltenyl Biotec Inc., Auburn, CA, USA). Cells were washed with 2 ml 0.5% BSA in PBS buffer and centrifuged at 300Xg for 10 minutes at 4 ^{o}C for removal of any unbounded beads from the pellet. Cell pellet was re-suspended in 500µl 0.5% BSA in PBS buffer, and then applied onto a prepped MACS MS column attached to an OctoMACS magnetic separator (Miltenyl Biotec Inc., Auburn, CA, USA). Flow through containing unlabeled cells was collected first, and $CD11b^{+}$ microglia were then collected by flushing out the magnetically labeled cells in the column into a microcentrifuge tube following the removal of the column from the magnetic separator. The flow through was immediately processed for astrocyte labeling using anti-ACSA-2 microbead kit (Miltenyl Biotec Inc., Auburn, CA, USA) according to the manufacturer's instructions. In a similar way to the magnetic separation step in $CD11b^{+}$ microglia isolation, $ACSA\text{-}2^{+}$ astrocytes were also purified and collected.

Behavioral and molecular data analyses

Results are presented as mean ± SEM. For behavioral data, statistical differences between groups were determined using two-way ANOVA followed by multiple two-stage linear step-up procedure of Benjamini, Krieger and Yekutieli multiple comparisons test. For molecular data, statistical differences between groups were determined using either one-way or two-way ANOVA followed by Bonferroni's or Tukey's HSD multiple comparison test. All statistical analyses were done in GraphPad Prism 8.0 (GraphPad Software, La Jolla, CA, USA).

2.4 RESULTS

Chronic nicotine and withdrawal alter microglial morphology in the nucleus accumbens.

Morphological changes and release of pro-inflammatory cytokines are canonical features of activated microglia (Bollinger et al 2016, Ding et al 2017, Qin et al 2004). To evaluate both features during chronic nicotine and withdrawal, mice were administered saline or nicotine (18 mg/kg/day) via osmotic minipump implantation, and at 2 weeks, a 48-h withdrawal was initiated by removal of implanted pumps in mice earmarked for nicotine withdrawal and their saline controls (Figure 2.1a). Our evaluation of striatal microglia morphology revealed region-specific alterations following chronic nicotine and withdrawal. In the nucleus accumbens of chronic nicotine and withdrawal mice, there were more microglia with larger cell area *($F = 18.24$, $p < 0.0001$, ANOVA; Saline versus Chronic nicotine mice: $p < 0.0001$, Saline versus Nicotine withdrawal mice: $p = 0.0169$, Post-hoc*

analyses), larger cell perimeter *(F = 6.390, p = 0.0018, ANOVA; Saline versus Chronic nicotine mice: p = 0.0026, Sal versus Nicotine withdrawal mice: p = 0.0254, Post-hoc analyses)*, but not process length *(F = 1.331, p = 0.2654, ANOVA)* compared to their saline counterparts; however, in the caudate putamen, we observed differences only between the microglial process length of chronic nicotine and withdrawal mice *(Cell area: F = 2.917, p = 0.0547, ANOVA; Cell perimeter: F = 1.121, p = 0.3264, ANOVA; Process length: F = 3.697, p = 0.0256, ANOVA; Saline versus Chronic nicotine mice: p = 0.1848, Sal versus Nicotine withdrawal mice: p = 0.6310, Chronic nicotine versus Nicotine withdrawal mice: p = 0.0292, Post-hoc analyses)* (Figure 2.1b – c, i - iii). While these data show that chronic nicotine and withdrawal induce microglia activation in the nucleus accumbens, our microglial process length data suggest that the observed activation phenotype may be early in the microglia activation spectrum. Next, we evaluated mRNA expression levels of TNFα and IL1β – pro-inflammatory cytokines associated with microglia activation, and our qPCR results revealed a differential mRNA profile of these cytokines in chronic nicotine and withdrawal mice. In the nucleus accumbens, TNFα *(F = 8.429, p = 0.0009, ANOVA; Saline versus Nicotine withdrawal mice: p = 0.0032, Chronic nicotine versus Nicotine withdrawal mice: p = 0.0015, Post-hoc analyses)* and IL1β *(F = 6.698, p = 0.0027, ANOVA; Saline versus Nicotine withdrawal mice: p = 0.0179, Chronic nicotine versus Nicotine withdrawal mice: p = 0.0023, Post-hoc analyses)* mRNA levels were elevated in the nicotine withdrawal mice compared to chronic saline and nicotine counterparts, suggesting a muted pro-inflammatory signal during chronic nicotine treatment. In

contrast, in the caudate-putamen, there was a significant decrease in IL1β mRNA expression *(F = 3.903, p = 0.0269, ANOVA; Saline versus Nicotine withdrawal mice: p = 0.0361, Chronic nicotine versus Nicotine withdrawal mice: p = 0.0415, Post-hoc analyses)*, but no significant change in TNFα mRNA expression *(F = 3.140, p = 0.0538, ANOVA)* between treatment groups (Figure 2.1d and e). Taken together, these results demonstrate that chronic nicotine and withdrawal induce microglial activation with distinct molecular features in the nucleus accumbens.

Nicotine withdrawal induces reactive oxygen species in the nucleus accumbens.

Given that excessive production of ROS is often associated with microglial activation (Ding et al 2017), we directly examined ROS generation in the nucleus accumbens and caudate putamen of saline, chronic nicotine, and nicotine withdrawal mice using a protein carbonylation assay. Carbonylated proteins are well-established markers for oxidative stress because they are representative products of protein oxidation, which occurs either by direct or indirect reaction of a protein with ROS or secondary by-products of oxidative stress (Suzuki et al 2010b, Zhang et al 2013) (Figure 2.2a; Protein and arrow icons were downloaded from Reactome (Sidiropoulos et al 2017)). In agreement to our previous observations of TNFα and IL1β mRNA levels, we found that nicotine withdrawal animals had increased levels of carbonylated proteins *(F = 9.125, p = 0.0004, ANOVA; Saline versus Nicotine withdrawal mice: p = 0.0012, Chronic nicotine versus Nicotine withdrawal mice: p = 0.0019, Post-hoc analyses)* in the nucleus accumbens

compared to the chronic saline and nicotine equivalents, while there were no changes *(F = 0.3290, p = 0.7247, ANOVA)* between treatment groups in the caudate putamen (Figure 2.2b and c). These data further reinforce that the observed dissimilar pro-inflammatory signaling during chronic nicotine and withdrawal is specific to the nucleus accumbens.

N-acetylcysteine prevents microglial signaling, but not activation, in the nucleus accumbens during nicotine withdrawal.

While we have shown that nicotine withdrawal induces ROS generation in the nucleus accumbens, it is unclear whether altered microglial morphology and signaling during nicotine withdrawal can be attenuated by ROS scavenging. To examine this, we utilized N-acetylcysteine (NAC), a well-described antioxidant (Aruoma et al 1989, Dekhuijzen 2004, Sun 2010). In this experiment, animals were administered saline or nicotine (18 mg/kg/day) via osmotic minipump implantation, and at 2 weeks, a 48 h withdrawal was initiated by removal of implanted pumps in animals earmarked for nicotine withdrawal and their saline controls. A day prior to withdrawal and each morning for the next 3 days, all animals received either vehicle or NAC (150 mg/kg per day) injection intraperitoneally (Figure 2.3a). First, we evaluated the impact of NAC on nicotine withdrawal-induced pro-inflammatory cytokines in the nucleus accumbens. Our TNFα qPCR results show that there was a main effect of nicotine withdrawal *(F(2, 88) = 13.51, p = 0.0001, ANOVA),* but no main effect of NAC injection *(F(1, 88) = 0.02802, p = 0.8674, ANOVA)* or an interaction effect *(F(2, 88) = 2.503, p = 0.0876, ANOVA)*. Post-hoc analyses

demonstrated vehicle-treated nicotine withdrawal mice showed increased TNFα mRNA expression in the nucleus accumbens compared to their nicotine counterparts and saline controls *(p = 0.0040; p = 0.0031, respectively)*. In addition, TNFα message also increased in the nucleus accumbens of the NAC-treated nicotine withdrawal mice compared to vehicle-treated nicotine mice and saline controls *(p = 0.0476; p = 0.0408, respectively)* (Figure 2.3b). Our IL1β mRNA expression data show there was a main effect of nicotine withdrawal *(F(2, 86) = 6.026, p = 0.0036, ANOVA)*, but no main effect of NAC injection *(F(1, 86) = 3.269, p = 0.0741, ANOVA)* or an interaction effect *(F(2, 86) = 1.041, p = 0.3575, ANOVA)*. Post-hoc analyses demonstrated that while vehicle-treated nicotine withdrawal mice showed increased IL1β mRNA expression in the nucleus accumbens compared to their nicotine counterparts and saline controls *(p = 0.0029; p = 0.0221, respectively)*, IL1β message in the nucleus accumbens of the NAC-treated nicotine withdrawal mice was not significantly different from their vehicle-treated nicotine mice and saline controls (Figure 2.3c). Similarly, analysis of carbonylated protein levels in the nucleus accumbens indicated a main effect of nicotine withdrawal *(F(2, 84) = 7.068, p = 0.0015, ANOVA)*, but no main effect of NAC treatment *(F(1, 84) = 1.148, p = 0.2870, ANOVA)* or an interaction effect *(F(2, 84) = 2.929, p = 0.0589, ANOVA)*. Post-hoc analyses showed that vehicle-treated nicotine withdrawal mice had increased amounts of carbonylated proteins compared to their nicotine equivalents and saline controls (p = 0.0049; p = 0.0028; respectively). In contrast, levels of this ROS marker were not significantly different between NAC-treated nicotine withdrawal mice and their respective vehicle-

treated nicotine mice and saline controls (p = 0.7903; p = 0.7941) (Figure 2.3d and e). Next, we evaluated the impact of NAC on WD-induced microglial activation, and we observed that the nucleus accumbens level of microgliosis was unchanged with respect to the cell area *(t(274) = 0.09383, p = 0.9253, unpaired t-test)*, cell perimeter *(t(275) = 0.8845, p = 0.3772, unpaired t-test)* and process length *(t(189) = 0.5959, p = 0.5520, unpaired t-test)* between nicotine withdrawal mice and their NAC-treated counterparts (Figure 2.4a and b, i - iii). Overall, these data show that while NAC treatment has no impact on morphological hallmarks of microglial activation, it was able to attenuate nicotine withdrawal-induced ROS in the nucleus accumbens.

N-acetylcysteine attenuates nicotine withdrawal-induced anxiogenic behavior in mice.

Given recent studies supporting the role of the nucleus accumbens in anxiety-related disorders (Kim et al 2008, Levita et al 2012), we evaluated NAC effect and withdrawal from chronic nicotine in two well-validated behavioral models of anxiety, the marble-burying (MB) test and the open field (OF) test. These behavioral tests were conducted 30 minutes post-injection at 24-h (OF test) and 48-h (MB test) withdrawal time points (refer to Figure 2.3a). In the MB test, there was a significant interaction between the main effects *(Treatment effect: F(2, 90) = 1.350, p = 0.2644, ANOVA; Injection effect: F(1,90) = 1.002, p = 0.3195, ANOVA; Interaction: F(2, 90) = 5.642, p = 0.0049, ANOVA)*. Post-hoc analyses showed that vehicle-treated nicotine withdrawal animals buried more marbles than their saline controls

(q = 0.0330), as well as their nicotine and NAC-treated equivalents *(q = 0.0148; q = 0.0148, respectively)* (Figure 2.5a), indicative of an anxiogenic effect. In the OF, there was a significant interaction between the main effects *(Treatment effect: F(2, 90) = 2.524, p = 0.0858, ANOVA; Injection effect: F(1,90) = 0.1591, p = 0.6910, ANOVA; Interaction: F(2, 90) = 5.079, p = 0.0081, ANOVA)*. From our post-hoc analyses, we discovered that vehicle-treated nicotine withdrawal animals spent less time in the center of the arena compared to their nicotine counterparts and saline controls *(q = 0.0042; q = 0.0042)*, indicating an anxiogenic response. This is in contrast to NAC-treated nicotine withdrawal animals, which were not significantly different from vehicle-treated nicotine mice and their saline controls (Figure 2.5b and c). Further, these effects were not due to alterations in locomotor activity, as there were no differences in distance traveled between any of the treatment groups *(Treatment effect: F(2, 91) = 2.713, p = 0.0717, ANOVA; Injection effect: F(1, 91) = 0.08425, p = 0.7723, ANOVA; Interaction: F(2, 91) = 2.379, p = 0.0984, ANOVA)* (Figure 2.5d). Altogether, these results suggest a role for nucleus accumbal oxidative stress in the development of nicotine withdrawal-related anxiety.

Microglia-related NADPH oxidase 2 is increased in the nucleus accumbens during nicotine withdrawal.

Among the many molecular mechanisms of intracellular ROS generation (Orient et al 2007), the NADPH oxidase (Nox) system is a major source of intracellular ROS production in the brain (Guilarte et al 2016, Rastogi et al 2016). Therefore, to

evaluate whether this system is the molecular source of WD-induced ROS, we examined the nucleus accumbens for changes in the primary Nox isoforms expressed in the brain. Quantitative PCR analysis of Nox1 *(Treatment effect: F(2, 91) = 0.7784, p = 0.4622, ANOVA; Injection effect: F(1, 91) = 0.7397, p = 0.3920, ANOVA; Interaction: F(2, 91) = 0.4887, p = 0.6150, ANOVA)* and Nox4 *(Treatment effect: F(2, 92) = 0.1001, p = 0.9049, ANOVA; Injection effect: F(1, 92) = 0.01189, p = 0.7310, ANOVA; Interaction: F(2, 92) = 1.521, p = 0.2240, ANOVA)* in the nucleus accumbens showed no significant differences between treatment groups. However, qPCR analyses of Nox2, which is primarily expressed in the microglia (Zhang et al 2016), showed significant treatment and interactive *effects (Treatment effect: F(2, 87) = 9.726, p = 0.0002, ANOVA; Injection effect: F(1, 87) = 3.563, p = 0.0624, ANOVA; Interaction: F(2, 87) = 3.731, p = 0.0279, ANOVA)*. Post-hoc analyses showed that Nox2 mRNA expression was significantly increased in the nucleus accumbens of vehicle-treated nicotine withdrawal mice compared to their saline controls *(p = 0.0006)*, as well as their nicotine and NAC-treated equivalents *(p = 0.0002; p = 0.0221, respectively)* (Figure 2.6a, i - iii). Of note, no significant differences in Nox2 mRNA expression were observed in the caudate putamen *(Treatment effect: F(2, 86) = 0.5177, p = 0.5977, ANOVA; Injection effect: F(1, 86) = 0.1992, p = 0.6565, ANOVA; Interaction: F(2, 86) = 1.142, p = 0.3238, ANOVA)* (Figure 2.6b). Further analyses investigating Nox2 protein show there was a main effect of nicotine withdrawal *(F(2, 79) = 5.405, p = 0.0063, ANOVA)*, but no main effect of NAC injection *(F(1, 79) = 0.01378, p = 0.9068, ANOVA)* or an interaction effect *(F(2, 79) = 0.5078, p = 0.6038, ANOVA)*. Post-hoc analyses demonstrated

that while vehicle-treated nicotine withdrawal mice showed increased Nox2 protein expression in the nucleus accumbens compared to their saline controls *(p = 0.0138)*, Nox2 levels in the nucleus accumbens of NAC-treated nicotine withdrawal mice was not significantly different from the levels in the vehicle-treated nicotine mice and their saline controls *(p = 0.9000; p = 0.1070, respectively)* (Figure 2.6c). Altogether, these data support that increased nucleus accumbal Nox2 during nicotine withdrawal contributes significantly to ROS production underlying nicotine withdrawal-related anxiety. Given that previous studies investigating Nox expression in brain cell-types induced Nox with lipopolysaccharide or examined Nox in pathological states (Nayernia et al 2014), we evaluated the enrichment of Nox isoforms at baseline in both neuronal and glial cell-types. We utilized magnetic activated cell sorting (MACS) for isolation and purification of cell-types in nucleus accumbens tissue. The purified cells were validated and investigated for Nox expression using qPCR. Our validation of microglia showed that $CD11b^+$ *(F = 344.1, p < 0.0001, ANOVA; Total Homogenate versus $CD11b^+$ microglia: p < 0.0001, Post-hoc analysis)*, Tmem119 *(F = 120.2, p < 0.0001, ANOVA; Total Homogenate versus $CD11b^+$ microglia: p < 0.0001, Post-hoc analysis)*, and P2ry12 *(F = 75.70, p < 0.0001, ANOVA; Total Homogenate versus $CD11b^+$ microglia: p < 0.0001, Post-hoc analysis)* were highly enriched in $CD11b^+$ microglia compared to total homogenate; however, there was no significant difference in expression of these microglia markers in total homogenate compared to ACSA II astrocytes, liver, neurons and oligodendrocytes (Figure 2.7a, i - iii). While Nox1 *(F = 6.452, p = 0.0032, ANOVA; Total Homogenate versus Liver: p = 0.0034, Post-*

hoc analysis) and Nox4 *(F = 10.31, p = 0.0006, ANOVA; Total Homogenate versus Liver: p = 0.0021, Post-hoc analysis)* mRNA analyses showed significant enrichment in the liver compared to total homogenate, there were no significant differences between total homogenate and the evaluated brain cell-types (Figure 2.7b, i and ii). In contrast, Nox2 mRNA is significantly enriched in both microglia *(F = 9.995, p = 0.0002, ANOVA; Total Homogenate versus CD11b^{+} microglia: p = 0.0005, Post-hoc analysis)* and liver *(F = 9.995, p = 0.0002, ANOVA; Total Homogenate versus Liver: p < 0.0305, Post-hoc analysis)* compared to total homogenate, which is not significantly different from ACSA II astrocytes, neurons and oligodendrocytes (Figure 2.7b, iii). Altogether, these data suggest that microglia-related Nox2 significantly contributes to excessive nucleus accumbal ROS generation and associated anxiety-like behavior during nicotine withdrawal.

Microglia depletion blocks increases in nicotine withdrawal-induced NADPH oxidase 2 and reactive oxygen species in the nucleus accumbens and attenuates nicotine withdrawal-related anxiety

Microglia are actively involved in the brain's functional organization (Perry et al 2010, Salter & Stevens 2017), which can be altered by chronic drug use or withdrawal. Our studies have demonstrated that withdrawal from chronic nicotine use, but not chronic nicotine treatment, elicits microglial morphological changes accompanied with pro-inflammatory signals in the nucleus accumbens (Figure 2.1, b - e). Therefore, to understand the contribution of this microglial phenotype in the development of withdrawal-related anxiety, we pharmacologically knocked down

microglia in saline and nicotine withdrawal animals using PLX5622, which is a colony stimulating factor-1 receptor (CSF1R) inhibitor. Both saline and nicotine withdrawal animals were fed either control- or PLX5622-chow 7 days after receiving chronic saline or nicotine treatment via osmotic minipump implantation. Withdrawal from chronic saline or nicotine lasted 48 h. OF and MB test were conducted at 24-h and 48-h withdrawal time points respectively (Figure 2.8a). Our evaluation of microglia density in the nucleus accumbens showed a significant main effect of PLX5622 chow and an interaction effect *(Treatment effect: $F(1, 17) = 0.02218$, $p = 0.8834$, ANOVA; Chow effect: $F(1, 17) = 54.39$, $p < 0.0001$, ANOVA; Interaction: $F(1, 17) = 4.705$, $p = 0.0445$, ANOVA).* Post-hoc analyses showed significant decrease in $Iba1^+$ cells / mm^2 *(Saline Control-chow versus Saline PLX5622-chow: $p < 0.0001$; Nicotine withdrawal Control-chow versus Nicotine withdrawal PLX5622-chow: $p = 0.0107$)* in the nucleus accumbens of the PLX5622-treated animals compared to their controls (Figure 2.8b, i and ii). Further, we evaluated microglia depletion in the nucleus accumbens using well-validated microglia markers. Both Tmem119 *(Treatment effect: $F(1, 34) = 0.06459$, $p = 0.8009$, ANOVA; Chow effect: $F(1, 34) = 917.4$, $p < 0.0001$, ANOVA; Interaction: $F(1, 34) = 1.632$, $p = 0.2101$, ANOVA)* and P2ry12 *(Treatment effect: $F(1, 34) = 0.03939$, $p = 0.8439$, ANOVA; Chow effect: $F(1, 34) = 461.5$, $p < 0.0001$, ANOVA; Interaction: $F(1, 34) = 0.2781$, $p = 0.6014$, ANOVA)* mRNA only showed significant main effect of PLX5622 chow. Similar to observations with $Iba1^+$ cells / mm^2 quantitation, our post-hoc analyses revealed significant reduction in Tmem119 *(Saline Control-chow versus Saline PLX5622-chow: $p < 0.0001$; Nicotine*

withdrawal Control-chow versus Nicotine withdrawal PLX5622-chow: p <0.0001) and P2ry12 *(Saline Control-chow versus Saline PLX5622-chow: p <0.0001; Nicotine withdrawal Control-chow versus Nicotine withdrawal PLX5622-chow: p <0.0001)* mRNA expression in PLX5622-treated animals compared to their controls (Figure 2.8c, i - ii). However, given that CSF1R are also expressed on macrophages, we examined whether there could be involvement of infiltrating macrophages in our study by comparing the expression profile of Tmem119 and P2ry12 to C-C-chemokine receptor 2 (Ccr2), which has been previously described by many studies as a critical element for trafficking and assembly of myeloid cells in the brain (Mizutani et al 2012, Morganti et al 2015, Prinz & Priller 2010, Saederup et al 2010). In the nucleus accumbens, our data showed an extremely low Ccr2 expression compared to Tmem119 and P2ry12 in all treatment groups. In addition, CSF1R inhibition did not reduce $Ccr2^{+}$ macrophages compared to controls in the nucleus accumbens (Figure 2.8d). Next, we examined the impact of microglia depletion on Nox2 expression in the nucleus accumbens during nicotine withdrawal. Similar to our validation of microglia depletion with microglia markers, our Nox2 qPCR analyses showed a significant chow effect *(Treatment effect: F(1, 32) = 4.077, p = 0.0519, ANOVA; Chow effect: F(1, 32) = 20.10, p < 0.0001, ANOVA; Interaction: F(1, 32) = 3.29, p = 0.0791, ANOVA).* Post-hoc analyses showed that Nox2 mRNA expression was significantly increased in the nucleus accumbens of control-chow nicotine withdrawal mice compared to their saline controls *(p = 0.0417)* and PLX5622-chow equivalents *(p = 0.0006)* (Figure 2.9a). Furthermore, we evaluated the effect of microglia knockdown on nicotine

withdrawal-induced ROS in the nucleus accumbens. We found a significant interactive effect between treatment and chow *(Treatment effect: F(1, 31) = 1.661, p = 0.2070, ANOVA; Chow effect: F(1, 31) = 2.371, p = 0.1337, ANOVA; Interaction: F(1, 31) = 4.447, p = 0.0431, ANOVA).* Similar to Nox2 mRNA evaluation in these animals, our post-hoc analyses showed an increase in carbonylated protein in the nucleus accumbens of control-chow nicotine withdrawal mice compared to their saline controls (p = 0.0412) and PLX5622-chow counterparts (p = 0.0270) (Figure 2.9b, i and ii). Finally, we assessed the behavioral impact of microglia depletion during nicotine withdrawal. For MB test, there was a significant main effect of nicotine withdrawal *(Treatment effect: F(1, 35) = 4.637, p = 0.0383, ANOVA; Chow effect: F(1, 35) = 1.733, p = 0.1966, ANOVA; Interaction: F(1, 35) = 1.937, p = 0.1728, ANOVA)*. While our post-hoc analyses showed an increase in the amount of marbles buried by the control-chow nicotine withdrawal mice compared to their saline controls (q = 0.0187), there was no observable difference between the PLX5622-chow nicotine withdrawal mice and their saline equivalents (q = 0.5630) (Figure 2.9c). Our OF analyses demonstrated a significant main effects of nicotine withdrawal and PLX5622 chow *(Treatment effect: F(1, 35) = 19.18, p = 0.0001, ANOVA; Chow effect: F(1, 35) = 5.736, p = 0.0221, ANOVA; Interaction: F(1, 35) = 0.08795, p = 0.7685, ANOVA).* From our post-hoc analyses, we found that control-chow nicotine withdrawal mice spent less time in the center of the arena compared to their PLX5622-chow counterparts (q = 0.0031) and saline controls (q = 0.0487) (Figure 2.9, d and e). There were no observed differences in distance moved between animals from all

treatment groups (Figure 2.9f). Overall, these data show that microglia depletion reduced aberrant nucleus accumbal oxidative signaling and associated anxiogenic behaviors.

2.5 DISCUSSION

Altered microglial signaling and associated neuroinflammation are well known key molecular events in the onset and progression of several neurodegenerative diseases (Chen et al 2016, Cunningham 2013, Perry et al 2010); however, their role in nicotine dependence has not been previously investigated. We show that chronic nicotine and withdrawal trigger microglial morphological changes with dissimilar activation phenotypes in the nucleus accumbens, and that the microglial activation phenotype during nicotine withdrawal is of a pro-inflammatory pattern. Further, we report elevated ROS levels in the nucleus accumbens only during nicotine withdrawal and show evidence that Nox2, which is highly enriched in microglia, is the major ROS-producing machinery. However, in contrast to our findings in the nucleus accumbens, we show that both chronic nicotine and withdrawal trigger none of these effects in the caudate putamen. Using a well-described antioxidant, we reveal a role for nucleus accumbal oxidative stress in the development of nicotine withdrawal-related anxiety. More directly, after depleting microglia to evaluate their role in connection to oxidative stress signals in the nucleus accumbens during nicotine withdrawal, we show reduced Nox2 mRNA and ROS in the nucleus accumbens, as well as associated nicotine withdrawal-related anxiety. Together, our study suggests that unlike other drugs of

abuse such as cocaine, which directly elicits a microglial activation phenotype associated with TNFα increase in the nucleus accumbens (Lewitus et al 2016a), nicotine exposure results in unchanged nucleus accumbal levels of TNFα regardless of microglial activation; however, acute withdrawal from nicotine provokes microglial activation as well as increased TNFα levels in the nucleus accumbens. Lastly, our data provide the first evidence that altered microglia morphology and function significantly contribute to the development of anxiety-like behavior during nicotine withdrawal.

Microglial Activation Phenotypes during Chronic Nicotine and Withdrawal in the Striatum.

Microglia are central players in an increasing number of brain disorders (Salter & Stevens 2017), and understanding their responsivity and role in nicotine dependence becomes increasingly urgent. In our model, both chronic nicotine and withdrawal induce remodeling of the highly adaptable resting microglia in the nucleus accumbens, but not in the caudate putamen, suggesting that microglial responsivity to drug cues may be shaped by the specialized role of their local CNS environment. For example, a recent study examining microglia transcriptome across the basal ganglia reported regional heterogeneity of resident microglia, and indicated local cues as a critical mediator of microglia phenotype and their diversity (De Biase et al 2017). In addition, this study also showed that genes associated with oxidative signaling and ROS homeostasis are among the top 10 abundant genes in nucleus accumbal microglia, but not microglia from other parts of the

basal ganglia (De Biase et al 2017). This is consistent with our findings that show disruption in ROS homeostasis in the nucleus accumbens, but not the caudate putamen, during nicotine withdrawal. Another important finding is the dissimilar expression of pro-inflammatory cytokines (TNFα, IL1β) and ROS in the nucleus accumbens during chronic nicotine and withdrawal. This suggests distinct pro-inflammatory profile, which may be partly driven by the diverse phenotype of activated microglia in both treatment conditions. In line with clinical studies that have shown nicotine's neuroprotective property in certain neurodegenerative diseases (Newhouse et al 2012, Villafane et al 2007), our findings show an absence of TNFα and IL1β mRNA induction during chronic nicotine treatment, suggesting a muted pro-inflammatory response in the striatum. However, the molecular attributes of activated microglia during withdrawal from chronic nicotine are characteristic of the pro-inflammatory phenotype. Of note, the few studies available on the role of microglia in drug dependence reported that microglial activation and related pro-inflammatory effects were directly elicited by the drugs of abuse examined, namely cocaine (Lewitus et al 2016a) and morphine (Hutchinson et al 2009, Schwarz & Bilbo 2013). Similar to our findings, microglial activation and elevated levels of pro-inflammatory signals in those studies were limited to the nucleus accumbens, but our findings contrast with those earlier studies in that activation of nucleus accumbal pro-inflammatory signals occur only during withdrawal from nicotine and not due to exposure to nicotine itself. Microglia are primarily involved in synaptic function and plasticity; however, their alteration within the nucleus accumbens, which is a critical brain circuit for addictive

processes, can enhance the development of aberrant synaptic connections and plasticity underlying nucleus accumbal adaptive changes in drug dependency (Grueter, Rothwell, & Malenka, 2012). Together, it is becoming clear that the synaptic cues specific to the nucleus accumbens during chronic nicotine and withdrawal influence its resident microglia signature.

Microglial NADPH Oxidase 2 Regulation in the Nucleus Accumbens during Nicotine Withdrawal

NADPH oxidase (Nox) systems are primarily implicated in disease-related aberrant ROS production (Panday et al 2015). Among the primary Nox isoforms in the brain – Nox1, Nox2, and Nox4 (Ma et al 2017), our findings implicate Nox2 as the primary source of excessive ROS in the nucleus accumbens during nicotine withdrawal. Many studies have reported that Nox2 is highly enriched in microglia compared to other brain cell-types (Guilarte et al 2016, Nayernia et al 2014, Zhang et al 2014, Zhang et al 2016) and a previous study also provided additional evidence showing that lipopolysaccharide (LPS) stimulation of BV2 microglial cell lines resulted in Nox2-dependent ROS production (Huo et al 2011). In our study, we find that among the brain cell-types, Nox2 is primarily expressed only in microglia at baseline. Overall, this study suggests that microglia-related Nox2 contributes significantly to aberrant ROS levels in the nucleus accumbens during nicotine withdrawal

N-acetylcysteine Effects and Anxiety-like Behavior during Nicotine Withdrawal.

Our behavioral findings provide a link between oxidative stress and anxiety-like behavior during nicotine withdrawal. NAC treatment prior to nicotine withdrawal precluded Nox2 induction and reduced ROS levels in the nucleus accumbens, a brain region well described for its critical role in anxiety (Kim et al 2008, Levita et al 2012, van der Kooij et al 2018). Together, NAC treatment results in attenuation of anxiety-like behavior during nicotine withdrawal. While this interpretation relies on NAC's well-documented antioxidant effects, other mechanisms describing NAC's effects in nicotine dependence phenotypes have been previously described (Gipson et al 2013, Knackstedt et al 2009). For example, Knackstedt et al (2009) demonstrated that NAC treatment in smokers reduced the number of cigarettes smoked by study participants. The authors attributed this effect in smokers to NAC's modulation of the astrocytic cystine-glutamate exchanger (xCT), which was initially shown to be compromised in their preclinical studies investigating nicotine seeking in rats (Knackstedt et al 2009). Of note, in their rodent experiment, while xCT was downregulated in rats that self-administered nicotine, the xCT was unchanged in animals that received nicotine via osmotic minipump, suggesting a motivational rather than a pharmacological basis for changes in xCT during nicotine exposure. Given that our findings are from mice treated with chronic nicotine via osmotic minipump, our results are unlikely to be due to NAC's modulatory effects on the xCT, but more likely due to its extensively described antioxidant activity (Aruoma et al 1989, Dekhuijzen 2004, Sun 2010). Furthermore,

while our studies demonstrated that NAC treatment effectively attenuated microglia-related ROS and the associated anxiety-like phenotypes, we also show that NAC is ineffective in altering the microglial activation phenotype during nicotine withdrawal. Given this limitation, combining NAC with therapeutics that can inhibit microglial reprogramming to an activation phenotype, such as minocycline (Suzuki et al 2010a, Zhu et al 2014), or those that can reverse the activation phenotype may offer more effective treatment for smoking cessation.

Microglia Depletion and Anxiety-like Behavior during Nicotine Withdrawal

Several studies have implicated microglial function in anxiety-related disorders (Li et al 2014, Stein et al 2017, Wang et al 2018); however, the role of microglia in nicotine withdrawal-related anxiety is unknown. Our study shows that depletion of microglia during nicotine withdrawal reduced Nox2 and ROS levels in the nucleus accumbens, and consequently attenuated nicotine withdrawal-related anxiety. These findings provide a strong link between microglia function and nicotine withdrawal-related anxiety, and further reinforce the contribution of microglial Nox2 and associated aberrant ROS production in the nucleus accumbens to the development of anxiety-like behavioral phenotype during nicotine withdrawal.

Perspectives on Future Smoking Cessation Pharmacotherapies

Currently, there are three FDA-approved pharmacotherapies for smoking cessation: varenicline (a nicotinic selective partial agonist), bupropion (a norepinephrine-dopamine reuptake inhibitor), and nicotine replacement therapy

(NRT, as patch, gum, etc.). While each of these therapeutics have quantifiable success as smoking cessation aids, the best in class medication, varenicline, results in only 40% abstinence success at 12 weeks and less than 20% at one year post-quit (Gonzales et al 2006). This underscores the urgent need for new drug targets in the development of new smoking cessation aids. We outline a series of novel findings implicating neuroinflammatory responses during nicotine withdrawal, arising not from the combustible contents of cigarettes, but from nicotine withdrawal itself. This suggests that withdrawal from two of the current smoking cessation aids, varenicline and NRT, may also alter neuroinflammatory responses in the mesolimbic circuitry. Further, with e-cigarette use on the rise particularly in adolescents and young adults, our findings lend mechanistic insight into why vaping during adolescence promotes progression to combustible cigarettes as adults (Leventhal et al 2015, Primack et al 2015). Long-term, further investigation into modulators of microglial function during nicotine withdrawal represents an untapped therapeutic avenue for smoking cessation.

2.6 FIGURES

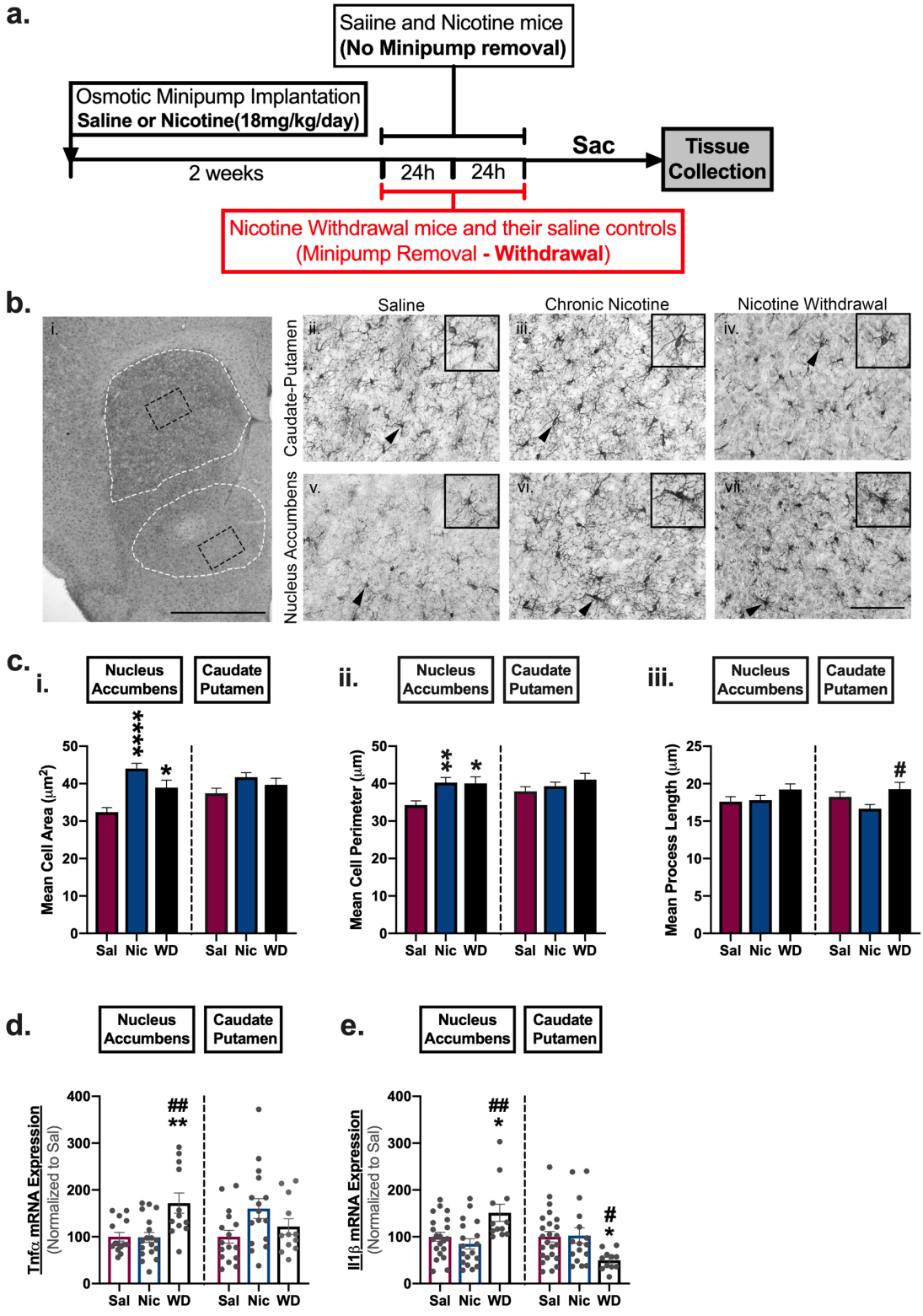

Figure 2.1: Chronic nicotine and withdrawal induce different microglial activation phenotypes in the nucleus accumbens. a. Experimental design. **b**. Representative images of IBA1-positive microglia in the caudate putamen and nucleus accumbens of saline (Sal), nicotine (Nic), and nicotine withdrawal (WD) mice. i) White dotted traces delineate the caudate-putamen (dorsal) and nucleus accumbens (ventral); black dotted traces indicate area where image iv – ix were taken. Scale bar = 1mm. ii) resting microglia, and iii) activated microglia. Scale bar = 20μm. Caudate-putamen of iv) Sal mice, v) Nic mice, and vi) WD mice. Nucleus accumbens of vii) Sal mice, viii) Nic mice, and ix) WD mice. Scale bar = 100μm. **c**. Quantitation of IBA1-positive microglia morphology in the caudate putamen and nucleus accumbens. i) Cell area, ii) Cell Perimeter, iii) Process length. **d**. Bar charts showing TNFα mRNA expression in the nucleus accumbens and caudate-putamen of Sal, Nic, and WD mice. **e**. Bar charts showing IL1β mRNA expression in the nucleus accumbens and caudate-putamen of Sal, Nic, and WD mice. (Compared to Sal – *P<0.05, **P<0.01, ****P<0.0001; Compared to Nic – $^{\#}$P<0.05, $^{\#\#}$P<0.01; **c**: n = minimum of 116 cells were quantified from 4-8 animals per treatment group; **d, e**: n=12-24 per treatment group).

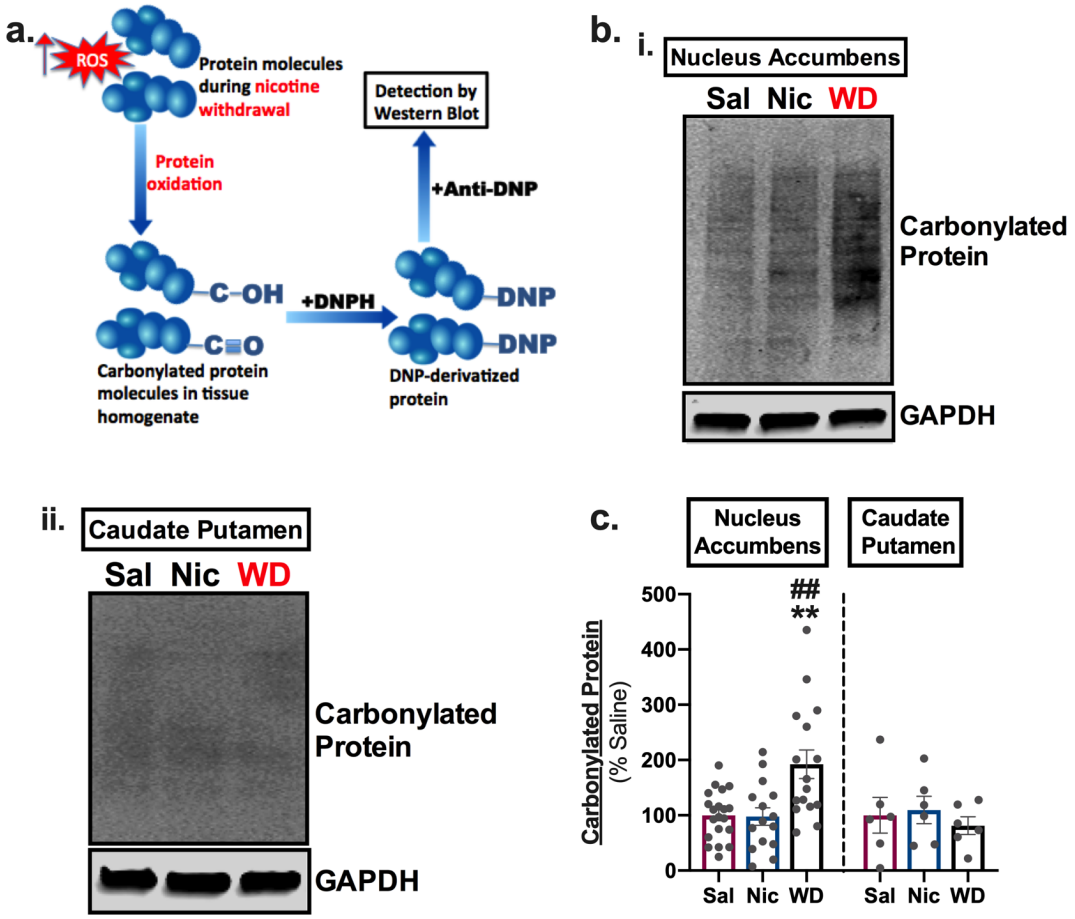

Figure 2.2: Nicotine withdrawal induces reactive oxygen species in the nucleus accumbens. a. Schematic diagram showing mechanism of ROS detection by protein carbonylation assay (Protein and arrow icons were downloaded from Reactome (Sidiropoulos et al., 2017)). **b**. Representative immunoblot showing the presence of carbonylated protein (reactive oxygen species indicator) in Sal, Nic, and WD mice i) nucleus accumbens, ii) caudate putamen. **c**. Quantitation of 2b. (Compared to Sal – **P<0.01; Compared to Nic – $^{\#\#}$P<0.01; **c:** n=6-19 per treatment group).

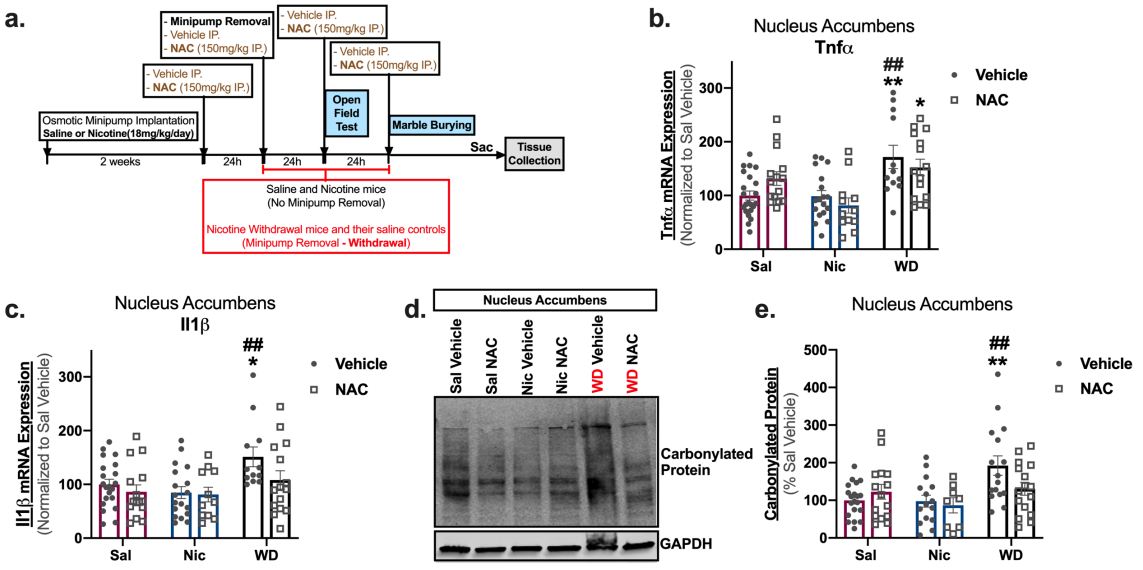

Figure 2.3: N-Acetylcysteine attenuates nicotine withdrawal-induced reactive oxygen species in the nucleus accumbens. a. Experimental design. **b**. Bar chart showing nucleus accumbal mRNA expression of TNFα in vehicle- and NAC-treated Sal, Nic and WD mice **c**. Bar chart showing nucleus accumbal mRNA expression of IL1β in vehicle- and NAC-treated Sal, Nic and WD mice **d**. Representative immunoblot showing the expression of carbonylated proteins in the nucleus accumbens of vehicle- and NAC-treated Sal, Nic and WD mice **e**. Quantitation of 3d. (Compared to Sal-Vehicle – *P<0.05, **P<0.01; Compared to Nic-Vehicle – $^{\#\#}$P<0.01; **b, c, and e**: n=12-23 per treatment group).

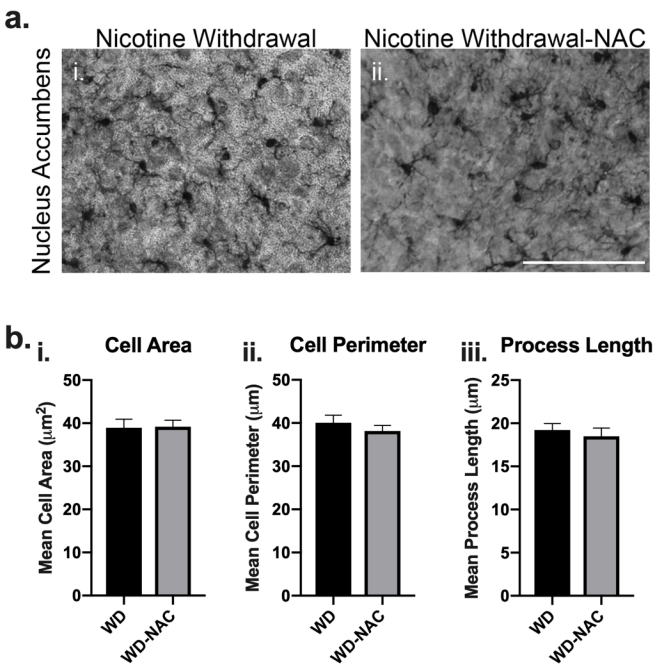

Figure 2.4: Nicotine withdrawal-induced microglia activation is unaltered by n-acetylcysteine treatment. a. Representative images of IBA-1 positive microglia in the nucleus accumbens of i) vehicle-treated, and ii) NAC-treated nicotine withdrawal mice. Scale bar = 100μm. **b.** Quantitation of 4a. i) Cell area, ii) Cell Perimeter, iii) Process length**.** **(b**: n = minimum of 87 cells were quantified from 4-5 animals per treatment group).

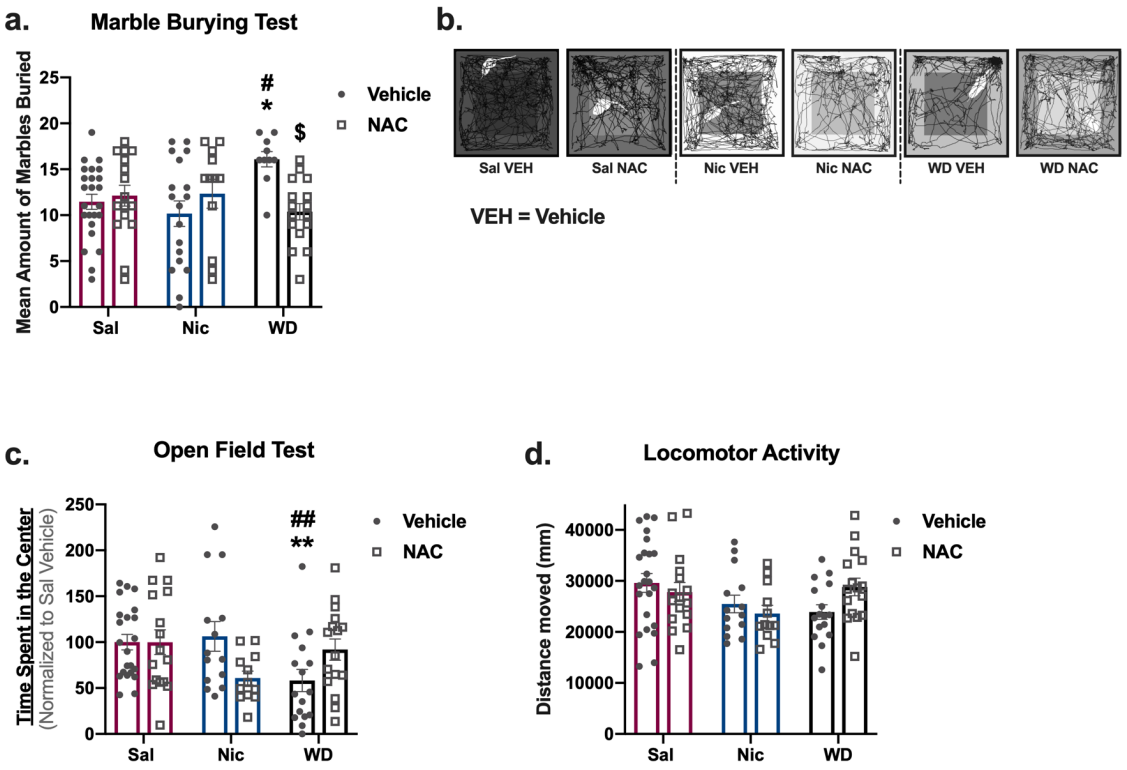

Figure 2.5: N-acetylcysteine treatment is anxiolytic during nicotine withdrawal. a. Marble-burying test: Bar graph showing the mean amount of marbles buried by vehicle- and NAC-treated Sal, Nic and WD mice. **b**. Representative open field traces of vehicle- and NAC-treated Sal, Nic and WD mice. **c**. Open field test: Bar chart showing percent time spent in the center of the open field arena by vehicle- and NAC-treated Sal, Nic and WD mice. **d**. Locomotor activity: Bar chart showing average distance moved in the open field arena by vehicle- and NAC-treated Sal, Nic and WD mice. (Compared to Sal-Vehicle – *q<0.05, **q<0.01; Compared to Nic-Vehicle – $^{\#}$q<0.05, $^{\#\#}$q<0.01; Compared to WD-Vehicle $^{\$}$q<0.05; **a, c, and d**: n=9-23 per treatment group**)**

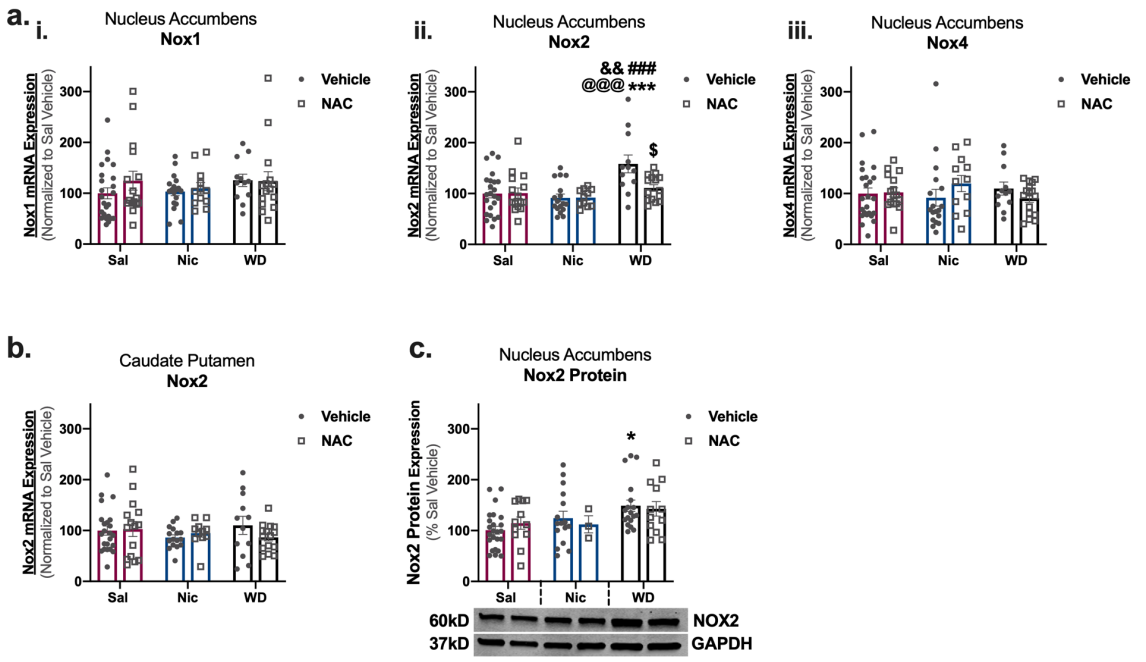

Figure 2.6: Nicotine withdrawal increases Nox2 expression in the nucleus accumbens. a. Bar graph showing quantitative PCR analysis of NOX isoforms (primarily expressed in the brain) in the nucleus accumbens of vehicle- and NAC-treated Sal, Nic and WD mice. i) Nox1, ii) Nox2, and iii) Nox4. **b**. Bar graph showing quantitative PCR analysis of Nox2 mRNA expression in the caudate-putamen of vehicle- and NAC-treated Sal, Nic and WD mice. **c**. Western blot image and quantification of nucleus accumbal Nox2 protein expression in vehicle- and NAC-treated Sal, Nic and WD mice. (Compared to Sal-Vehicle – *P<0.05, ***P<0.001; Compared to Sal-NAC – $^{\&\&}$P<0.01; Compared to Nic-Vehicle – $^{\#\#\#}$P<0.001; Compared to Nic-NAC – $^{@@@}$P<0.001; Compared to WD-Vehicle – $^{\$}$P<0.05).

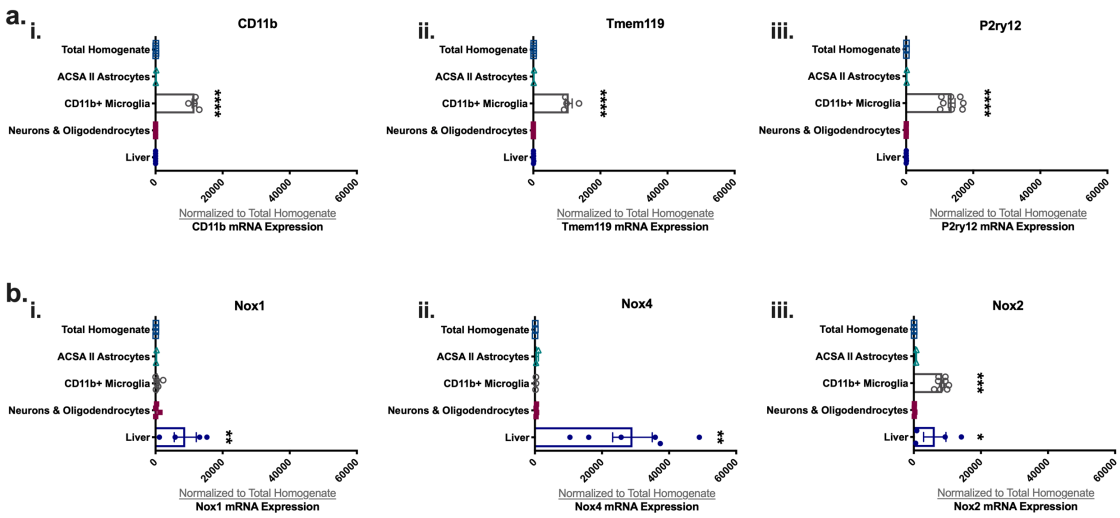

Figure 2.7: Nox2 is expressed in microglia. a. Bar graph showing quantitative PCR analysis of microglia markers in the liver, brain cell-types and tissue (Total homogenate). i) CD11b, ii) Tmem119, and iii) P2ry12. **b**. Bar graph showing quantitative PCR analysis of Nox isoforms in the liver, brain cell-types and tissue. i) Nox1, ii) Nox4, and iii) Nox2. (Compared to Total homogenate – *P<0.05, **P<0.01, ***P<0.001, ****P<0.0001; **a, b**: n=2-9 per treatment group).

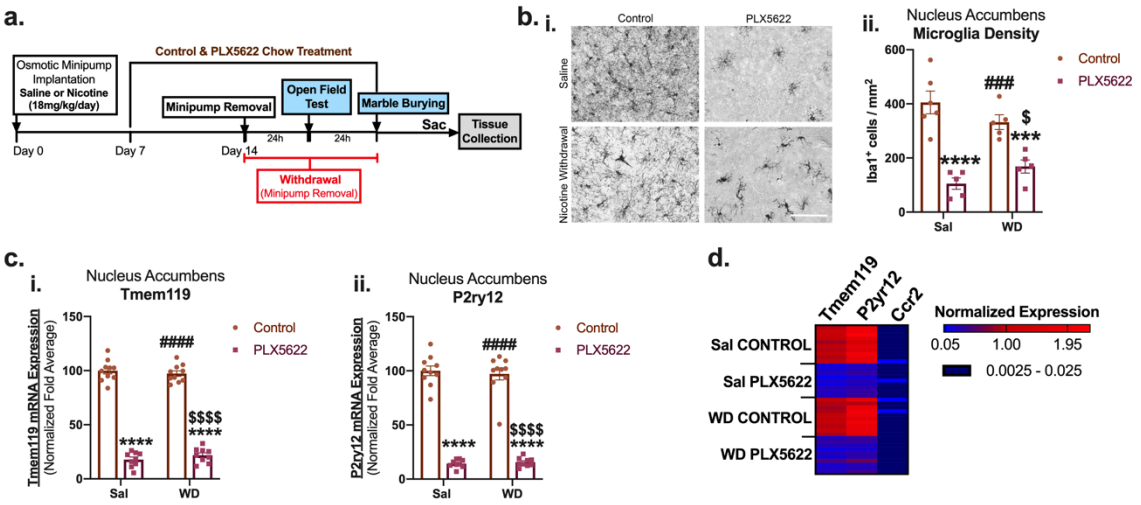

Figure 2.8: Inhibition of CSF1 receptor (CSF1R) depletes microglia in the nucleus accumbens. **a**. Experimental design. **b**. i) Representative images of IBA1-positive microglia in the nucleus accumbens of Control- and PLX5622-chow Sal, as well as their WD equivalents. ii) Quantitation of 8bi. **c**. Bar graph showing quantitative PCR analysis of microglia markers in the nucleus accumbens of Control- and PLX5622-chow Sal, as well as their WD equivalents. i) Tmem119, and ii) P2ry12. **d**. Heatmap showing normalized expression profile of Tmem119, P2ry12, and Ccr2 in the nucleus accumbens of Control- and PLX5622-chow Sal, as well as their WD equivalents. (Compared to Sal-Control – ***P<0.001, ****P<0.0001; Compared to Sal-PLX5622 – $^{###}$P<0.001, $^{####}$P<0.0001; Compared to WD-Control – $^{\$}$P<0.05, $^{\$\$\$\$}$P<0.0001; **b**ii: n=5 per treatment group; **c, d**: n=10 per treatment group).

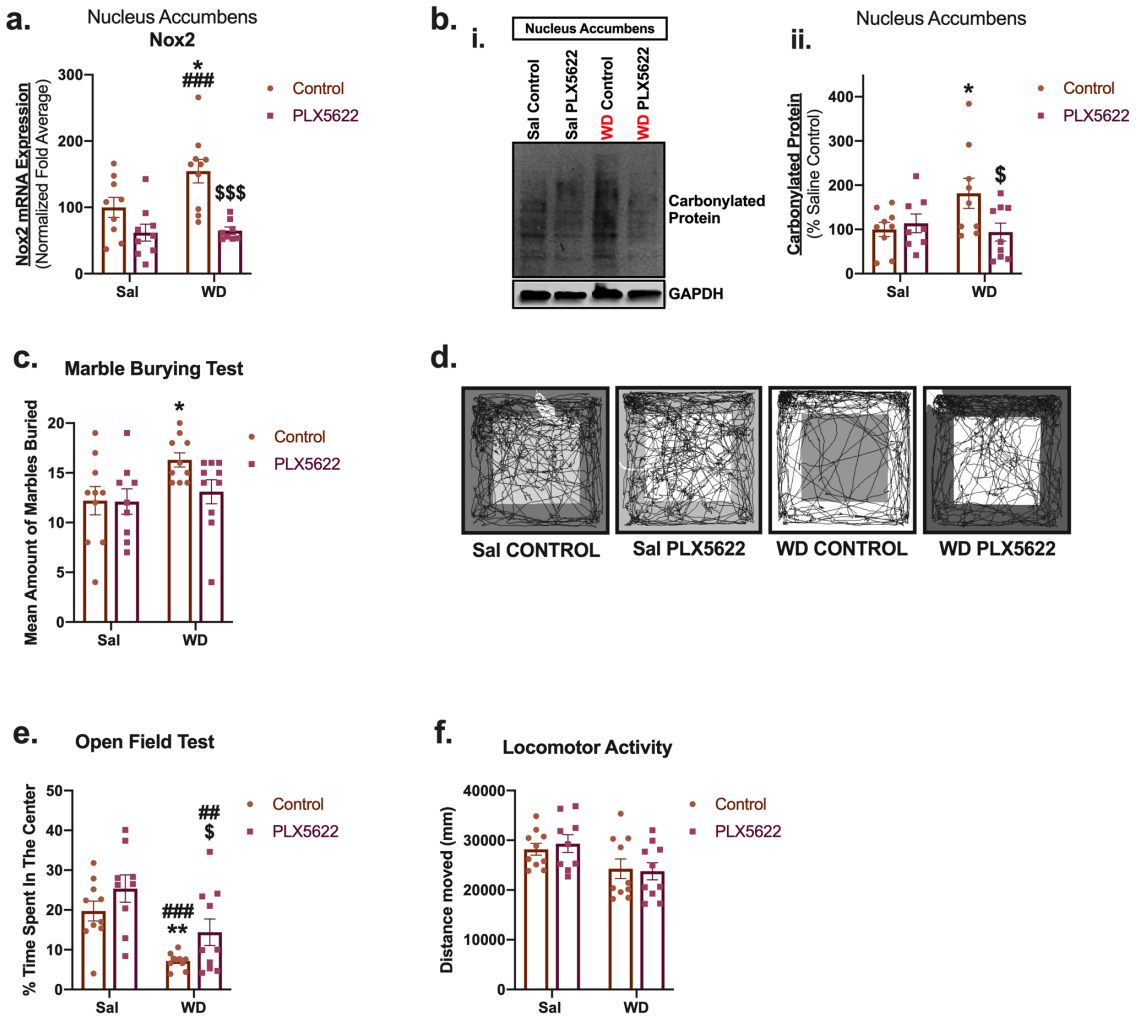

Figure 2.9: Microglia depletion attenuates nicotine withdrawal-related anxiety. a. Bar graph showing quantitative PCR analysis of Nox2 in the nucleus accumbens of Control- and PLX5622-chow Sal, as well as their WD equivalents. **b**. i) Representative immunoblot showing the expression of carbonylated proteins in the nucleus accumbens of Control- and PLX5622-chow Sal, as well as their WD equivalents. ii) Quantitation of 9bi. **c**. Marble-burying test: Bar graph showing the mean amount of marbles buried by Control- and PLX5622-chow Sal, as well as their WD equivalents. **d**. Representative open field traces of Control- and PLX5622-chow Sal, as well as their WD equivalents. **e**. Open field test: Bar chart showing percent time spent in the center of the open field arena by Control- and PLX5622-chow Sal, as well as their WD equivalents. **f**. Locomotor activity: Bar chart showing average distance moved in the open field arena by Control- and PLX5622-chow Sal, as well as their WD equivalents. (Compared to Sal-Control – *P<0.05, **P<0.01; Compared to Sal-PLX5622 – $^{\#\#}$P<0.01, $^{\#\#\#}$P<0.001; Compared to WD-Control – $^{\$}$P<0.05, $^{\$\$\$}$P<0.001; **a**, **b**ii, **c, e, and f**: n=9-10 per treatment group)

CHAPTER 3

TRANSCRIPTIONAL REMODELING IN RESPONSE TO CHRONIC NICOTINE AND WITHDRAWAL IN ASTROCYTES AND MICROGLIA[1]

[1] Adewale Adeluyi and Jill R. Turner. In preparation.

3.1 ABSTRACT

Transcriptional programs are genomic regulatory code instructing the formation, maintenance, and functions of diverse brain cell types and distinct brain structures. Tissue- and cell type-specific evaluation of whole transcriptome can advance current understanding of the role of genes in CNS health and disorders such as nicotine dependence. Here, we performed whole transcriptome sequencing on nucleus accumbens microglia, astrocytes, and its whole tissue at different withdrawal timepoints (24 h and 48 h). We show temporally-dependent activation of distinct gene programs in the nucleus accumbens during chronic nicotine and withdrawal. Differential gene expression analysis suggests that chronic nicotine treatment activates subset of genes that are neuroprotective while withdrawal from nicotine provokes neuroinflammation and oxidative stress- related transcriptional programs in the nucleus accumbens. Our cell type-specific RNA seq data support our tissue-level observation. Gene programs associated with neuroinflammation were suppressed in microglia following nicotine treatment while nicotine withdrawal triggers microglial pro-inflammatory networks. Further, our transcriptome data suggest astrocytes assume a reactive phenotype during nicotine withdrawal. Finally, we find subset of genes that are enriched in nucleus accumbens tissue and either of the nucleus accumbens cell types examined during nicotine withdrawal. Taken together, our study provides the first insight into cell type-specific and tissue-level transcriptional remodeling in the nucleus accumbens during chronic nicotine and withdrawal.

3.2 INTRODUCTION

Tobacco addiction impacts an estimated 1.2 billion people globally. While ability to successfully quit smoking remarkably reduces smoking-related deaths and diseases, about 80% of smokers attempting to quit fail (Benowitz 2010) due to the effect of nicotine, which is the addictive component of tobacco. Smoking cessation often leads to nicotine withdrawal symptoms, which usually manifest negative behavioral signs a few hours after discontinuation of nicotine use. These behavioral patterns are collections of affective and cognitive manifestations, which are both predictors of smoking relapse (Ashare et al 2014). Chronic exposure to drugs of abuse such as nicotine induces a number of neuroadaptations that result in drug dependence (Koob & Kreek 2007, Turner et al 2014). Such adaptations in neural circuits and associated functions are often required for maintenance of nicotine dependence. While the molecular mechanisms underlying the long-lasting nature of negative behaviors associated with nicotine dependence are not yet completely understood, it is recently becoming clearer that changes in specific gene programs in plastic neural circuits may underlie the development and persistence of these behaviors (Brunzell et al 2003, Nestler 2008, Turner et al 2014).

The nucleus accumbens (NAc) is a heterogeneous structure that plays a central role in the mesolimbic reward pathway. Chronic exposure to many drugs of abuse including nicotine disrupt plasticity in the NAc circuitry, and these NAc-related drug-induced neuroadaptations are known to underlie reward-related behaviors, which markedly contributes to relapse vulnerability in drug dependency.

Besides several frequently-reported neuroadaptive changes in the NAc following chronic nicotine exposure, a few studies have demonstrated transcriptional changes relating to CREB (cAMP-response element-binding protein) and FosB (a Fos family protein) in this neurocircuitry (Brunzell et al 2009, Brunzell et al 2003, Nestler 2008). Alteration of transcription factors such as CREB and FosB is one of the common molecular mechanisms through which nicotine and other drugs of abuse regulate gene expression, which may underlie the persistence of addictive behaviors (Madsen et al 2012). Therefore, evaluation of NAc transcriptomic changes during chronic nicotine and withdrawal may reveal tissue-level bulk gene programs driving nicotine dependency. However, while quantification of tissue-level transcriptome data may be a critical step towards advancing current understanding of nicotine dependence, this level of transcriptomic analyses may lack the actual resolution to better characterize the molecular phenotype associated with addictive disorders. In the complex multicellular NAc structure, there are neuronal and non-neuronal cell types such as astrocytes and microglia, which all together interact to maintain the integrity and adaptation of this neural circuitry (Allen & Barres 2009). Hence, evaluation of transcriptome-wide responses at cell-type specific resolution will provide a better understanding and a less complex insight into NAc-related molecular processes driving nicotine dependency.

In this study, we use RNA sequencing (RNA-seq) to capture temporal gene expression changes in nucleus accumbens tissue during chronic nicotine and withdrawal at different timepoints (24h and 48 h). Further, we explored

transcriptomic changes in the nucleus accumbens at cell type-specific resolution during chronic nicotine and 48 h withdrawal. We uncover multiple dysregulated genes and molecular pathways that are related to nicotine dependence. Our study provides the first direct evidence of transcriptome remodeling in the nucleus accumbens at cell type-specific and tissue-level resolution during chronic nicotine and withdrawal.

3.3 MATERIALS AND METHODS

Animals

Male B6/129SF1 mice were purchased from Jackson Laboratories (Bar Harbor, ME, USA; 8 weeks of age; 20 – 31 g). Mice were housed in groups of four or five, and randomly assigned to treatment conditions. They were maintained on a 12-h light/dark cycle with food and water *ad libitum* in accordance to the University of South Carolina Animal Care and Use Committee. All behavioral testing sessions were conducted between the 0900 and 1300 hours.

Osmotic drug delivery and treatment

(-)-Nicotine tartrate (MP Biomedicals, Solon, OH, USA) was dissolved in sterile 0.9% sodium chloride solution, and then infused subcutaneously via osmotic minipumps (Alzet model 2002; DURECT Corporation, Cupertino, CA, USA) at a dose of 18 mg/kg/day for 15 days. The control group was infused with saline for the same period of time. Chronic treatment with nicotine at this dose yields a plasma level of approximately 0.3μM in mice (reported as nicotine free base

molecular weight), a concentration comparable to that observed in human smokers consuming an average of 17 cigarettes a day (plasma levels between 0.06 - 0.31μM) (Matta et al 2007). Prior to the start of surgery, mice were anesthetized with isoflurane/ oxygen mixture (1-3%), and minipumps were inserted using aseptic techniques. Surgical wounds were closed with 7mm stainless steel wound clips (Reflex, Cellpoint Scientific, Gaithersburg, MD, USA), after which mice were left to recover on the recovery pad before they were returned to their individual cages. After 14 days of chronic administration of either saline or nicotine via osmotic minipumps, mice earmarked for withdrawal from chronic nicotine and their assigned saline controls were subjected to spontaneous withdrawal by the removal of their osmotic minipumps using a similar aseptic surgical approach as above. Tissues were collected from mice after 24 h or 48 h withdrawal.

Isolation of nucleus accumbal microglia and astrocytes by magnetic activated cell sorting (MACS)

Nucleus accumbal tissues (10 pooled animals per N) from animals in the 48-h withdrawal experiment were diced with a sterile scalpel into small pieces in a sterile petri dish containing 2ml of cold Hank's buffered saline solution (HBSS, minus Ca^{2+}, Mg^{2+}; Life Technologies Corporation, Grand Island, NY, USA). This suspension was transferred into a 15ml centrifuge tube, and then, spun at 300Xg for 2mins at 4°C. Supernatant was discarded, and tissue was processed into single-cell suspension by enzyme dissociation using Miltenyl's adult brain dissociation kit (Miltenyl Biotec Inc., Auburn, CA, USA) according to the

manufacturer's instructions. Following complete dissociation, cell suspension was applied to pre-wet MACS Smart Strainer (70µm; Miltenyl Biotec Inc., Auburn, CA, USA), and the flow through was processed for microglia labeling with $CD11b^+$ microbeads (Miltenyl Biotec Inc., Auburn, CA, USA). Cells were washed with 2ml 0.5% BSA in PBS buffer and centrifuged at 300Xg for 10mins at 4^oC for removal of any unbounded beads from the pellet. Cell pellet was re-suspended in 500µl 0.5% BSA in PBS buffer, and then applied onto a prepped MACS MS column attached to an OctoMACS magnetic separator (Miltenyl Biotec Inc., Auburn, CA, USA). Flow through containing unlabeled cells was collected first, and $CD11b^+$ microglia were then collected by flushing out the magnetically labeled cells in the column into a microcentrifuge tube following the removal of the column from the magnetic separator. The flow through was immediately processed for astrocyte labeling using anti-ACSA-2 microbead kit (Miltenyl Biotec Inc., Auburn, CA, USA) according to the manufacturer's instructions. In a similar way to the magnetic separation step in $CD11b^+$ microglia isolation, $ACSA\text{-}2^+$ astrocytes were also purified and collected.

RNA extraction and purification

Total RNA was extracted and purified from nucleus accumbal $CD11b^+$ microglia and $ACSA\text{-}2^+$ astrocytes using TRIzol (Invitrogen) and RNeasy Mini Kit (QIAGEN, Valencia, CA) according to manufacturer's instructions. Similarly, RNA was also isolated and purified from nucleus accumbens tissues collected from animals in the 24-h and 48-h withdrawal experiments.

Library preparation

For nucleus accumbal CD11b^{+} microglia and ACSA-2^{+} astrocytes, RNA sequencing libraries were prepared using the NuGEN Ovation RNA Ultra Low Input kit (500pg minimum) (Tecan Genomics Inc., Redwood City, CA) while RNA libraries for 24-h and 48-h withdrawal nucleus accumbens RNA samples were prepared using NEBNext Ultra II RNA Directional RNA Library Prep kit (NEB, Ipswich, MA).

RNA sequencing

Nucleus accumbal CD11b^{+} microglia and ACSA-2^{+} astrocytes libraries were indexed and sequenced as 2X75bp paired-end reads over 4 lanes on an Illumina HiSeq4000. For the 24-h and 48-h withdrawal experiment, nucleus accumbens RNA libraries were indexed and sequenced as 2X75bp paired-end reads using Illumina NextSeq500.

Sequencing data preprocessing analyses

To ensure there were no sequencing errors, demultiplexed fastq files from both Illumina HiSeq4000 and Illumina NextSeq500 were checked for quality using FastQC (v0.11.8). Reads that failed certain quality criteria were trimmed and filtered using BBDuk tool (sourceforge.net/projects/bbmap/) for quality improvement prior to the alignment step. Reads were then aligned to the mouse genome (mm10, downloaded from iGenomes, Illumina) using STAR aligner (Dobin et al 2013). Average input read counts were 53.75 million, 49.72 million, and 43.79

million for CD11b$^+$ microglia, ACSA-2$^+$ astrocytes, and nucleus accumbens tissue samples (24 h and 48 h) respectively. Average percentage of uniquely mapped reads were 74.96%, 73.96%, and 88.15% for CD11b$^+$ microglia, ACSA-2$^+$ astrocytes, and nucleus accumbens tissue samples (24 h and 48 h) respectively. Fragments counts were obtained using featureCounts (Liao et al 2014). Low read counts were filtered prior to differential expression analysis.

Differential expression analyses

DESeq2 (Love et al 2014) was used to assess differential gene expression (DGE) at a false discovery rate (FDR) < 0.2 and 0.25 for nucleus accumbens tissue samples (24 h and 48 h) and cell types (CD11b$^+$ microglia and ACSA-2$^+$ astrocytes), respectively.

Principal component analysis and correlation analysis

Principal component analysis and correlation analysis using hierarchical clustering function were performed to identify outliers in our samples.

Pathway Enrichment Analysis

Enrichr (Kuleshov et al 2016) was used in identifying and testing statistically significant differentially expressed genes for overrepresentation in canonical pathways.

3.4 RESULTS

Experimental Design

Three separate set of experiments were performed with the nucleus accumbens – the 24hWD, 48hWD, and 48hWD cell type-specific (astrocytes and microglia) experiments. Each experiment has three treatment groups – Saline, Nicotine and Withdrawal. The withdrawal mice in the 24hWD study were subjected to 24 h withdrawal while in the 48hWD study, mice undergoing withdrawal from nicotine were subjected to 48 h withdrawal. Nucleus accumbens tissues were utilized for both 24WD and 48hWD studies; however, these tissues were processed for cell sorting (microglia and astrocytes isolation/purification) in the cell type-specific experiment. RNA seq libraries were constructed for each of these experiments, and then sequenced (Figure 3.1a).

Transcriptional alterations in the nucleus accumbens during 24 h and 48 h withdrawal from nicotine

Given that symptoms associated with nicotine withdrawal are usually intense within 24 - 48 h of abstinence (Stoker et al 2008), we examined temporal transcriptional changes in the nucleus accumbens of mice that underwent withdrawal for 24 h or 48 h, in addition to their respective nicotine-treated and saline controls using RNA-seq. For each of these treatment groups, we have 3 - 4 biological replicates. We compare the transcriptome profile of 24hWD (n=3) and 48hWD tissue samples (n=3) using a correlation matrix. Our data show that sample replicates of similar withdrawal timepoints are highly correlated (Spearman ‘s rank correlation, mean r

(24-h withdrawal replicates) = 0.93 ; Spearman 's rank correlation, mean r *(48-h withdrawal replicates)* = 0.84) while replicates across timepoints have low correlations (Spearman 's rank correlation, mean r *(24-h withdrawal replicates vs 48-h withdrawal replicates)* = 0.33) (Figure 3.1b). These data suggest a minimal overlap between differentially expressed genes (DEGs) at 24-h and 48-h withdrawal timepoints. However, while temporal transcriptional changes are expected during withdrawal from nicotine, it is important to note that our different library preparation approaches (Ribosomal depletion for 24hWD experiment; Poly-A enrichment for 48hWD experiment) may have introduced further transcriptome variation between the 24hWD and 48hWD experiments. Next, we analyzed transcriptomic changes between treatment groups by performing pairwise differential gene expression (DGE) analysis (i.e. saline versus nicotine, saline versus withdrawal, and nicotine versus withdrawal). Genes that we statistically determined as differentially expressed are those with varying expression levels between treatment groups at false discovery rate (FDR) less than 0.2. This FDR cutoff was selected a priori since we do not expect large magnitude changes in brain transcriptome during chronic nicotine treatment and withdrawal. In the 24hWD experiment, 207 genes (122 downregulated, 85 upregulated) were differentially expressed between saline and nicotine groups, 1050 DEGs (565 downregulated, 485 upregulated) were revealed between saline and withdrawal groups, and the expression levels of 75 genes (25 downregulated, 50 upregulated) were altered between nicotine and withdrawal groups. However, in the 48hWD experiment, DGE analysis revealed 11 DEGs (3 downregulated, 8 upregulated)

between saline and nicotine groups, 653 DEGs (343 downregulated, 310 upregulated) between saline and withdrawal groups, and 1485 DEGs (549 downregulated, 936 upregulated) between nicotine and withdrawal groups. In order to visualize and identify statistically significant DEGs at our designated cutoff – fold changes ($|log2FC| > 0.5$) and adjusted p-values ($FDR < 0.2$), we generated a color-coded volcano plot for both 24hWD and 48hWD experiments, indicating upregulated genes in red and downregulated genes in blue (Figure 3.1c, i and ii). Further, we constructed a heatmap showing pairwise comparison of statistically significant DEGs between treatment groups. Our 24hWD data show there were no statistically significant DEGs between saline and nicotine; however, 63 (22 downregulated, 41 upregulated) and 34 DEGs (5 downregulated, 29 upregulated) were statistically significant between saline and withdrawal, and nicotine and withdrawal groups, respectively (Figure 3.2a, i and ii.). Similarly, 48hWD pairwise comparison revealed 5 (2 downregulated, 3 upregulated), 359 (200 downregulated, 159 upregulated), 972 (295 downregulated, 677 upregulated) statistically significant between saline and nicotine, saline and withdrawal, and nicotine and withdrawal groups, respectively (Figure 3.2b, i - iii). Pathway enrichment analysis of statistically significant DEGs indicates that genes involved in overrepresented pathways such as cholinergic synapse (Gng4, Gng2, Adcy8), glutamatergic synapse (Gng4, Gng2, Grik1, Adcy8), chemokine signaling (Gng4, Gng2, Adcy8), oxidative stress (Gpx3), glutathione metabolism (Gpx3) and nuclear receptors (Nr2f2, Rxrg) are upregulated during 24 h withdrawal (Figure 3.3a, i and ii). Similarly, in our 48hWD experiment, genes associated with enriched pathways

such as fatty acid beta oxidation (Lpl), adipogenesis (Lpl), Alzheimer's disease (Lpl), cholesterol metabolism (Lpl) and Tnf-alpha Nf-kβ signaling (Traip) were upregulated following nicotine treatment (Figure 3.3bi). Further analyses also revealed that genes upregulated during 48 h withdrawal timepoint are connected to enriched pathways such as inflammatory response (Thbs1,Tnfrsf1a, Col1a1), type II interferon signaling (Cybb, Isg15, Icam1, Ifit2, Prkcd, Gbp2b), microglia pathogen phagocytosis (Cybb, Trem2, Rac2, Cyba, Itgb2), macrophage markers (Rac2, Lyz2, Cd74, Cd83), complement and coagulation cascades (F2rl2, Itgb2, Serpind1, Serping1, C3, C2, C7, Cfb), complement activation and classical pathway (C3, C2, C7, C151) and TGFβ signaling (Lef1, Spp1, Smad9, Thbs1, Zfp423, Bmp4) (Figure 3.3b, ii and iii). In contrast to the enriched pathways that are altered during 24 h withdrawal timepoint, pathway analysis data at 48 h withdrawal timepoint showed perturbation of microglia-related pathways. Altogether, these data show temporal changes in nicotine withdrawal-induced transcriptional programs in the nucleus accumbens.

Transcriptome remodeling in nucleus accumbal microglia and astrocytes during 48 h withdrawal from nicotine

Non-neuronal cell types such as astrocytes and microglia are actively involved in the formation, maintenance and adaptations of neural circuitry (Allen & Barres 2009). However, given possible disruption of molecular pathways related to microglia during 48 h withdrawal (as demonstrated by our pathway analysis), we evaluated nucleus accumbal microglia- and astrocyte-specific transcriptomic

changes during chronic nicotine and 48 h withdrawal. For this experiment, we generated 3 biological replicates (n =3) for each treatment – saline, nicotine and withdrawal. To arrive at each n, we pooled dissected nucleus accumbens tissues from 10 mice to improve our sample yield and maximize biological diversity. Then, we utilized magnetic activated cell sorting (MACS) for isolation and purification of microglia and astrocytes from pooled nucleus accumbens samples. Purified ACSA II astrocytes and $Cd11b^+$ microglia population were validated using quantitative PCR. Our validation of microglia showed enrichment of microglia markers (Cd11b, Tmem119 and P2ry12) in $Cd11b^+$ microglia compared to total homogenate, liver and other brain cell types (previously shown in Chapter 2, Figure 2.7a. i - iii). Similarly, our astrocyte validation showed that astrocytes markers (Gfap and S100β) are highly expressed in ACSA II astrocytes population compared to total homogenate, liver and other brain cell types (Figure 3.4a, i and ii). RNA extracted from purified cell populations were checked for quality and we found that our samples' RNA integrity number (RIN) range from 4.1 – 8.6. We constructed RNA-seq libraries and performed deep sequencing on these libraries. To evaluate the reproducibility of our sequencing data and conservation across biological replicates, we computed correlations across all RNA-seq samples and found high correlations among $Cd11b^+$ microglia (Spearman's rank correlation, mean r = 0.77) or ACSA II astrocytes replicates (Spearman's rank correlation, mean r = 0.70) and low correlations between both cell type replicates (Spearman's rank correlation, mean r = 0.27). Hierarchical clustering of all RNA-seq samples in the correlation matrix revealed two samples, one from $Cd11b^+$ microglia replicates and another

from ACSA II astrocytes replicates, as potential outliers (Figure 3.4b). This was further supported by our principal component analysis (PCA) data (Figure 3.4c, i and ii). Following outlier removal, we observed a tighter correlation within cell type replicates and a more distinct separation between cell type replicates (Figure 3.4d). Then, we examined the purity of isolated brain cell types (microglia and astrocytes) by probing transcriptome data for expression of cell type-specific markers for microglia and astrocytes and found that these markers were highly and specifically expressed in their corresponding cell types (Figure 3.4e). To analyze microglia and astrocytes for treatment-related transcriptomic differences, we performed pairwise DGE analysis and created a heatmap representation of DEGs (cutoff = $|\log2FC| > 0.5$, FDR < 0.25). In $Cd11b^+$ microglia, 2458 genes (1009 downregulated, 1449 upregulated) were differentially expressed following nicotine treatment; however, there was no significant transcriptomic alteration in ACSA II astrocytes under the same treatment condition (Figure 3.5 a). Further, in $Cd11b^+$ microglia, DGE analysis revealed 31 DEGs (5 downregulated, 26 upregulated) between saline and withdrawal groups, and 32 DEGs (18 downregulated, 14 upregulated) between nicotine and withdrawal groups (Figure 3.5a, ii and iii). However, in ACSA II astrocytes, 92 (42 downregulated, 50 upregulated) and 17 genes (13 downregulated, 4 upregulated) were differentially expressed between saline and withdrawal, and nicotine and withdrawal groups, respectively (Figure 3.5b, i and ii). Pathway analysis of DEGs obtained from pairwise DGE analysis of saline and nicotine $Cd11b^+$ microglia shows that genes involved in enriched pathways such as TYROBP causal network, microglia pathogen phagocytosis,

type II interferon signaling, chemokine signaling, TGFβ signaling, IL-1 signaling, macrophage markers, toll-like receptor signaling, inflammatory response, and oxidative damage are downregulated while some of the upregulated genes are involved in overrepresented pathways like nicotine addiction and hypothetical network of drug addiction pathways (Figure 3.6ai). However, during 48 h withdrawal, pathway analysis showed that upregulated $Cd11b^{+}$ microglia DEGs are involved in overrepresented pathways such as inflammation mediated by chemokine and cytokine signaling, toll-like receptor signaling, cytokine-cytokine receptor interaction, macrophage markers, and Tnf signaling (Figure 3.6a, ii and iii). Furthermore, pathway analysis of ACSA II astrocytes DEGs showed that genes that are upregulated during 48 h withdrawal are involved in overrepresented pathways including biogenic amine synthesis, taurine and hypotaurine metabolism, insulin secretion, butanoate metabolism, endocrine and other factor-regulated calcium reabsorption, beta-alanine metabolism, and type I diabetes mellitus (Figure 3.6b, i and ii). Taken together, these data suggest that nicotine has a direct modulatory effect on microglia but not astrocytes. In addition, 48 h withdrawal from nicotine provokes microglial pro-inflammatory signaling while vital metabolic processes are disrupted in astrocytes.

Comparison of DEGs in nucleus accumbens bulk tissue, microglia and astrocytes during chronic nicotine and withdrawal

To identify and visualize both unique and overlapping DEGs between nucleus accumbens bulk tissue (24hWD and 48hWD experiments) and cell types

(astrocytes and microglia) during chronic nicotine and withdrawal, we constructed a Venn diagram and found that all DEGs resulting from pairwise DGE analysis of saline and nicotine in nucleus accumbens tissue and cell type-specific experiments were unique (no overlap) (Figure 3.7a). However, for pairwise DGE analysis of saline and withdrawal, we found 8 overlapping DEGs (Btg2, Syt17, Nr4a3, Slc6a11, Sparc, Gpr165, Nr2f2, Itih3) between 24hWD and 48hWD experiments, 1 (Scn4b) between 24hWD and astrocytes, 2 (Tsc22d3, Pdk4) between 24hWD and microglia, 2 (Npas4, Pak6) between 48hWD and astrocytes, 3 (Mybpc1, Dio2, Gjb6) between 48hWD and microglia, and 1 (6330403K07Rik) between astrocytes and microglia experiments (Figure 3.7b). Further, two-way DGE analysis of nicotine and withdrawal produced overlapping DEGs between 24hWD and 48hWD (9 – Resp, Syt14, Ccdc108, Ngb, Gpx3, Gpr165, Nr2f2, Itih3, Pnoc), 48hWD and astrocytes (3 – Trf, Kcnj5, F2rl2), and 48hWD and microglia (4 – Doc2g, Unc13c, Plekhg3, Kif5a) experiments (Figure 3.7c). First, these data reveal nucleus accumbal gene programs that are consistently driving or contributing to nicotine withdrawal effects between 24 to 48 h withdrawal timeframe. In addition, these data uncover a subset of genes that are differentially expressed both in nucleus accumbens tissue and in either of the cell types evaluated at during nicotine withdrawal.

3.5 DISCUSSION

Transcriptional programs are genomic regulatory code instructing the formation, maintenance, and functions of diverse brain cell types and distinct brain structures.

Tissue- and cell type-specific evaluation of whole transcriptome can advance current understanding of the role of genes in CNS health and disorders such as nicotine dependence. In this study, we demonstrate that transcriptional programs are temporally-regulated in the nucleus accumbens during chronic nicotine and withdrawal. Additional investigation of transcriptome-wide responses to chronic nicotine treatment and withdrawal at cell-type specific resolution shows that unlike astrocytes, microglia are directly modulated by nicotine, resulting in myriad changes in microglial gene expression. Our cell type-specific RNA-seq data further show that during 48h withdrawal from nicotine, molecular pathways related to metabolic processes are overrepresented in astrocytes while pathways associated with inflammatory responses are overrepresented in microglia. Finally, during nicotine withdrawal, we find subset of genes that are enriched in nucleus accumbens tissue and either of the nucleus accumbens cell types examined. Taken together, our study provides the first insight into cell type-specific and tissue-level transcriptional remodeling in the nucleus accumbens in nicotine dependence.

Temporal Transcriptional Changes in the Nucleus Accumbens during Nicotine Withdrawal

Studies have shown that threshold levels of somatic signs and affective nicotine withdrawal symptoms such as anxiety increase 24 h post nicotine administration and completely wane by 96 h (Stoker et al 2008); however, transcriptional mechanisms underlying the development and brief maintenance of these

behavioral symptoms are still unknown. First, in our differential gene expression analysis data for saline versus nicotine, statistically significant enriched genes were only found at 48hWD but not at 24hWD experiment. This is most likely due to the variation in sequencing depth of our samples in both experiments since nicotine treatment period was the same in both studies. Additionally, only 5 DEGs were observed during nicotine treatment in the 48hWD experiment, suggesting more sequencing depth is required in our 24hWD experiment to observe such a small change. Lpl and Traip are part of the upregulated DEGs following nicotine treatment. We found Lpl in overrepresented pathways related to lipid metabolism and transport while Traip is associated with Tnfα-Nfkβ signaling pathway. It is suggested that reduced Lpl levels may contribute to neurite pathology and reduced neurogenesis potential in Alzheimer's (Gong et al 2013) while Traip has been shown to inhibit activation of Nfkβ mediated by Tnfα (Lee et al 1997). This suggest upregulation of both genes during nicotine treatment may be neuroprotective. Furthermore, our whole transcriptome studies show distinct gene programs in the nucleus accumbens at 24 h and 48 h withdrawal timepoints. These findings suggest that temporal transcriptional changes may underlie differential emergence and diminishing thresholds of behavioral symptoms during the early periods of nicotine withdrawal. However, further analyses show that a total (pairwise DGE analysis between saline and withdrawal = 8 genes, and nicotine and withdrawal = 9 genes) of 14 unique enriched genes (Resp18, Sytl4, Ccdc108, Ngb, Gpx3, Gpr165, Nr2f2, Itih3, Pnoc, Btg2, Syt17, Nr4a3, Slc6a11, Sparc) overlap between DEGs at 24 h and 48 h withdrawal timepoints. These genes all have similar

directionality (all upregulated) during 24 h and 48 h withdrawal, except for Ccdc108, Syt17 and Nr4a3 that were upregulated at 24 h but downregulated at 48 h, and Btg2 that was consistently downregulated regardless of withdrawal period. Interestingly, a number of these genes (Gpx3, Itih3, Ngb) have been shown to respond to oxidative stress conditions (Herault et al 2012, Maes et al 2011, Wang et al 2007, Watanabe et al 2012, Wickramasekara et al 2018), suggesting their upregulation indicates oxidative imbalance during nicotine withdrawal. This is further supported by increased Sparc expression, which is connected to elevation of reactive oxygen species (ROS). Sparc gene deletion or deficiency have been shown to have protective effect against oxidative stress (Aseer et al 2017, Peixoto et al 2016). In addition, studies have shown that Btg2 is a coactivator for Nrf2 in upregulating cellular antioxidant defenses (Karve & Rosen 2012); however, Btg2 was downregulated at 24 h and 48 h nicotine withdrawal timepoints. These findings further suggest altered ROS homeostasis during nicotine withdrawal. One distinct transcriptomic feature observed during 48 h withdrawal but not evident in 24 h withdrawal is the enrichment of signaling pathways related to microglial pro-inflammatory cascades. Taken together, further studies may lead to transcriptomic characterization of molecular events associated with behavioral symptomatology in nicotine dependence.

Transcriptome Remodeling in Microglia during Chronic Nicotine and Withdrawal

Recently, microglia have emerged as central players in many brain disorders (Salter & Stevens 2017), including drug addiction (Lewitus et al 2016b, Schwarz & Bilbo 2013, Schwarz et al 2013); however, their role in nicotine dependence is completely unknown. To study microglial transcriptomic changes in response to chronic nicotine and withdrawal, we utilized cell type-specific RNA-seq. Our bulk tissue RNA-seq studies capture RNAs from all cell types en masse; therefore, transcriptomic composition of individual cell types is diluted and missed. First, our data suggest that nicotine directly interacts with microglia, provoking myriad transcriptome remodeling.

One of the notable changes is the upregulation of α4 and β2 nAChR subunits following nicotine treatment. Further analysis revealed that both genes are part of the nicotine addiction pathway, which is overrepresented in microglia. Our findings show that α4β2 nAChR is upregulated in microglia in response to nicotine treatment, suggesting a direct mechanism through which nicotine interacts with microglia. Prior to this study, it is unclear whether or how nicotine interacts with microglia. However, in contrast to our study, previous studies evaluating nicotine's effect on microglia using immortalized cell lines or primary microglial cultures have reported the expression of homomeric α7-nAChR on microglia (De Simone et al 2005, King et al 2017, Mencel et al 2013, Shytle et al 2004, Suzuki et al 2006), suggesting nicotine may directly interact with this receptor subtype on microglia to elicit its effect. While these studies may have provided mechanistic insights into

nicotine's modulation of microglia, it is noteworthy that our approach, which involves isolation and purification of microglia from fresh nucleus accumbens tissue, presents microglia in a more natural state and provides better translatability to in vivo situations. Another important consideration is the differences in brain region from which microglia was prepared or isolated, as nAChR subtypes are differentially expressed across brain regions. Furthermore, nicotine can also have an indirect modulatory effect on microglia through enhancement of neuron-microglia communication. One of the important bidirectional communication between neurons and microglia is the interaction between fractalkine, Cx3cl1, which is constitutively expressed in neurons and its receptor, Cx3cr1, which is primarily expressed on microglia. Cx3cl1-Cx3cr1 signaling is required to keep microglia in a surveying phenotype, and activation of Cx3cr1 provokes signal cascades that modulates apoptotic, proliferative, transcriptional and migratory functions in microglia (Szepesi et al 2018). However, our findings show that Cx3cr1 and other chemokines that could mediate neuron-microglia communication (Ccl2, Ccl12, and CxCl9) were all downregulated following nicotine treatment, reinforcing our previous findings. Furthermore, our data show that overrepresented pathways including inflammatory responses, oxidative damage, toll-like receptor signaling, macrophage markers, and microglia pathogen phagocytosis are downregulated in microglia following nicotine treatment. These findings support previous studies that have demonstrated nicotine's neuroprotective property in neurodegenerative disorders such as Alzheimer's (Newhouse et al 2012, Wilson et al 1995) and Parkinson's (Villafane et al 2007), two disorders with extensive links to microglial

activation and inflammatory responses (Amor et al 2010). However, during 48 h nicotine withdrawal, enriched pathways such as inflammation mediated by chemokine and cytokine signaling, toll-like receptor signaling, macrophage markers are upregulated in microglia, suggesting nicotine withdrawal-induced microglial pro-inflammatory signaling as well as microglia proliferation. Overall, these data provide evidence for nicotine's direct modulatory effect on microglia as well as its suppression of microglial pro-inflammatory networks, which were all activated during nicotine withdrawal.

Transcriptome Remodeling in Astrocytes during Chronic Nicotine and Withdrawal

Astrocytes are actively involved in regulating the overall architecture and activity of neuronal circuits (Szepesi et al 2018). While the role of astrocytes have been studied in addiction to some drugs of abuse (Goins & Bajic 2018, Ikeda et al 2010, Turner et al 2013a), their contributions in nicotine dependency is still unclear. We found no enriched genes in astrocytes following nicotine treatment, suggesting that nicotine does not have a direct modulatory effect on astrocytes. However, during nicotine withdrawal, numerous genes were differentially expressed, suggesting astrocyte reactivity to withdrawal-related insults within their local microenvironment. Further, our data show that overrepresented pathways including biogenic amine synthesis, taurine and hypotaurine metabolism, butanoate metabolism, beta-alanine metabolism and iron homeostasis are upregulated in astrocytes, suggesting that astrocytes upregulate these metabolic

pathways in response to withdrawal-related insults on neurons. Usually, astrocytes optimize their metabolism to provide energy to the neurons that are deprived of nutrients upon insult. These metabolic changes that astrocyte develop following neuronal insult are one of the defining features of reactive astrocytes (Ben Haim et al 2015, Iglesias et al 2017). Our data show that GAD1 and GAD2 (both glutamate decarboxylases), which are both upregulated in our study, are involved in many of the metabolic processes overrepresented in astrocytes during nicotine withdrawal. GADs deplete glutamate levels in the brain to produce gamma aminobutyric acid (GABA). Therefore, GAD upregulation may indicate alterations in glutamate homeostasis and elevated GABA levels, which are both features associated with reactive astrocyte (Ben Haim et al 2015). In fact, a study reported that astrocytes can modulate microglia activity via GABA release (Lee et al 2011). On the other hand, this supports the concept that astrocyte reactivity may be a response to activated microglia, and not necessarily a direct response to neuronal insult. Altogether, our astrocyte transcriptome data suggest that astrocyte undergo transformation to the reactive phenotype, which may be a response to neuronal insult or microglial activation during nicotine withdrawal.

3.6 FIGURES

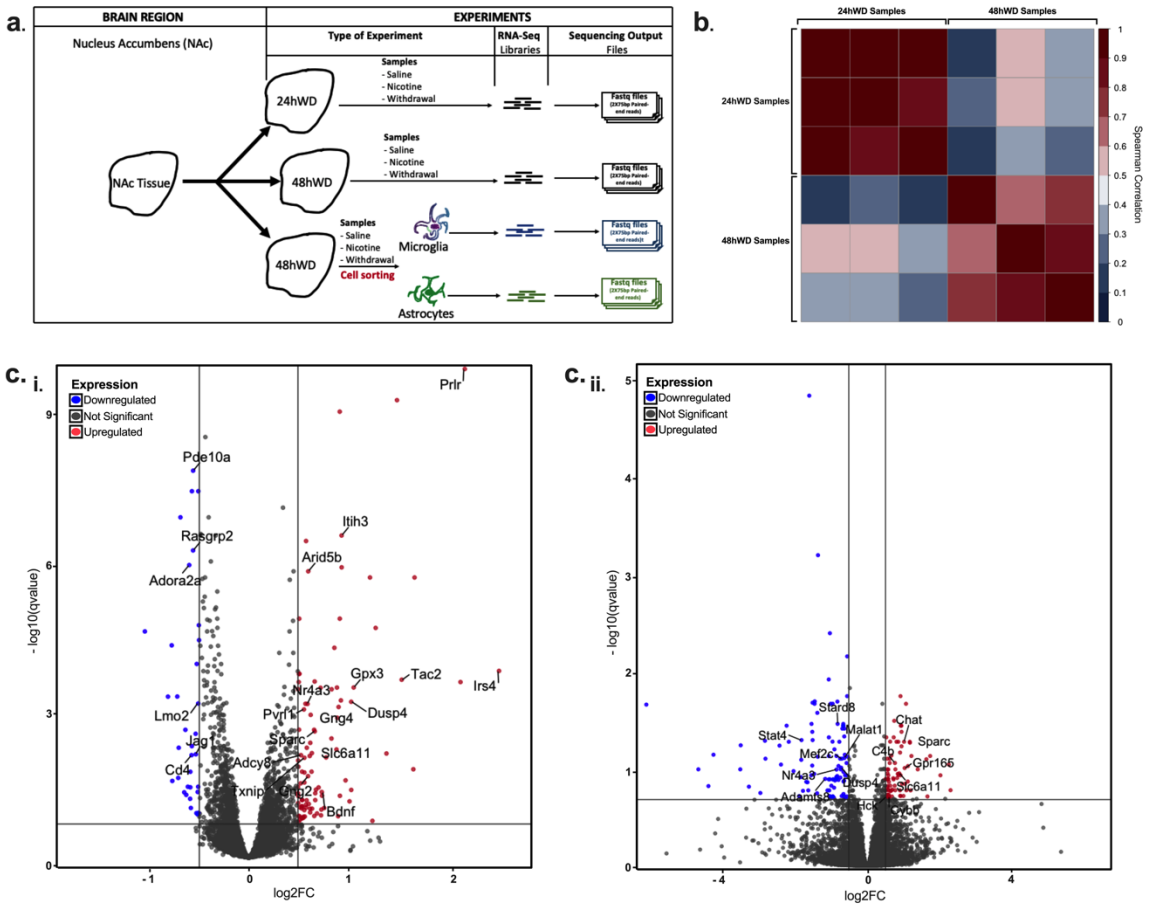

Figure 3.1. Differentially expressed genes in the nucleus accumbens during chronic nicotine and withdrawal. a. Experimental design. **b.** Correlation matrix showing relationships between withdrawal samples from 24hWD and 48hWD experiment. **c.** Volcano plot showing statistically significant differentially expressed genes in i) 24hWD, ii) 48hWD experiments.

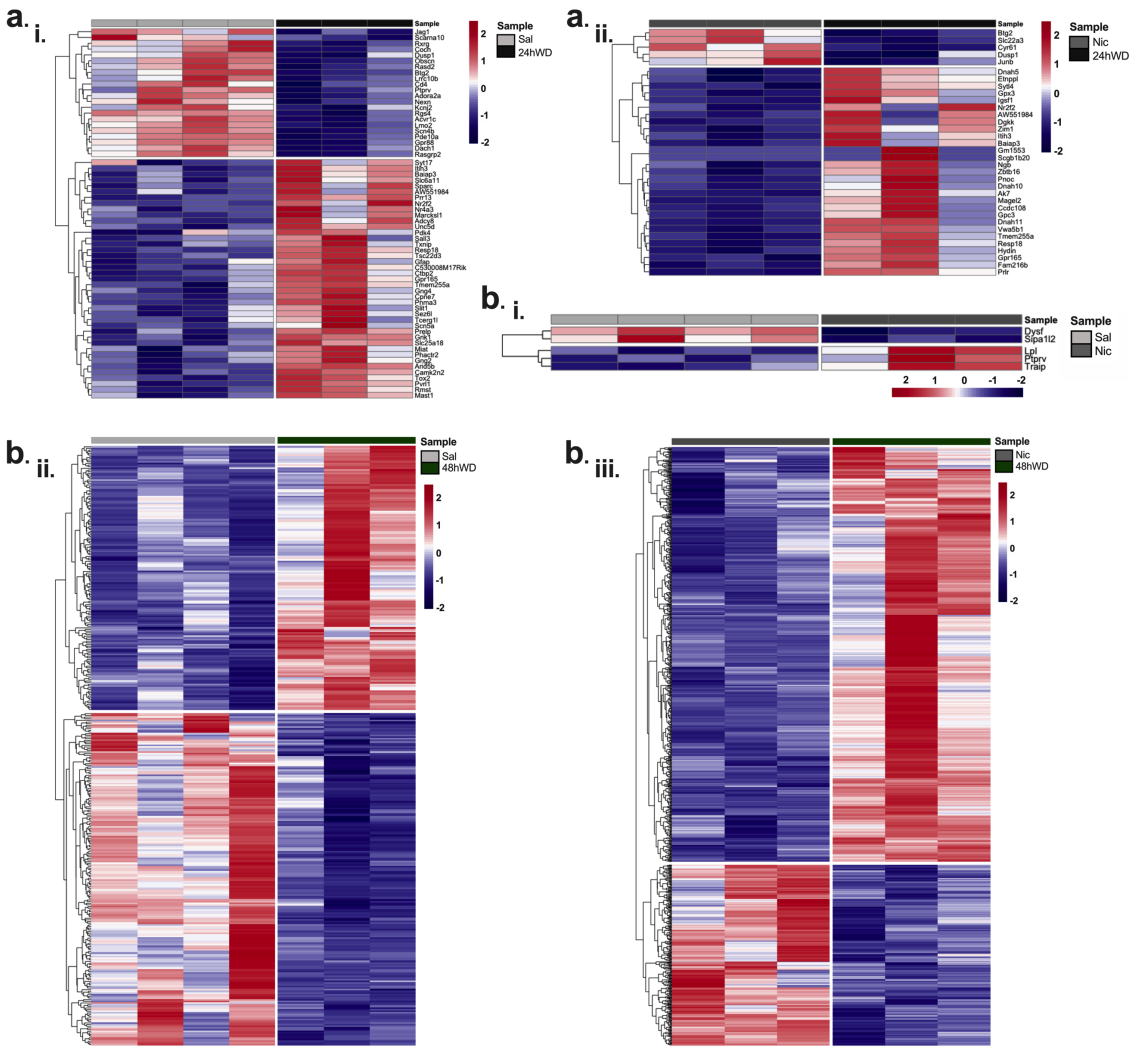

Figure 3.2. Distinct gene programs are altered in the nucleus accumbens of mice in the 24hWD and 48hWD experiments.
Heat map representation showing differentially expressed genes obtained from pairwise DGE analysis of **a.** 24hWD experiment i) Sal (Saline) and 24 h withdrawal (24hWD), ii) Nic (Nicotine) and 24 h withdrawal. **b.** 48hWD experiment i) Sal and Nic, ii) Sal and 48 h withdrawal (48hWD), iii) Nic and 48 h withdrawal.

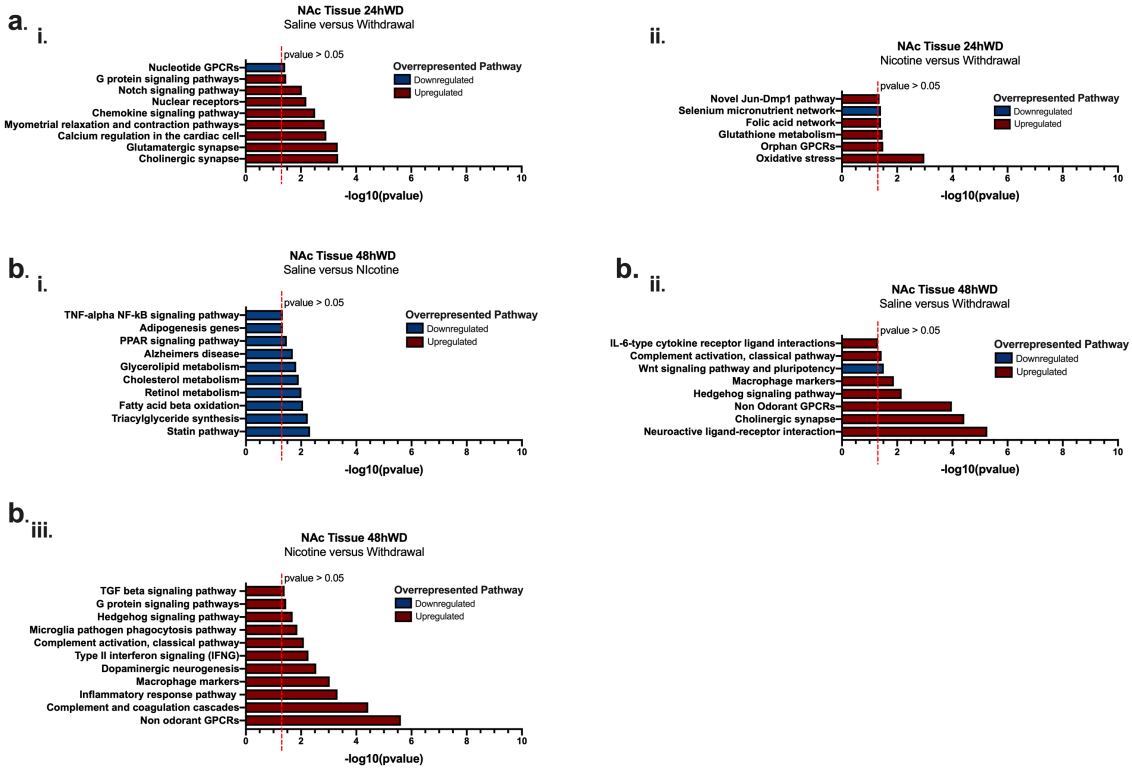

Figure 3.3. Overrepresented pathways in the nucleus accumbens during chronic nicotine and withdrawal in the 24hWD and 48hWD experiments.
Pathway enrichment analysis highlighting some of the overrepresented pathways in **a.** 24hWD experiment i) Sal and 24 h withdrawal, ii) Nic and 24 h withdrawal. **b.** 48hWD experiment i) Sal and Nic, ii) Sal and 48 h withdrawal, iii) Nic and 48 h withdrawal

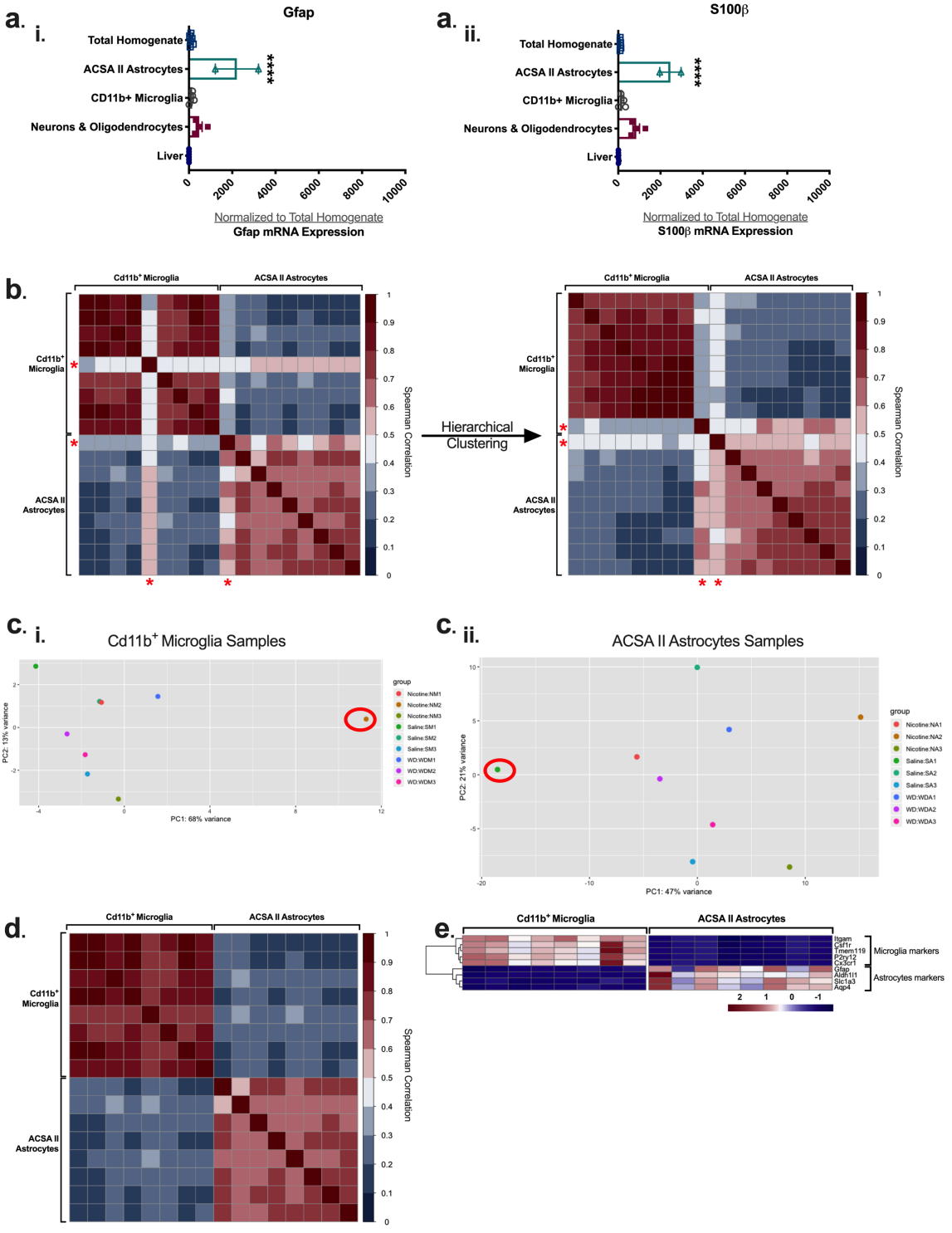

Figure 3.4. Evaluating the reproducibility of our data and conservation across biological replicates. a. Bar graph showing quantitative PCR analysis of astrocytes markers in the liver, brain cell-types and tissue (Total homogenate). i) Gfap, ii) S100β. **b.** Correlation matrix showing relationships between nucleus accumbal Cd11b^{+} microglia and ACSA II astrocytes samples. Sample clustering identify two potential outliers (in red-

colored asterisks). **c.** Separate principal component analysis plot showing variation between i) $Cd11b^+$ microglia, ii) ACSA II astrocytes samples. Potential outlier samples (same samples observed in 3.4b) are encircled by the red-colored ring. **d.** Correlation matrix showing relationships between nucleus accumbal $Cd11b^+$ microglia and ACSA II astrocytes samples post-outlier removal. **e.** Heatmap showing the expression of classical cell type markers in nucleus accumbal $Cd11b^+$ microglia and ACSA II astrocytes samples

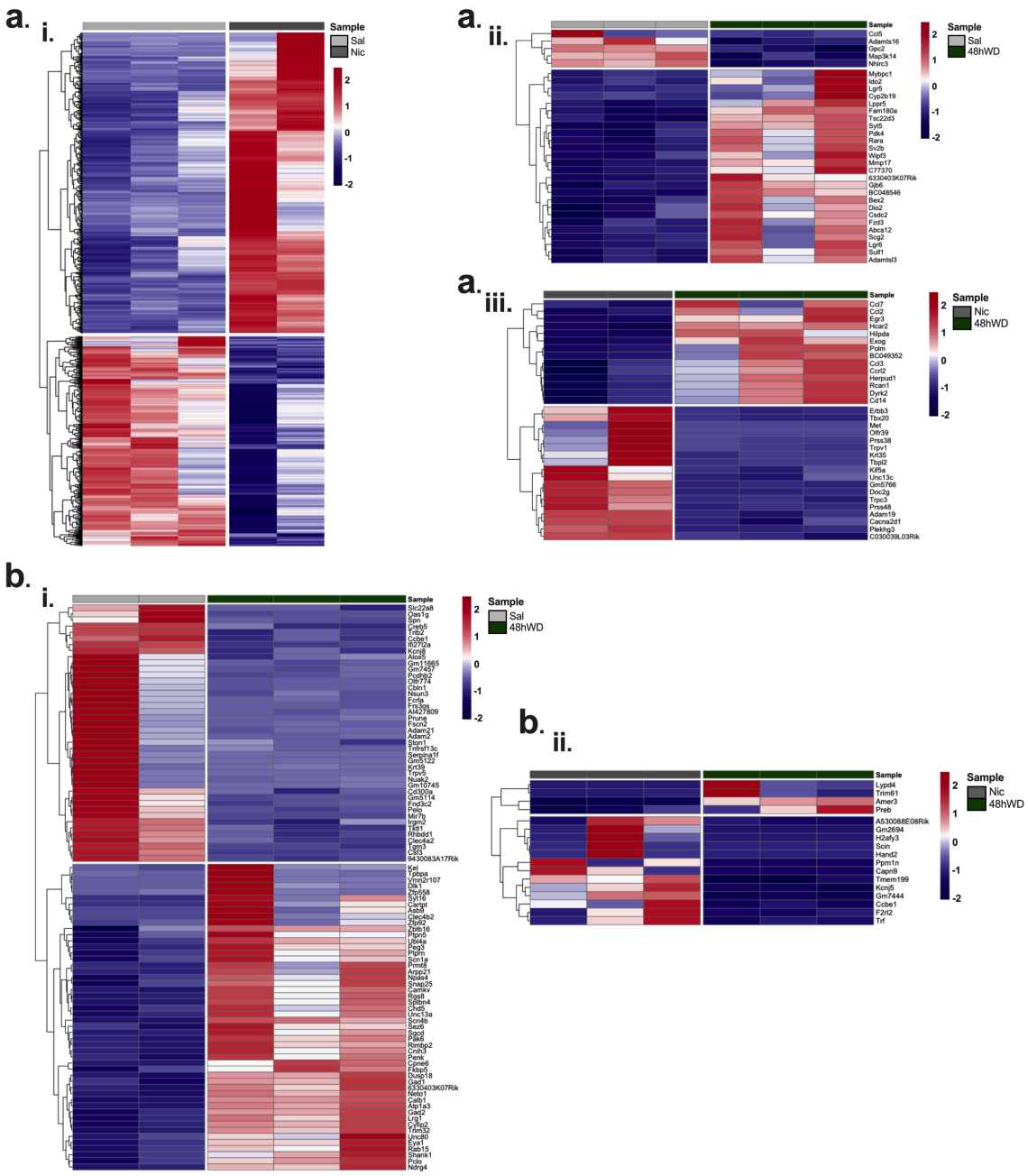

Figure 3.5. Transcriptional programs in nucleus accumbal Cd11b$^+$ microglia and ACSA II astrocytes during chronic nicotine and 48 h withdrawal.
Heat map representation showing differentially expressed genes obtained from pairwise DGE analysis of **a.** Cd11b$^+$ microglia i) Sal and Nic, ii) Sal and 48 h withdrawal, iii) Nic and 48 h withdrawal. **b.** ACSA II astrocytes i) Sal and 48 h withdrawal, ii) Nic and 48 h withdrawal.

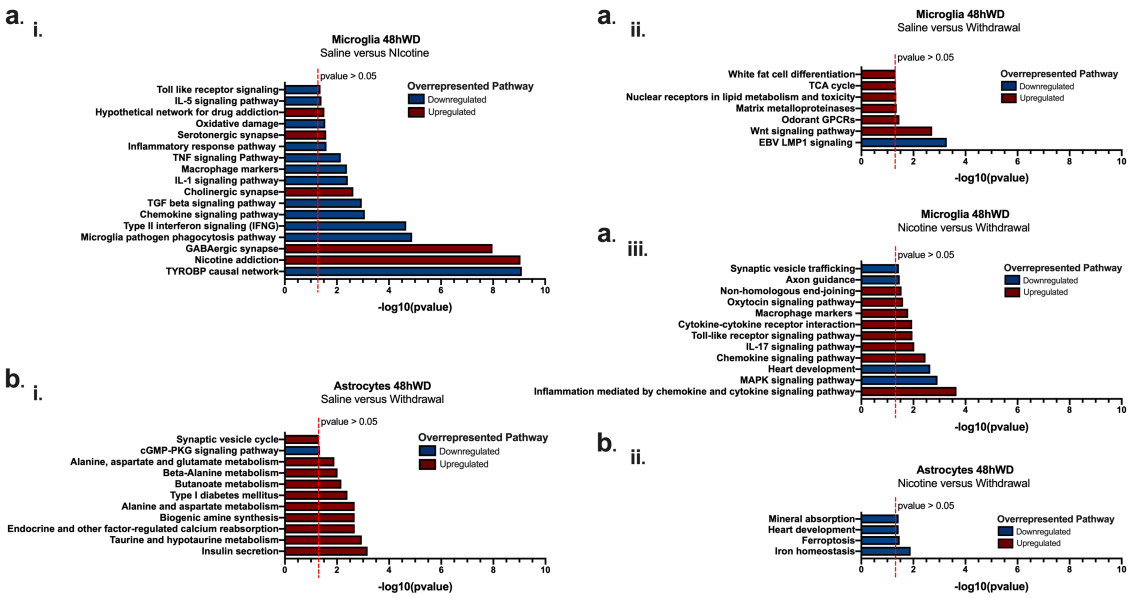

Figure 3.6. Overrepresented pathways in nucleus accumbal Cd11b^{+} microglia and ACSA II astrocytes during chronic nicotine and 48 h withdrawal.
Pathway enrichment analysis showing some of the overrepresented pathways in **a.** Cd11b^{+} microglia i) Sal and Nic, ii) Sal and 48 h withdrawal, iii) Nic and 48 h withdrawal. **b.** ACSA II astrocytes i) Sal and 48 h withdrawal, ii) Nic and 48 h withdrawal.

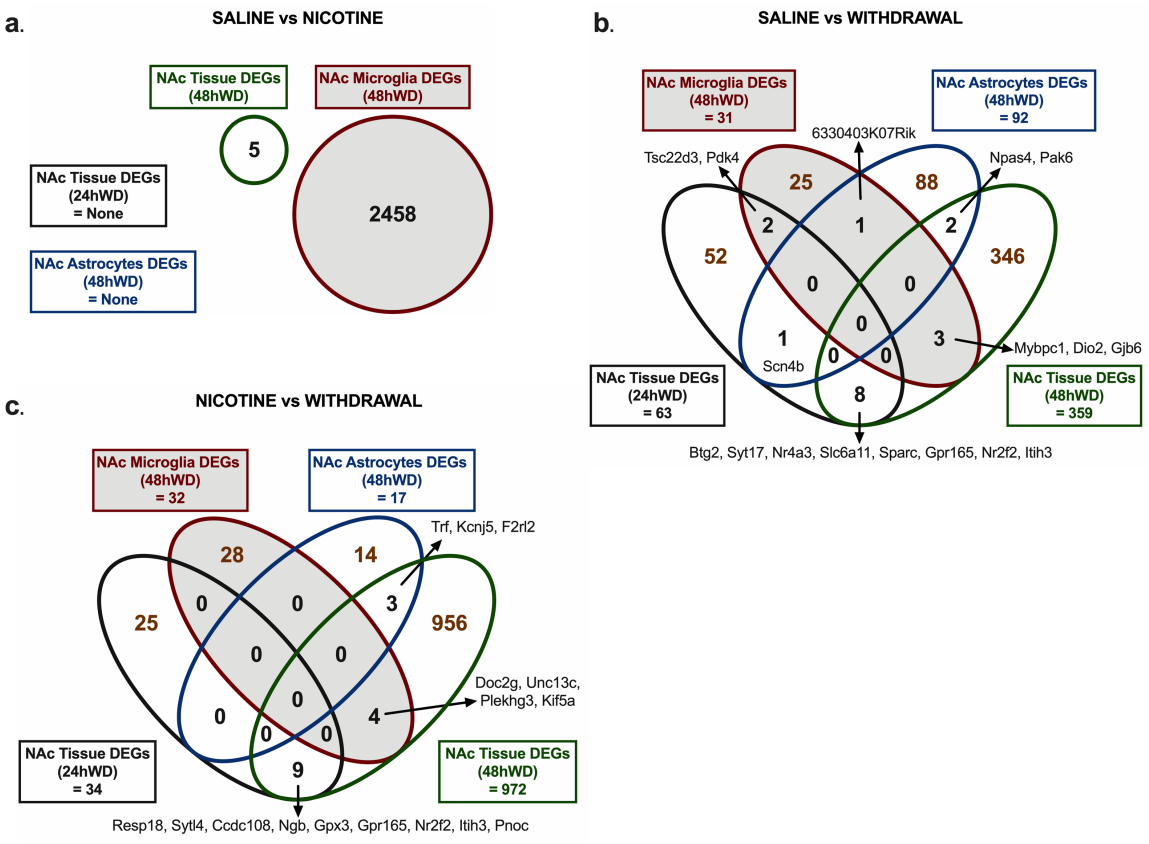

Figure 3.7. Graphical overview of unique and overlapping differentially expressed gene in all RNA sequencing experiments.
Venn diagram showing relationships between differentially expressed genes in **a.** Sal and Nic, **b.** Sal and Withdrawal, **c.** Nic and Withdrawal.

CHAPTER 4

CONCLUSION

Neurons are the primary research target in the exploration and development of novel smoking cessation pharmacotherapies. These investigations have led to the discovery and development of three FDA-approved smoking cessation aids – nicotine replacement therapy, varenicline, and bupropion, each of which elicit their effects via modulation of neuronal function. However, while each of these therapeutics have quantifiable success as smoking cessation aids, about 80% of smokers attempting to quit still fail. This may be substantially due to inability of these current aids to address some critical aspects of nicotine dependency. Therefore, there is an urgent need to extend attention to non-neuronal cell types such as astrocytes and microglia, which are both active participants in neuroplastic events underlying drug addiction. This chapter will highlight the salient aspects of this study and recommend experimental approaches to advance this project.

4.1 CHAPTER 2 SUMMARY

In Chapter 2, we conducted series of experiments that demonstrated a link between oxidative stress signaling and nicotine withdrawal-related anxiety. Neurons are particularly susceptible to oxidative stress insults, and it is thought that these insults can activate neuronal signaling pathways that are associated with the development of anxiety-like behavior during nicotine withdrawal. Our

results showed that both pro-inflammatory signaling and oxidative stress during nicotine withdrawal are limited to the nucleus accumbens, which has a critical role in anxiety. Given that Nox system is the major source of intracellular ROS and Nox2 subtype is primarily expressed in microglia, we hypothesized that oxidative stress and nicotine withdrawal-related anxiety are direct consequences of microglial morphological remodeling. Our findings provide the first evidence of microglial involvement in nicotine dependence.

Future direction

While our molecular findings were based on the evaluation of striatum, our behavioral data may result from molecular events within multiple neural substrates of anxiety. Therefore, future studies may need to examine other neural substrates of anxiety for the same molecular events (pro-inflammatory signaling, oxidative stress, microglial morphological remodeling) observed in the nucleus accumbens during nicotine withdrawal. Additional studies should also include region-specific depletion of microglia or inhibition of microglia functions such as their pro-inflammatory signaling prior to behavioral and molecular assessments. Together, this will elucidate brain regions that are actually associated with nicotine-withdrawal related anxiety.

4.2 CHAPTER 3 SUMMARY

Based on our findings in chapter 2, we extended our study to capture tissue-level transcriptome changes in the nucleus accumbens during chronic nicotine and

withdrawal (24 h and 48 h). This study uncovered temporal transcriptome changes during the early stages of withdrawal (24 h to 48 h). Interestingly, we found a substantial proportion of overlapping genes at these withdrawal timepoints to be associated with dysregulation of ROS homeostasis and oxidative imbalance. This corroborates our findings in chapter 2. More specifically, during 48 h withdrawal, we found enrichment of gene subsets connected to microglia pro-inflammatory signaling pathways.

To have a finer resolution that aid better characterization of transcriptomic changes during chronic nicotine and withdrawal, we performed cell type-specific RNA sequencing (RNA-seq) and evaluated astrocyte- and microglia-specific transcriptome changes during chronic nicotine and 48 h withdrawal. In contrast to previous suggestions of α7 nAChR on microglia, we identified α4β2 nAChR as the potential receptor through which nicotine interacts directly with microglia. Chronic nicotine treatment suppresses pro-inflammatory pathways in microglial transcriptome while 48 h withdrawal activates them. This is consistent with many studies assessing neuroinflammation in neurodegenerative disorders. For astrocytes, we found that nicotine has no impact on their transcriptome; however, during 48 h withdrawal, metabolic pathways in astrocytes are activated. Nicotine's activation of microglia but not astrocytes, and the type of responses from both cell types during withdrawal present a consistent pattern with several studies that demonstrated that activated microglia promotes reactive astrocytes in many neurodegenerative diseases (Liu et al 2011).

Compared to our nucleus accumbens tissue RNA-seq, astrocytes- and microglia-specific RNA-seq gave us a less complex insight into the transcriptomic changes observed at tissue-level during chronic nicotine and withdrawal.

Future direction

Future studies can include weighted correlation network analysis or weighted gene co-expression network analysis (WGCNA) to determine clusters (modules) of highly correlated genes in our enriched gene datasets (tissue and cell type-specific). Correlation networks aid network-based gene screening approaches that can be used to determine candidate biomarkers or therapeutic targets. These biomarkers or gene targets from WGCNA can then be validated using quantitative PCR. Following validation, functional genomics studies should be performed to study the function of these targets, as well as their impact on nicotine withdrawal-relevant behavioral phenotypes.

Finally, moving biomarkers or gene targets with therapeutic potential from the laboratory to the point at which it is available as a medication is a long, rigorous and expensive process. However, going forward, we do not doubt the translatability of our findings given that certain modulators of microglia differentiation and survival has already been developed and commercially available.

REFERENCES

Allen NJ, Barres BA. 2009. Neuroscience: Glia — more than just brain glue. *Nature* 457: 675-77

Amor S, Puentes F, Baker D, van der Valk P. 2010. Inflammation in neurodegenerative diseases. *Immunology* 129: 154-69

Aruoma OI, Halliwell B, Hoey BM, Butler J. 1989. The antioxidant action of N-acetylcysteine: its reaction with hydrogen peroxide, hydroxyl radical, superoxide, and hypochlorous acid. *Free radical biology & medicine* 6: 593-7

Aseer KR, Silvester AJ, Kumar A, Choi MS, Yun JW. 2017. SPARC paucity alleviates superoxide-mediated oxidative stress, apoptosis, and autophagy in diabetogenic hepatocytes. *Free radical biology & medicine* 108: 874-95

Ashare RL, Falcone M, Lerman C. 2014. Cognitive function during nicotine withdrawal: Implications for nicotine dependence treatment. *Neuropharmacology* 76 Pt B: 581-91

Babizhayev MA. 2014. The detox strategy in smoking comprising nutraceutical formulas of non-hydrolyzed carnosine or carcinine used to protect human health. *Human & experimental toxicology* 33: 284-316

Balfour DJK. 2008. The psychobiology of nicotine dependence. *European Respiratory Review* 17: 172-

Barreto GE, Iarkov A, Moran VE. 2014. Beneficial effects of nicotine, cotinine and its metabolites as potential agents for Parkinson's disease. *Frontiers in aging neuroscience* 6: 340

Ben Haim L, Carrillo-de Sauvage MA, Ceyzeriat K, Escartin C. 2015. Elusive roles for reactive astrocytes in neurodegenerative diseases. *Frontiers in cellular neuroscience* 9: 278

Benowitz NL. 1999. Nicotine addiction. *Prim Care* 26: 611-31

Benowitz NL. 2008a. Clinical pharmacology of nicotine: implications for understanding, preventing, and treating tobacco addiction. *Clinical pharmacology and therapeutics* 83: 531-41

Benowitz NL. 2008b. Neurobiology of nicotine addiction: implications for smoking cessation treatment. *Am J Med* 121: S3-10

Benowitz NL. 2010. Nicotine Addiction. *New England Journal of Medicine* 362: 2295-303

Bollinger JL, Bergeon Burns CM, Wellman CL. 2016. Differential effects of stress on microglial cell activation in male and female medial prefrontal cortex. *Brain, behavior, and immunity* 52: 88-97

Brunzell DH, Mineur YS, Neve RL, Picciotto MR. 2009. Nucleus accumbens CREB activity is necessary for nicotine conditioned place preference. *Neuropsychopharmacology : official publication of the American College of Neuropsychopharmacology* 34: 1993-2001

Brunzell DH, Russell DS, Picciotto MR. 2003. In vivo nicotine treatment regulates mesocorticolimbic CREB and ERK signaling in C57Bl/6J mice. *J Neurochem* 84: 1431-41

Buisson B, Bertrand D. 2001. Chronic exposure to nicotine upregulates the human (alpha)4((beta)2 nicotinic acetylcholine receptor function. *The Journal of neuroscience : the official journal of the Society for Neuroscience* 21: 1819-29

Buisson B, Bertrand D. 2002. Nicotine addiction: the possible role of functional upregulation. *Trends Pharmacol Sci* 23: 130-6

Butovsky O, Jedrychowski MP, Moore CS, Cialic R, Lanser AJ, et al. 2014. Identification of a unique TGF-β–dependent molecular and functional signature in microglia. *Nature neuroscience* 17: 131-43

Butovsky O, Weiner HL. 2018. Microglial signatures and their role in health and disease. *Nat Rev Neurosci* 19: 622-35

Cao L, Li L, Zuo Z. 2012. N-acetylcysteine reverses existing cognitive impairment and increased oxidative stress in glutamate transporter type 3 deficient mice. *Neuroscience* 220: 85-9

Cao Y-J, Surowy CS, Puttfarcken PS. 2005. Different nicotinic acetylcholine receptor subtypes mediating striatal and prefrontal cortical [3H]dopamine release. *Neuropharmacology* 48: 72-79

Cerbai F, Lana D, Nosi D, Petkova-Kirova P, Zecchi S, et al. 2012. The neuron-astrocyte-microglia triad in normal brain ageing and in a model of neuroinflammation in the rat hippocampus. *PloS one* 7: e45250

Changeux J-P. 2010. Nicotine addiction and nicotinic receptors: lessons from genetically modified mice. *Nature Reviews Neuroscience* 11: 389-401

Changeux JP, Devillers-Thiery A, Chemouilli P. 1984. Acetylcholine receptor: an allosteric protein. *Science* 225: 1335-45

Chen WW, Zhang X, Huang WJ. 2016. Role of neuroinflammation in neurodegenerative diseases (Review). *Molecular medicine reports* 13: 3391-6

Clarke R, Adermark L. 2015. Dopaminergic Regulation of Striatal Interneurons in Reward and Addiction: Focus on Alcohol. *Neural Plast* 2015: 814567

Cleck JN, Ecke LE, Blendy JA. 2008. Endocrine and gene expression changes following forced swim stress exposure during cocaine abstinence in mice. *Psychopharmacology* 201: 15-28

Coe JW, Brooks PR, Vetelino MG, Wirtz MC, Arnold EP, et al. 2005. Varenicline: an alpha4beta2 nicotinic receptor partial agonist for smoking cessation. *Journal of medicinal chemistry* 48: 3474-7

Cohen A, Young RW, Velazquez MA, Groysman M, Noorbehesht K, et al. 2009. Anxiolytic effects of nicotine in a rodent test of approach-avoidance conflict. *Psychopharmacology* 204: 541-9

Cosci F. 2011. Nicotine dependence and psychological distress: outcomes and clinical implications in smoking cessation. *Psychology Research and Behavior Management*: 119

Cunningham C. 2013. Microglia and neurodegeneration: the role of systemic inflammation. *Glia* 61: 71-90

D'Souza MS, Markou A. 2011. Neuronal mechanisms underlying development of nicotine dependence: implications for novel smoking-cessation treatments. *Addict Sci Clin Pract* 6: 4-16

D'Souza MS, Markou A. 2013. The "Stop" and "Go" of Nicotine Dependence: Role of GABA and Glutamate. *Cold Spring Harbor Perspectives in Medicine* 3: a012146-a46

Dani JA, De Biasi M. 2013. Mesolimbic Dopamine and Habenulo-Interpeduncular Pathways in Nicotine Withdrawal. *Cold Spring Harbor Perspectives in Medicine* 3: a012138-a38

Darsow T, Booker TK, Pina-Crespo JC, Heinemann SF. 2005. Exocytic trafficking is required for nicotine-induced up-regulation of alpha 4 beta 2 nicotinic acetylcholine receptors. *The Journal of biological chemistry* 280: 18311-20

Davis JA, James JR, Siegel SJ, Gould TJ. 2005. Withdrawal from chronic nicotine administration impairs contextual fear conditioning in C57BL/6 mice. *The Journal of neuroscience : the official journal of the Society for Neuroscience* 25: 8708-13

De Biase LM, Schuebel KE, Fusfeld ZH, Jair K, Hawes IA, et al. 2017. Local Cues Establish and Maintain Region-Specific Phenotypes of Basal Ganglia Microglia. *Neuron* 95: 341-56 e6

De Biasi M, Dani JA. 2011. Reward, addiction, withdrawal to nicotine. *Annu Rev Neurosci* 34: 105-30

De Simone R, Ajmone-Cat MA, Carnevale D, Minghetti L. 2005. Activation of alpha7 nicotinic acetylcholine receptor by nicotine selectively up-regulates

cyclooxygenase-2 and prostaglandin E2 in rat microglial cultures. *J Neuroinflammation* 2: 4

Dekhuijzen PN. 2004. Antioxidant properties of N-acetylcysteine: their relevance in relation to chronic obstructive pulmonary disease. *The European respiratory journal* 23: 629-36

Ding X, Zhang M, Gu R, Xu G, Wu H. 2017. Activated microglia induce the production of reactive oxygen species and promote apoptosis of co-cultured retinal microvascular pericytes. *Graefe's archive for clinical and experimental ophthalmology = Albrecht von Graefes Archiv fur klinische und experimentelle Ophthalmologie* 255: 777-88

Dobin A, Davis CA, Schlesinger F, Drenkow J, Zaleski C, et al. 2013. STAR: ultrafast universal RNA-seq aligner. *Bioinformatics* 29: 15-21

Dulawa SC, Hen R. 2005. Recent advances in animal models of chronic antidepressant effects: the novelty-induced hypophagia test. *Neurosci Biobehav Rev* 29: 771-83

Ernst M, Matochik JA, Heishman SJ, Van Horn JD, Jons PH, et al. 2001. Effect of nicotine on brain activation during performance of a working memory task. *Proceedings of the National Academy of Sciences of the United States of America* 98: 4728-33

Ficklin MB, Zhao S, Feng G. 2005. Ubiquilin-1 regulates nicotine-induced up-regulation of neuronal nicotinic acetylcholine receptors. *The Journal of biological chemistry* 280: 34088-95

Fisher ML, LeMalefant RM, Zhou L, Huang G, Turner JR. 2017. Distinct Roles of CREB Within the Ventral and Dorsal Hippocampus in Mediating Nicotine Withdrawal Phenotypes. *Neuropsychopharmacology : official publication of the American College of Neuropsychopharmacology* 42: 1599-609

Fowler CD, Arends MA, Kenny PJ. 2008. Subtypes of nicotinic acetylcholine receptors in nicotine reward, dependence, and withdrawal: evidence from genetically modified mice. *Behav Pharmacol* 19: 461-84

Fujiyama F, Sohn J, Nakano T, Furuta T, Nakamura KC, et al. 2011. Exclusive and common targets of neostriatofugal projections of rat striosome neurons: a single neuron-tracing study using a viral vector. *Eur J Neurosci* 33: 668-77

Galloway A, Adeluyi A, O'Donovan B, Fisher ML, Rao CN, et al. 2018. Dopamine triggers CTCF-dependent morphological and genomic remodeling of astrocytes. *The Journal of Neuroscience*: 3349-17

Gipson CD, Reissner KJ, Kupchik YM, Smith AC, Stankeviciute N, et al. 2013. Reinstatement of nicotine seeking is mediated by glutamatergic plasticity. *Proceedings of the National Academy of Sciences of the United States of America* 110: 9124-9

Goins EC, Bajic D. 2018. Astrocytic hypertrophy in the rat ventral tegmental area following chronic morphine differs with age. *J Neurol Neurorehabilit Res* 3: 14-21

Gong H, Dong W, Rostad SW, Marcovina SM, Albers JJ, et al. 2013. Lipoprotein lipase (LPL) is associated with neurite pathology and its levels are markedly

reduced in the dentate gyrus of Alzheimer's disease brains. *J Histochem Cytochem* 61: 857-68

Gonzales D, Rennard SI, Nides M, Oncken C, Azoulay S, et al. 2006. Varenicline, an alpha4beta2 nicotinic acetylcholine receptor partial agonist, vs sustained-release bupropion and placebo for smoking cessation: a randomized controlled trial. *Jama* 296: 47-55

Gotti C, Clementi F. 2004. Neuronal nicotinic receptors: from structure to pathology. *Prog Neurobiol* 74: 363-96

Gould TJ, Portugal GS, Andre JM, Tadman MP, Marks MJ, et al. 2012. The duration of nicotine withdrawal-associated deficits in contextual fear conditioning parallels changes in hippocampal high affinity nicotinic acetylcholine receptor upregulation. *Neuropharmacology* 62: 2118-25

Govind AP, Vezina P, Green WN. 2009. Nicotine-induced upregulation of nicotinic receptors: underlying mechanisms and relevance to nicotine addiction. *Biochem Pharmacol* 78: 756-65

Grady SR, Salminen O, Laverty DC, Whiteaker P, McIntosh JM, et al. 2007. The subtypes of nicotinic acetylcholine receptors on dopaminergic terminals of mouse striatum. *Biochemical Pharmacology* 74: 1235-46

Graham AJ, Ray MA, Perry EK, Jaros E, Perry RH, et al. 2003. Differential nicotinic acetylcholine receptor subunit expression in the human hippocampus. *J Chem Neuroanat* 25: 97-113

Grunberg NE. 2007. A neurobiological basis for nicotine withdrawal. *Proceedings of the National Academy of Sciences* 104: 17901-02

Guilarte TR, Loth MK, Guariglia SR. 2016. TSPO Finds NOX2 in Microglia for Redox Homeostasis. *Trends Pharmacol Sci* 37: 334-43

Harada K, Kamiya T, Tsuboi T. 2015. Gliotransmitter Release from Astrocytes: Functional, Developmental, and Pathological Implications in the Brain. *Front Neurosci* 9: 499

Harkness PC, Millar NS. 2002. Changes in conformation and subcellular distribution of alpha4beta2 nicotinic acetylcholine receptors revealed by chronic nicotine treatment and expression of subunit chimeras. *The Journal of neuroscience : the official journal of the Society for Neuroscience* 22: 10172-81

Herault O, Hope KJ, Deneault E, Mayotte N, Chagraoui J, et al. 2012. A role for GPx3 in activity of normal and leukemia stem cells. *J Exp Med* 209: 895-901

Huo Y, Rangarajan P, Ling EA, Dheen ST. 2011. Dexamethasone inhibits the Nox-dependent ROS production via suppression of MKP-1-dependent MAPK pathways in activated microglia. *BMC neuroscience* 12: 49

Hutchinson MR, Lewis SS, Coats BD, Skyba DA, Crysdale NY, et al. 2009. Reduction of opioid withdrawal and potentiation of acute opioid analgesia by systemic AV411 (ibudilast). *Brain, behavior, and immunity* 23: 240-50

Hyman SE, Malenka RC, Nestler EJ. 2006. NEURAL MECHANISMS OF ADDICTION: The Role of Reward-Related Learning and Memory. *Annual Review of Neuroscience* 29: 565-98

Iglesias J, Morales L, Barreto GE. 2017. Metabolic and Inflammatory Adaptation of Reactive Astrocytes: Role of PPARs. *Mol Neurobiol* 54: 2518-38

Ikawa M, Okazawa H, Kudo T, Kuriyama M, Fujibayashi Y, Yoneda M. 2011. Evaluation of striatal oxidative stress in patients with Parkinson's disease using [62Cu]ATSM PET. *Nuclear medicine and biology* 38: 945-51

Ikeda H, Miyatake M, Koshikawa N, Ochiai K, Yamada K, et al. 2010. Morphine modulation of thrombospondin levels in astrocytes and its implications for neurite outgrowth and synapse formation. *The Journal of biological chemistry* 285: 38415-27

Jackson KJ, Martin BR, Changeux JP, Damaj MI. 2008. Differential role of nicotinic acetylcholine receptor subunits in physical and affective nicotine withdrawal signs. *The Journal of pharmacology and experimental therapeutics* 325: 302-12

Jackson KJ, McIntosh JM, Brunzell DH, Sanjakdar SS, Damaj MI. 2009. The role of alpha6-containing nicotinic acetylcholine receptors in nicotine reward and withdrawal. *The Journal of pharmacology and experimental therapeutics* 331: 547-54

Jiloha R. 2010. Biological basis of tobacco addiction: Implications for smoking-cessation treatment. *Indian Journal of Psychiatry* 52: 301

Jiloha RC. 2014. Pharmacotherapy of smoking cessation. *Indian J Psychiatry* 56: 87-95

Karve TM, Rosen EM. 2012. B-cell translocation gene 2 (BTG2) stimulates cellular antioxidant defenses through the antioxidant transcription factor NFE2L2 in

human mammary epithelial cells. *The Journal of biological chemistry* 287: 31503-14

Khakh BS, Sofroniew MV. 2015. Diversity of astrocyte functions and phenotypes in neural circuits. *Nature neuroscience* 18: 942-52

Kim K, Lee SG, Kegelman TP, Su ZZ, Das SK, et al. 2011. Role of excitatory amino acid transporter-2 (EAAT2) and glutamate in neurodegeneration: opportunities for developing novel therapeutics. *J Cell Physiol* 226: 2484-93

Kim KS, Lee KW, Baek IS, Lim CM, Krishnan V, et al. 2008. Adenylyl cyclase-5 activity in the nucleus accumbens regulates anxiety-related behavior. *J Neurochem* 107: 105-15

King JR, Gillevet TC, Kabbani N. 2017. A G protein-coupled alpha7 nicotinic receptor regulates signaling and TNF-alpha release in microglia. *FEBS Open Bio* 7: 1350-61

Knackstedt LA, LaRowe S, Mardikian P, Malcolm R, Upadhyaya H, et al. 2009. The role of cystine-glutamate exchange in nicotine dependence in rats and humans. *Biological psychiatry* 65: 841-5

Koob G, Kreek MJ. 2007. Stress, dysregulation of drug reward pathways, and the transition to drug dependence. *Am J Psychiatry* 164: 1149-59

Kuleshov MV, Jones MR, Rouillard AD, Fernandez NF, Duan Q, et al. 2016. Enrichr: a comprehensive gene set enrichment analysis web server 2016 update. *Nucleic acids research* 44: W90-7

Kutlu MG, Gould TJ. 2016. Effects of drugs of abuse on hippocampal plasticity and hippocampus-dependent learning and memory: contributions to development and maintenance of addiction. *Learning & memory* 23: 515-33

Lee BG, Anastasia A, Hempstead BL, Lee FS, Blendy JA. 2015. Effects of the BDNF Val66Met Polymorphism on Anxiety-Like Behavior Following Nicotine Withdrawal in Mice. *Nicotine & tobacco research : official journal of the Society for Research on Nicotine and Tobacco* 17: 1428-35

Lee M, Schwab C, McGeer PL. 2011. Astrocytes are GABAergic cells that modulate microglial activity. *Glia* 59: 152-65

Lee SY, Lee SY, Choi Y. 1997. TRAF-interacting protein (TRIP): a novel component of the tumor necrosis factor receptor (TNFR)- and CD30-TRAF signaling complexes that inhibits TRAF2-mediated NF-kappaB activation. *J Exp Med* 185: 1275-85

Leventhal AM, Ameringer KJ, Osborn E, Zvolensky MJ, Langdon KJ. 2013. Anxiety and depressive symptoms and affective patterns of tobacco withdrawal. *Drug Alcohol Depend* 133: 324-9

Leventhal AM, Strong DR, Kirkpatrick MG, Unger JB, Sussman S, et al. 2015. Association of Electronic Cigarette Use With Initiation of Combustible Tobacco Product Smoking in Early Adolescence. *Jama* 314: 700-7

Levita L, Hoskin R, Champi S. 2012. Avoidance of harm and anxiety: A role for the nucleus accumbens. *NeuroImage* 62: 189-98

Lewitus GM, Konefal SC, Greenhalgh AD, Pribiag H, Augereau K, Stellwagen D. 2016a. Microglial TNF-alpha Suppresses Cocaine-Induced Plasticity and Behavioral Sensitization. *Neuron* 90: 483-91

Lewitus Gil M, Konefal Sarah C, Greenhalgh Andrew D, Pribiag H, Augereau K, Stellwagen D. 2016b. Microglial TNF-α Suppresses Cocaine-Induced Plasticity and Behavioral Sensitization. *Neuron* 90: 483-91

Li G, Gong J, Lei H, Liu J, Xu XZS. 2016. Promotion of behavior and neuronal function by reactive oxygen species in C. elegans. *Nature Communications* 7: 13234

Li Z, Ma L, Kulesskaya N, Voikar V, Tian L. 2014. Microglia are polarized to M1 type in high-anxiety inbred mice in response to lipopolysaccharide challenge. *Brain, behavior, and immunity* 38: 237-48

Liao Y, Smyth GK, Shi W. 2014. featureCounts: an efficient general purpose program for assigning sequence reads to genomic features. *Bioinformatics* 30: 923-30

Liu W, Tang Y, Feng J. 2011. Cross talk between activation of microglia and astrocytes in pathological conditions in the central nervous system. *Life Sci* 89: 141-6

Liu Y, Zeng X, Hui Y, Zhu C, Wu J, et al. 2015. Activation of alpha7 nicotinic acetylcholine receptors protects astrocytes against oxidative stress-induced apoptosis: implications for Parkinson's disease. *Neuropharmacology* 91: 87-96

Livak KJ, Schmittgen TD. 2001. Analysis of relative gene expression data using real-time quantitative PCR and the 2(-Delta Delta C(T)) Method. *Methods* 25: 402-8

Lopez-Hidalgo M, Salgado-Puga K, Alvarado-Martinez R, Medina AC, Prado-Alcala RA, Garcia-Colunga J. 2012. Nicotine uses neuron-glia communication to enhance hippocampal synaptic transmission and long-term memory. *PloS one* 7: e49998

Lorberbaum JP, Kose S, Johnson MR, Arana GW, Sullivan LK, et al. 2004. Neural correlates of speech anticipatory anxiety in generalized social phobia. *Neuroreport* 15: 2701-5

Love MI, Huber W, Anders S. 2014. Moderated estimation of fold change and dispersion for RNA-seq data with DESeq2. *Genome Biol* 15: 550

Lu JYD, Su P, Barber JEM, Nash JE, Le AD, et al. 2017. The neuroprotective effect of nicotine in Parkinson's disease models is associated with inhibiting PARP-1 and caspase-3 cleavage. *PeerJ* 5: e3933

Lull ME, Block ML. 2010. Microglial activation and chronic neurodegeneration. *Neurotherapeutics : the journal of the American Society for Experimental NeuroTherapeutics* 7: 354-65

Ma MW, Wang J, Zhang Q, Wang R, Dhandapani KM, et al. 2017. NADPH oxidase in brain injury and neurodegenerative disorders. *Molecular Neurodegeneration* 12

Madore C, Baufeld C, Butovsky O. 2017. Microglial confetti party. *Nature neuroscience* 20: 762-63

Madsen HB, Brown RM, Lawrence AJ. 2012. Neuroplasticity in addiction: cellular and transcriptional perspectives. *Front Mol Neurosci* 5: 99

Maes M, Galecki P, Chang YS, Berk M. 2011. A review on the oxidative and nitrosative stress (O&NS) pathways in major depression and their possible contribution to the (neuro)degenerative processes in that illness. *Prog Neuropsychopharmacol Biol Psychiatry* 35: 676-92

Manhaes AC, Guthierrez MC, Filgueiras CC, Abreu-Villaca Y. 2008. Anxiety-like behavior during nicotine withdrawal predict subsequent nicotine consumption in adolescent C57BL/6 mice. *Behavioural brain research* 193: 216-24

Markou A. 2008. Neurobiology of nicotine dependence. *Philosophical Transactions of the Royal Society B: Biological Sciences* 363: 3159-68

Matta SG, Balfour DJ, Benowitz NL, Boyd RT, Buccafusco JJ, et al. 2007. Guidelines on nicotine dose selection for in vivo research. *Psychopharmacology* 190: 269-319

McCarthy MM. 2017. Location, Location, Location: Microglia Are Where They Live. *Neuron* 95: 233-35

McLaughlin I, Dani JA, De Biasi M. 2015. Nicotine Withdrawal In *The Neuropharmacology of Nicotine Dependence*, ed. DJK Balfour, MR Munafò, pp. 99-123. Cham: Springer International Publishing

Mencel M, Nash M, Jacobson C. 2013. Neuregulin upregulates microglial alpha7 nicotinic acetylcholine receptor expression in immortalized cell lines: implications for regulating neuroinflammation. *PloS one* 8: e70338

Miyamoto A, Wake H, Ishikawa AW, Eto K, Shibata K, et al. 2016. Microglia contact induces synapse formation in developing somatosensory cortex. *Nat Commun* 7: 12540

Mizutani M, Pino PA, Saederup N, Charo IF, Ransohoff RM, Cardona AE. 2012. The fractalkine receptor but not CCR2 is present on microglia from embryonic development throughout adulthood. *Journal of immunology* 188: 29-36

Morganti JM, Jopson TD, Liu S, Riparip LK, Guandique CK, et al. 2015. CCR2 antagonism alters brain macrophage polarization and ameliorates cognitive dysfunction induced by traumatic brain injury. *The Journal of neuroscience : the official journal of the Society for Neuroscience* 35: 748-60

Morud J, Strandberg J, Andren A, Ericson M, Soderpalm B, Adermark L. 2018. Progressive modulation of accumbal neurotransmission and anxiety-like behavior following protracted nicotine withdrawal. *Neuropharmacology* 128: 86-95

Nayernia Z, Jaquet V, Krause KH. 2014. New insights on NOX enzymes in the central nervous system. *Antioxidants & redox signaling* 20: 2815-37

Nestler EJ. 2008. Review. Transcriptional mechanisms of addiction: role of DeltaFosB. *Philos Trans R Soc Lond B Biol Sci* 363: 3245-55

Newhouse P, Kellar K, Aisen P, White H, Wesnes K, et al. 2012. Nicotine treatment of mild cognitive impairment: a 6-month double-blind pilot clinical trial. *Neurology* 78: 91-101

Ng M, Freeman MK, Fleming TD, Robinson M, Dwyer-Lindgren L, et al. 2014. Smoking Prevalence and Cigarette Consumption in 187 Countries, 1980-2012. *Jama* 311: 183

Orient A, Donko A, Szabo A, Leto TL, Geiszt M. 2007. Novel sources of reactive oxygen species in the human body. *Nephrology, dialysis, transplantation : official publication of the European Dialysis and Transplant Association - European Renal Association* 22: 1281-8

Panday A, Sahoo MK, Osorio D, Batra S. 2015. NADPH oxidases: an overview from structure to innate immunity-associated pathologies. *Cellular & molecular immunology* 12: 5-23

Pang X, Liu L, Ngolab J, Zhao-Shea R, McIntosh JM, et al. 2016. Habenula cholinergic neurons regulate anxiety during nicotine withdrawal via nicotinic acetylcholine receptors. *Neuropharmacology* 107: 294-304

Parikh V, Cole RD, Patel PJ, Poole RL, Gould TJ. 2016. Cognitive control deficits during mecamylamine-precipitated withdrawal in mice: Possible links to frontostriatal BDNF imbalance. *Neurobiology of learning and memory* 128: 110-6

Patki G, Solanki N, Atrooz F, Allam F, Salim S. 2013. Depression, anxiety-like behavior and memory impairment are associated with increased oxidative stress and inflammation in a rat model of social stress. *Brain research* 1539: 73-86

Patterson F, Jepson C, Strasser AA, Loughead J, Perkins KA, et al. 2009. Varenicline improves mood and cognition during smoking abstinence. *Biological psychiatry* 65: 144-9

Peixoto A, Fernandes E, Gaiteiro C, Lima L, Azevedo R, et al. 2016. Hypoxia enhances the malignant nature of bladder cancer cells and concomitantly antagonizes protein O-glycosylation extension. *Oncotarget* 7: 63138-57

Peng X, Gerzanich V, Anand R, Whiting PJ, Lindstrom J. 1994. Nicotine-induced increase in neuronal nicotinic receptors results from a decrease in the rate of receptor turnover. *Molecular pharmacology* 46: 523-30

Perry VH, Nicoll JA, Holmes C. 2010. Microglia in neurodegenerative disease. *Nature reviews. Neurology* 6: 193-201

Picciotto MR, Addy NA, Mineur YS, Brunzell DH. 2008. It is not "either/or": activation and desensitization of nicotinic acetylcholine receptors both contribute to behaviors related to nicotine addiction and mood. *Prog Neurobiol* 84: 329-42

Piper ME, Cook JW, Schlam TR, Jorenby DE, Baker TB. 2011. Anxiety diagnoses in smokers seeking cessation treatment: relations with tobacco dependence, withdrawal, outcome and response to treatment. *Addiction* 106: 418-27

Polosa R, Benowitz NL. 2011. Treatment of nicotine addiction: present therapeutic options and pipeline developments. *Trends Pharmacol Sci* 32: 281-9

Portugal GS, Gould TJ. 2007. Bupropion dose-dependently reverses nicotine withdrawal deficits in contextual fear conditioning. *Pharmacology, biochemistry, and behavior* 88: 179-87

Portugal GS, Kenney JW, Gould TJ. 2008. Beta2 subunit containing acetylcholine receptors mediate nicotine withdrawal deficits in the acquisition of contextual fear conditioning. *Neurobiology of learning and memory* 89: 106-13

Portugal GS, Wilkinson DS, Turner JR, Blendy JA, Gould TJ. 2012. Developmental effects of acute, chronic, and withdrawal from chronic nicotine on fear conditioning. *Neurobiology of learning and memory* 97: 482-94

Primack BA, Soneji S, Stoolmiller M, Fine MJ, Sargent JD. 2015. Progression to Traditional Cigarette Smoking After Electronic Cigarette Use Among US Adolescents and Young Adults. *JAMA pediatrics* 169: 1018-23

Prinz M, Priller J. 2010. Tickets to the brain: role of CCR2 and CX3CR1 in myeloid cell entry in the CNS. *J Neuroimmunol* 224: 80-4

Prochaska JJ, Benowitz NL. 2016. The Past, Present, and Future of Nicotine Addiction Therapy. *Annual Review of Medicine* 67: 467-86

Qin L, Liu Y, Wang T, Wei SJ, Block ML, et al. 2004. NADPH oxidase mediates lipopolysaccharide-induced neurotoxicity and proinflammatory gene expression in activated microglia. *The Journal of biological chemistry* 279: 1415-21

Quik M, Huang LZ, Parameswaran N, Bordia T, Campos C, Perez XA. 2009. Multiple roles for nicotine in Parkinson's disease. *Biochem Pharmacol* 78: 677-85

Ransohoff RM. 2016. A polarizing question: do M1 and M2 microglia exist? *Nature neuroscience* 19: 987-91

Rastogi R, Geng X, Li F, Ding Y. 2016. NOX Activation by Subunit Interaction and Underlying Mechanisms in Disease. *Frontiers in cellular neuroscience* 10: 301

Reitsma MB, Fullman N, Ng M, Salama JS, Abajobir A, et al. 2017. Smoking prevalence and attributable disease burden in 195 countries and territories, 1990–2015: a systematic analysis from the Global Burden of Disease Study 2015. *The Lancet* 389: 1885-906

Rezvani K, Teng Y, Shim D, De Biasi M. 2007. Nicotine regulates multiple synaptic proteins by inhibiting proteasomal activity. *The Journal of neuroscience : the official journal of the Society for Neuroscience* 27: 10508-19

Rollema H, Chambers LK, Coe JW, Glowa J, Hurst RS, et al. 2007. Pharmacological profile of the alpha4beta2 nicotinic acetylcholine receptor partial agonist varenicline, an effective smoking cessation aid. *Neuropharmacology* 52: 985-94

Ross GW, Petrovitch H. 2001. Current evidence for neuroprotective effects of nicotine and caffeine against Parkinson's disease. *Drugs & aging* 18: 797-806

Russo SJ, Nestler EJ. 2013. The brain reward circuitry in mood disorders. *Nature Reviews Neuroscience* 14: 609-25

Saederup N, Cardona AE, Croft K, Mizutani M, Cotleur AC, et al. 2010. Selective chemokine receptor usage by central nervous system myeloid cells in CCR2-red fluorescent protein knock-in mice. *PloS one* 5: e13693

Salim S, Sarraj N, Taneja M, Saha K, Tejada-Simon MV, Chugh G. 2010. Moderate treadmill exercise prevents oxidative stress-induced anxiety-like behavior in rats. *Behavioural brain research* 208: 545-52

Sallette J, Pons S, Devillers-Thiery A, Soudant M, Prado de Carvalho L, et al. 2005. Nicotine upregulates its own receptors through enhanced intracellular maturation. *Neuron* 46: 595-607

Salter MW, Stevens B. 2017. Microglia emerge as central players in brain disease. *Nature medicine* 23: 1018-27

Samet JM. 2013. Tobacco smoking: the leading cause of preventable disease worldwide. *Thoracic surgery clinics* 23: 103-12

Saravia R, Ten-Blanco M, Grande MT, Maldonado R, Berrendero F. 2019. Anti-inflammatory agents for smoking cessation? Focus on cognitive deficits associated with nicotine withdrawal in male mice. *Brain, behavior, and immunity* 75: 228-39

Schieber M, Chandel NS. 2014. ROS function in redox signaling and oxidative stress. *Current biology : CB* 24: R453-62

Schwarz JM, Bilbo SD. 2013. Adolescent morphine exposure affects long-term microglial function and later-life relapse liability in a model of addiction. *The*

Journal of neuroscience : the official journal of the Society for Neuroscience 33: 961-71

Schwarz JM, Smith SH, Bilbo SD. 2013. FACS analysis of neuronal–glial interactions in the nucleus accumbens following morphine administration. *Psychopharmacology* 230: 525-35

Seo JS, Park JY, Choi J, Kim TK, Shin JH, et al. 2012. NADPH oxidase mediates depressive behavior induced by chronic stress in mice. *The Journal of neuroscience : the official journal of the Society for Neuroscience* 32: 9690-9

Sharma G, Vijayaraghavan S. 2001. Nicotinic cholinergic signaling in hippocampal astrocytes involves calcium-induced calcium release from intracellular stores. *Proceedings of the National Academy of Sciences of the United States of America* 98: 4148-53

Sharples CGV, Kaiser S, Soliakov L, Marks MJ, Collins AC, et al. 2000. UB-165: A Novel Nicotinic Agonist with Subtype Selectivity Implicates the α4β2* Subtype in the Modulation of Dopamine Release from Rat Striatal Synaptosomes. *The Journal of Neuroscience* 20: 2783-91

Shytle RD, Mori T, Townsend K, Vendrame M, Sun N, et al. 2004. Cholinergic modulation of microglial activation by alpha 7 nicotinic receptors. *J Neurochem* 89: 337-43

Sidiropoulos K, Viteri G, Sevilla C, Jupe S, Webber M, et al. 2017. Reactome enhanced pathway visualization. *Bioinformatics* 33: 3461-67

Sofroniew MV, Vinters HV. 2010. Astrocytes: biology and pathology. *Acta Neuropathologica* 119: 7-35

Spencer S, Kalivas PW. 2017. Glutamate Transport: A New Bench to Bedside Mechanism for Treating Drug Abuse. *Int J Neuropsychopharmacol* 20: 797-812

Stansley B, Post J, Hensley K. 2012. A comparative review of cell culture systems for the study of microglial biology in Alzheimer's disease. *J Neuroinflammation* 9: 115

Stein DJ, Vasconcelos MF, Albrechet-Souza L, Cereser KMM, de Almeida RMM. 2017. Microglial Over-Activation by Social Defeat Stress Contributes to Anxiety- and Depressive-Like Behaviors. *Front Behav Neurosci* 11: 207

Stoker AK, Semenova S, Markou A. 2008. Affective and somatic aspects of spontaneous and precipitated nicotine withdrawal in C57BL/6J and BALB/cByJ mice. *Neuropharmacology* 54: 1223-32

Streit WJ. 2002. Microglia as neuroprotective, immunocompetent cells of the CNS. *Glia* 40: 133-9

Sun SY. 2010. N-acetylcysteine, reactive oxygen species and beyond. *Cancer biology & therapy* 9: 109-10

Suzuki H, Sugimura Y, Iwama S, Suzuki H, Nobuaki O, et al. 2010a. Minocycline prevents osmotic demyelination syndrome by inhibiting the activation of microglia. *Journal of the American Society of Nephrology : JASN* 21: 2090-8

Suzuki T, Hide I, Matsubara A, Hama C, Harada K, et al. 2006. Microglial alpha7 nicotinic acetylcholine receptors drive a phospholipase C/IP3 pathway and modulate the cell activation toward a neuroprotective role. *J Neurosci Res* 83: 1461-70

Suzuki YJ, Carini M, Butterfield DA. 2010b. Protein carbonylation. *Antioxidants & redox signaling* 12: 323-5

Szepesi Z, Manouchehrian O, Bachiller S, Deierborg T. 2018. Bidirectional Microglia-Neuron Communication in Health and Disease. *Frontiers in cellular neuroscience* 12: 323

Tang Y, Le W. 2016. Differential Roles of M1 and M2 Microglia in Neurodegenerative Diseases. *Mol Neurobiol* 53: 1181-94

Tariq M, Khan HA, Elfaki I, Al Deeb S, Al Moutaery K. 2005. Neuroprotective effect of nicotine against 3-nitropropionic acid (3-NP)-induced experimental Huntington's disease in rats. *Brain research bulletin* 67: 161-8

Teaktong T, Graham A, Court J, Perry R, Jaros E, et al. 2003. Alzheimer's disease is associated with a selective increase in alpha7 nicotinic acetylcholine receptor immunoreactivity in astrocytes. *Glia* 41: 207-11

Torregrossa MM, Corlett PR, Taylor JR. 2011. Aberrant learning and memory in addiction. *Neurobiology of learning and memory* 96: 609-23

Torres L, Danver J, Ji K, Miyauchi JT, Chen D, et al. 2016. Dynamic microglial modulation of spatial learning and social behavior. *Brain, behavior, and immunity* 55: 6-16

Torres OV, Pipkin JA, Ferree P, Carcoba LM, O'Dell LE. 2015. Nicotine withdrawal increases stress-associated genes in the nucleus accumbens of female rats in a hormone-dependent manner. *Nicotine & tobacco research : official journal of the Society for Research on Nicotine and Tobacco* 17: 422-30

Tumkosit P, Kuryatov A, Luo J, Lindstrom J. 2006. Beta3 subunits promote expression and nicotine-induced up-regulation of human nicotinic alpha6* nicotinic acetylcholine receptors expressed in transfected cell lines. *Molecular pharmacology* 70: 1358-68

Turner JR, Ecke LE, Briand LA, Haydon PG, Blendy JA. 2013a. Cocaine-related behaviors in mice with deficient gliotransmission. *Psychopharmacology* 226: 167-76

Turner JR, Ray R, Lee B, Everett L, Xiang J, et al. 2014. Evidence from mouse and man for a role of neuregulin 3 in nicotine dependence. *Mol Psychiatry* 19: 801-10

Turner JR, Wilkinson DS, Poole RLF, Gould TJ, Carlson GC, Blendy JA. 2013b. Divergent Functional Effects of Sazetidine-A and Varenicline During Nicotine Withdrawal. *Neuropsychopharmacology : official publication of the American College of Neuropsychopharmacology* 38: 2035-47

van der Kooij MA, Hollis F, Lozano L, Zalachoras I, Abad S, et al. 2018. Diazepam actions in the VTA enhance social dominance and mitochondrial function in the nucleus accumbens by activation of dopamine D1 receptors. *Molecular Psychiatry* 23: 569-78

Victor VM, Rocha M, De la Fuente M. 2003. Regulation of macrophage function by the antioxidant N-acetylcysteine in mouse-oxidative stress by endotoxin. *International immunopharmacology* 3: 97-106

Villafane G, Cesaro P, Rialland A, Baloul S, Azimi S, et al. 2007. Chronic high dose transdermal nicotine in Parkinson's disease: an open trial. *European journal of neurology* 14: 1313-6

Volkow ND, Li T-K. 2004. Science and Society: Drug addiction: the neurobiology of behaviour gone awry. *Nature Reviews Neuroscience* 5: 963-70

Volkow Nora D, Morales M. 2015. The Brain on Drugs: From Reward to Addiction. *Cell* 162: 712-25

Wang X, Pal R, Chen XW, Kumar KN, Kim OJ, Michaelis EK. 2007. Genome-wide transcriptome profiling of region-specific vulnerability to oxidative stress in the hippocampus. *Genomics* 90: 201-12

Wang YL, Han QQ, Gong WQ, Pan DH, Wang LZ, et al. 2018. Microglial activation mediates chronic mild stress-induced depressive- and anxiety-like behavior in adult rats. *J Neuroinflammation* 15: 21

Watanabe S, Takahashi N, Uchida H, Wakasugi K. 2012. Human neuroglobin functions as an oxidative stress-responsive sensor for neuroprotection. *The Journal of biological chemistry* 287: 30128-38

Weinhard L, di Bartolomei G, Bolasco G, Machado P, Schieber NL, et al. 2018. Microglia remodel synapses by presynaptic trogocytosis and spine head filopodia induction. *Nat Commun* 9: 1228

Whiting PJ, Lindstrom JM. 1988. Characterization of bovine and human neuronal nicotinic acetylcholine receptors using monoclonal antibodies. *The Journal of neuroscience : the official journal of the Society for Neuroscience* 8: 3395-404

Wickramasekara RN, Morrill S, Farhat Y, Smith SJ, Yilmazer-Hanke D. 2018. Glutathione and Inter-alpha-trypsin inhibitor heavy chain 3 (Itih3) mRNA levels in nicotine-treated Cd44 knockout mice. *Toxicol Rep* 5: 759-64

Wilson AL, Langley LK, Monley J, Bauer T, Rottunda S, et al. 1995. Nicotine patches in Alzheimer's disease: pilot study on learning, memory, and safety. *Pharmacology, biochemistry, and behavior* 51: 509-14

Wonnacott S. 1990. The paradox of nicotinic acetylcholine receptor upregulation by nicotine. *Trends Pharmacol Sci* 11: 216-9

World Health Organization. 2012. WHO global report: mortality attributable to tobacco.Geneva,Switzerland. http://apps.who.int/iris/bitstream/10665/44815/1/9789241564434_eng.pdf.

Xiao C, Nashmi R, McKinney S, Cai H, McIntosh JM, Lester HA. 2009. Chronic Nicotine Selectively Enhances 4 2* Nicotinic Acetylcholine Receptors in the Nigrostriatal Dopamine Pathway. *Journal of Neuroscience* 29: 12428-39

Xiao Y, Fan H, Musachio JL, Wei ZL, Chellappan SK, et al. 2006. Sazetidine-A, a novel ligand that desensitizes alpha4beta2 nicotinic acetylcholine receptors without activating them. *Molecular pharmacology* 70: 1454-60

Yager LM, Garcia AF, Wunsch AM, Ferguson SM. 2015. The ins and outs of the striatum: role in drug addiction. *Neuroscience* 301: 529-41

Yohn NL, Turner JR, Blendy JA. 2014. Activation of alpha4beta2*/alpha6beta2* nicotinic receptors alleviates anxiety during nicotine withdrawal without upregulating nicotinic receptors. *The Journal of pharmacology and experimental therapeutics* 349: 348-54

Zhang T, Zhang L, Liang Y, Siapas AG, Zhou FM, Dani JA. 2009. Dopamine Signaling Differences in the Nucleus Accumbens and Dorsal Striatum Exploited by Nicotine. *Journal of Neuroscience* 29: 4035-43

Zhang W, Xiao S, Ahn DU. 2013. Protein oxidation: basic principles and implications for meat quality. *Critical reviews in food science and nutrition* 53: 1191-201

Zhang Y, Chen K, Sloan SA, Bennett ML, Scholze AR, et al. 2014. An RNA-sequencing transcriptome and splicing database of glia, neurons, and vascular cells of the cerebral cortex. *The Journal of neuroscience : the official journal of the Society for Neuroscience* 34: 11929-47

Zhang Y, Sloan SA, Clarke LE, Caneda C, Plaza CA, et al. 2016. Purification and Characterization of Progenitor and Mature Human Astrocytes Reveals Transcriptional and Functional Differences with Mouse. *Neuron* 89: 37-53

Zhu F, Zheng Y, Ding YQ, Liu Y, Zhang X, et al. 2014. Minocycline and risperidone prevent microglia activation and rescue behavioral deficits induced by neonatal intrahippocampal injection of lipopolysaccharide in rats. *PloS one* 9: e93966

Zoli M, Moretti M, Zanardi A, McIntosh JM, Clementi F, Gotti C. 2002. Identification of the nicotinic receptor subtypes expressed on dopaminergic terminals in

the rat striatum. *The Journal of neuroscience : the official journal of the Society for Neuroscience* 22: 8785

APPENDIX A

CODE FOR RNA SEQUENCING ANALYSIS

```
######################################################################
##################RNA-Seq Data Analysis Pipeline on UNIX #############
#mm10 genome was downloaded from iGenomes
#https://support.illumina.com/sequencing/sequencing_software/igenome.html

#Generating genome indexes
module load gcc/4.9.1
module load star/2.5

STAR --runThreadN 20 --runMode genomeGenerate --genomeDir
/work/adeluyi/mm10genome_indexes --genomeFastaFiles
/work/adeluyi/mm10genome/mm10genome.fa --sjdbGTFfile
/work/adeluyi/mm10genome/mm10genes.gtf --sjdbOverhang 75

#Checking read quality using FastQC
module load fastqc/0.11.5

for i in /work/adeluyi/input_folder/cat_files/*fastq.gz;
do fastqc --outdir /work/adeluyi/output_folder/fq_files -t 10 $i;
```

```
done

#For reads that need adapter trimming
module load bbmap/gcc/38.16

for i in `ls -1 /work/adeluyi/input_folder/ fastq_file/*_1.fastq.gz | sed
's/_1.fastq.gz//'`
do bbduk.sh in1=$i\_1.fastq.gz in2=$i\_2.fastq.gz
out1=$i\_clean_1.fastq.gz out2=$i\_clean_2.fastq.gz ktrim=r k=21
literal=GATCGGAAGAGCACACGTCTGAACTCCAGTCACTGATCACGATCTCG
TATGCCGTCTTCTGCTTGAAAAAAAAAA,GATCGGAAGAGCGTCGTGTAGGG
AAAGAGTGTCGTGATCAGTGTAGATCTCGGTGGTCGCCGTATCATTAAAAAA
,ATCGGAAGAGCACACGTCTGAACTCCAGTCACCCACATTGATCTCGTATGC
CGTCTTCTGCTTGAAAAAAAAAAA,ATCGGAAGAGCGTCGTGTAGGGAAAGA
GTGTCAATGTGGGTGTAGATCTCGGTGGTCGCCGTATCATTAAAAAAA,AAA
AAAAAAAAAAAAAAAAAAAAAAAAAAAAAAAAAAAAAAAAAAAAAAAAAAA
AAAAAAAAAAAAAAAAAA,TTTTTTTTTTTTTTTTTTTTTTTTTTTTTTTTTT
TTTTTTTTTTTTTTTTTTTTTTTTTTTTTTTTTT tbo tpe
done

#Mapping reads to genome
module load gcc/4.9.1
module load star/2.5
```

```
for i in $(ls /work/adeluyi/input folder/cat_files | sed s/_[12].fastq.gz// | sort -u);

do STAR --genomeDir /work/adeluyi/mm10genome_indexes --readFilesIn
/work/adeluyi/input folder/cat_files/${i}_1.fastq.gz
/work/adeluyi/input_folder/cat_files/${i}_2.fastq.gz
--runThreadN 20 --outFileNamePrefix
/work/adeluyi/output_folder/mapped_reads/$i.
--sjdbGTFfile /work/adeluyi/mm10genome/mm10genes.gtf
--sjdbOverhang 75 --readFilesCommand zcat;
done

#Read count and summarization
module load subread/1.5.3

featureCounts -p -s 2 -t exon -g gene_id -a
/work/adeluyi/mm10genome/mm10genes.gtf -o
/work/adeluyi/output_folder/count_files/ count.txt
/work/adeluyi/input_folder/mapped_reads/*Aligned.out.sam*
```

```
#####################################################################
################## Statistical Data Analysis on R Software##################
#For this part, I am using the analysis of NAc48hWD experiment as an example. Other experiments (NAc24hWD, Microglia-specific and Astrocyte-specific experiments) were passed through the same analysis pipeline.

NAc = read.csv("NAc48hWD_count.csv", header = T)
head(NAc)

####### Filter out low read counts
lowread = apply(NAc,1,max)
whcount = which(lowread<5)
length(whcount)
NAc_data = NAc[-whcount,]
dim(NAc_data)
rownames(NAc_data) = NAc_data$Geneid
head(NAc_data)
NAc_data = NAc_data[,-1]
head(NAc_data)
NAc_data1=data.frame(Gene=rownames(NAc_data),Sal1=NAc_data$Sal1,Sal2
=NAc_data$Sal2,Sal3=NAc_data$Sal3,Sal4=NAc_data$Sal4,Nic1=NAc_data$Ni
c5,Nic2=NAc_data$Nic6,Nic3=NAc_data$Nic7,WD1=NAc_data$WD8,WD2=NAc
_data$WD9,WD3=NAc_data$WD10)
```

```
rownames(NAc_data1) = NAc_data1$Gene

head(NAc_data1)

NAc_data1 = NAc_data1[,-1]

head(NAc_data1)

Nlen = as.vector(NAc_data$Length)


########## Differential Expression Analysis

NAc_col= read.csv("NAc_metadata.csv",header = T)

head(NAc_col)

NAc_col=data.frame(Sample=NAc_col$Sample,Treatment= NAc_col$Treatment)


BiocManager::install(c("DESeq2","GenomicFeatures", "AnnotationDbi"))

BiocManager::install(c("rtracklayer","GenomicAlignments", "Rsamtools"))

library("DESeq2")

library("AnnotationDbi")

library("GenomicFeatures")

library("rtracklayer")

library("Rsamtools")

library("GenomicAlignments")


NAc_dds = DESeqDataSetFromMatrix(NAc_data1,NAc_col,~Treatment)

NAc_dds1<-DESeq(NAc_dds)

res_NAc<-results(NAc_dds1)
```

```
head(res_NAc)

plotMA(res_NAc, main="MA Plot with DESeq2: 48hWD Nicotine Studies")
tsig_NAc = table(res_NAc[,6]<0.2)
tsig_res_NAc = which(res_NAc[,6]<0.2)
sig_NAc = res_NAc[tsig_res_NAc,]
head(sig_NAc)
rownames(sig_NAc)

sig_ordNAc = sig_NAc[order(sig_NAc$log2FoldChange,decreasing = TRUE),]
head(sig_ordNAc)
DEG=data.frame(Gene=rownames(sig_ordNAc),log2FC=sig_ordNAc$log2FoldC
hange,pvalue=sig_ordNAc$pvalue,padj=sig_ordNAc$padj)
row.names(DEG)<- NULL
write.csv(DEG,"NAc_DEG(48hWD).csv", row.names = FALSE)
NAc48hWD_cutoff = DEG[DEG$log2FC>0.5|DEG$log2FC < -0.5,]
write.csv(NAc48hWD_cutoff,"NAc48hWD_cutoff.csv", row.names = FALSE)

############ PCA plot
N_rld <- rlog(NAc_dds1, blind=FALSE)
plotPCA(N_rld, intgroup=c("Sample", "Treatment"))
```

```
############ Volcano plot
install.packages("ggrepel")
library("ggrepel")
install.packages("plyr")
library("plyr")
library("dplyr")

# Cutoff for differential expression
fc = 0.5
cf = -0.5
pval = 0.2

DEG1=data.frame(Gene=rownames(sig_ordNAc),log2FC=(1*sig_ordNAc$log2F
oldChange),pvalue=sig_ordNAc$pvalue,qvalue=sig_ordNAc$padj)
head(DEG1)
Ntex=c("Nr4a3","C4b","Cybb","Sparc","Malat1","Chat","Adamts14","Dusp4","Ada
mts8","Stard8","CD38","Stat4","Gpr165","Mef2c","Slc6a11","Hck","Egln3","Itih3")
N_genes = DEG1[DEG1$Gene %in% Ntex,]
N_res=data.frame(Gene=rownames(res_NAc),log2FC=(1*res_NAc$log2FoldCha
nge),pvalue=res_NAc$pvalue,qvalue=res_NAc$padj)
head(N_res)
Nlog_res=data.frame(log2FC=(-1*res_NAc$log2FoldChange),neglogP=-
log10(res_NAc$pvalue),neglogFDR=-log10(res_NAc$padj))
```

```
rownames(Nlog_res) = rownames(res_NAc)
head(Nlog_res)

N_resmut=mutate(N_res,Expression=ifelse(Nlog_res$log2FC>fc&
Nlog_res$neglogFDR> -log10(pval), "Upregulated", ifelse(Nlog_res$log2FC<cf &
Nlog_res$neglogFDR> -log10(pval),"Downregulated”,” Not significant")))
table(N_resmut$Expression)
head(N_resmut)
volc=ggplot(na.omit(N_resmut)) + aes(x=log2FC, y=-log10(qvalue)) +
geom_point(aes(color = Expression),alpha=0.65) +
scale_color_manual(values = c("blue","grey40","firebrick3")) + xlim(c(-6.5, 6)) +
ylim(c(0,5)) +
ggtitle("VOLCANO PLOT","Differentially Expressed Genes")+
geom_vline(xintercept = c(-0.5,0.5), colour = "grey30") +
geom_hline(yintercept = 0.69, colour = "grey30") +
theme(plot.background = element_rect(), panel.grid.major=element_blank(),
panel.grid.minor=element_blank(),panel.background=element_rect(fill = "white"))

volc+geom_text_repel(data=N_genes, aes(label = Gene), size = 5,
        box.padding = unit(0.5, "lines"),
        point.padding = unit(0.15, "lines"),segment.size = 0.5, direction = c("both") )
```

```
###########Transcript per million (TPM) normalization
tpm <- function(coun,leng) {
  x <- coun/leng
  return(t(t(x)*1e6/colSums(x)))
}
N_TPM = tpm(NAc_data1, Nlen)
head(N_TPM)

########### Heatmap
install.packages("pheatmap")
library("pheatmap")

#For All Genes
N_TPM = as.data.frame(N_TPM)
head(N_TPM)
N_TPMmeans = rowMeans(N_TPM)
head(N_TPMmeans)
N_TPMsd<- vector(length=nrow(N_TPM), mode="numeric")
for(i in 1:nrow(N_TPM)){N_TPMsd[i]<-sd(N_TPM[i,])}
head(N_TPMsd)
N_TPMZscore<- (N_TPM-N_TPMmeans)/N_TPMsd
head(N_TPMZscore)
N_TPMZscore = na.omit(N_TPMZscore)
```

```
N_TPMpheat<-as.matrix(N_TPMZscore)

N_annot = data.frame(Sample = factor(rep(c("Sal","Nic","48hWD"),c(4,3,3))))
N_ann = list(Sample = c(Sal="grey80",Nic="grey50","48hWD" ="darkgreen"))
rownames(N_annot) = colnames(N_TPMpheat)
pheatmap(N_TPMpheat, cluster_cols = FALSE,gaps_col = c(4,7),labels_col =
c("","","","","","","","","","","),color = colorRampPalette(c("navy","white","firebrick3"
))(50),annotation_col = N_annot, annotation_colors = N_ann)

# Extracting DEGs (that passed the cutoff) from the matrix
N_TPM1 = NAc_data1[rownames(NAc_data1)%in%NAc48hWD_cutoff$Gene,]
Nlen1 = NAc[NAc$Geneid %in% NAc48hWD_cutoff$Gene,]
Nlen1 = Nlen1$Length
N_TPM1 = tpm(N_TPM1,Nlen1)
head(N_TPM1)
N_TPM2 = as.data.frame(N_TPM1)
head(N_TPM2)
N2_TPMmeans = rowMeans(N_TPM2)
head(N2_TPMmeans)
N2_TPMsd<- vector(length=nrow(N_TPM2), mode="numeric")
for(i in 1:nrow(N_TPM2)){N2_TPMsd[i]<-sd(N_TPM2[i,])}
head(N2_TPMsd)
N2_TPMZscore<- (N_TPM2-N2_TPMmeans)/N2_TPMsd
```

```
head(N2_TPMZscore)
N_pheat<-as.matrix(N2_TPMZscore)

N_annot = data.frame( Sample = factor(rep(c("Sal","Nic","48hWD"),c(4,3,3))))
N_ann = list(Sample = c(Sal="grey80",Nic="grey50","48hWD" ="darkgreen"))
rownames(N_annot) = colnames(N_pheat)
pheatmap(N_pheat,cluster_cols=FALSE,gaps_col=c(4,7),cutree_rows=2,labels_
col=c("","","","","","","","","",""),color=colorRampPalette(c("navy","white","firebrick3"
))(50),annotation_col = N_annot, annotation_colors = N_ann)

##########Two-way Analysis
#Extracting the dataframe of sample treatments to be compared from the dataframe containing all samples
NAc_SN = NAc_data1[,-(8:10)]
head(NAc_SN)
NAc_SWD = NAc_data1[,-(5:7)]
head(NAc_SWD)
NAc_NWD = NAc_data1[,-(1:4)]
head(NAc_NWD)
SN_col = NAc_col[-(8:10),]
head(SN_col)
SWD_col = NAc_col[-(5:7),]
head(SWD_col)
```

```
NWD_col = NAc_col[-(1:4),]
head(NWD_col)

######## Sal vs Nic
SN_dds = DESeqDataSetFromMatrix(NAc_SN,SN_col,~Treatment)
SN_dds1<-DESeq(SN_dds)
res_SN<-results(SN_dds1)
head(res_SN)

plotMA(res_SN, main="MA Plot with DESeq2: 48hWD Nicotine Studies")
tsig_SN = table(res_SN[,6]<0.2)
tsig_res_SN = which(res_SN[,6]<0.2)
sig_SN = res_SN[tsig_res_SN,]
head(sig_SN)

sig_ordSN = sig_SN[order(sig_SN$log2FoldChange,decreasing = TRUE),]
head(sig_ordSN)
SN_DEG=data.frame(Gene=rownames(sig_ordSN),log2FC=sig_ordSN$log2Fold
Change,pvalue=sig_ordSN$pvalue,padj=sig_ordSN$padj)
row.names(SN_DEG)<- NULL
write.csv(SN_DEG,"Sal_Nic_DEG(48hWD).csv", row.names = FALSE)
SN48hWD_cutoff = SN_DEG[SN_DEG$log2FC>0.5|SN_DEG$log2FC < -0.5,]
write.csv(SN48hWD_cutoff,"Sal_Nic(48hWD)cutoff.csv", row.names = FALSE)
```

```
####### Sal vs 24hWD
SWD_dds = DESeqDataSetFromMatrix(NAc_SWD,SWD_col,~Treatment)
SWD_dds1<-DESeq(SWD_dds)
res_SWD<-results(SWD_dds1)
head(res_SWD)

plotMA(res_SWD, main="MA Plot with DESeq2: 48hWD Nicotine Studies")
tsig_SWD = table(res_SWD[,6]<0.2)
tsig_res_SWD = which(res_SWD[,6]<0.2)
sig_SWD = res_SWD[tsig_res_SWD,]
head(sig_SWD)

sig_ordSWD = sig_SWD[order(sig_SWD$log2FoldChange,decreasing = TRUE),]
head(sig_ordSWD)
SWD_DEG=data.frame(Gene=rownames(sig_ordSWD),log2FC=sig_ordSWD$lo
g2FoldChange,pvalue=sig_ordSWD$pvalue,padj=sig_ordSWD$padj)
row.names(SWD_DEG)<- NULL
write.csv(SWD_DEG,"Sal_WD_DEG(48hWD).csv", row.names = FALSE)
SWD48hWD_cutoff = SWD_DEG[SWD_DEG$log2FC>0.5|SWD_DEG$log2FC <
-0.5,]
write.csv(SWD48hWD_cutoff,"Sal_WD(48hWD)cutoff.csv", row.names = FALSE)
```

```
####### Nic vs 24hWD
NWD_dds = DESeqDataSetFromMatrix(NAc_NWD,NWD_col,~Treatment)
NWD_dds1<-DESeq(NWD_dds)
res_NWD<-results(NWD_dds1)
head(res_NWD)

plotMA(res_NWD, main="MA Plot with DESeq2: 48hWD Nicotine Studies")
tsig_NWD = table(res_NWD[,6]<0.2)
tsig_res_NWD = which(res_NWD[,6]<0.2)
sig_NWD = res_NWD[tsig_res_NWD,]
head(sig_NWD)

sig_ordNWD = sig_NWD[order(sig_NWD$log2FoldChange,decreasing = TRUE),]
head(sig_ordNWD)
NWD_DEG=data.frame(Gene=rownames(sig_ordNWD),log2FC=sig_ordNWD$lo
g2FoldChange,pvalue=sig_ordNWD$pvalue,padj=sig_ordNWD$padj)
row.names(NWD_DEG)<- NULL
write.csv(NWD_DEG,"Nic_WD_DEG(48hWD).csv", row.names = FALSE)
NWD48hWD_cutoff = NWD_DEG[NWD_DEG$log2FC>0.5|NWD_DEG$log2FC <
-0.5,]
write.csv(NWD48hWD_cutoff,"Nic_WD(48hWD)cutoff.csv", row.names = FALSE)
```

```
#####################################################################
# Determining overlapping genes between experiments. The output was used for
the construction of Venn Diagram.
SN24hWD = No DEGs at the cutoff
SWD24hWD = read.csv("Sal_WD(24hWD)cutoff.csv", header = T)
NWD24hWD = read.csv("Nic_WD(24hWD)cutoff.csv", header = T)
SN48hWD = read.csv("Sal_Nic(48hWD)cutoff.csv", header = T)
SWD48hWD = read.csv("Sal_WD(48hWD)cutoff.csv", header = T)
NWD48hWD = read.csv("Nic_WD(48hWD)cutoff.csv", header = T)
SN_Mic = read.csv("Microglia_SN DEGs (Untrimmed).csv", header = T)
SWD_Mic = read.csv("Microglia_SWD DEGs (Untrimmed).csv", header = T)
NWD_Mic = read.csv("Microglia_NWD DEGs (Untrimmed).csv", header = T)
SN_Ast = No DEGs at the cutoff
SWD_Ast = read.csv("Astrocytes_SWD DEGs (Untrimmed).csv", header = T)
NWD_Ast = read.csv("Astrocytes_NWD DEGs (Untrimmed).csv", header = T)

######## SAL vs NIC
# Two-way Sal/Nic in NAc48hWD experiment vs Microglia48hWD experiment
SN_Mic_48hWD_tab = table(SN48hWD$Gene %in% SN_Mic$X)
SN_Mic_48hWD_overlap = SN48hWD$Gene[which(SN48hWD$Gene %in%
SN_Mic$X)]
```

```
######## SAL vs WD
# Two-way Sal/WD in NAc24hWD experiment vs NAc48hWD experiment
SWD_24h_48hWD_tab = table(SWD24hWD$Gene %in% SWD48hWD$Gene)
SWD_24h_48hWD_overlap = SWD24hWD$Gene[which(SWD24hWD$Gene
%in% SWD48hWD$Gene)]

# Two-way Sal/WD in NAc24hWD experiment vs Astrocytes48hWD experiment
SWD_Ast_24hWD_tab = table(SWD24hWD$Gene %in% SWD_Ast$X)
SWD_Ast_24hWD_overlap = SWD24hWD$Gene[which(SWD24hWD$Gene
%in% SWD_Ast$X)]

# Two-way Sal/WD in NAc24hWD experiment vs Microglia48hWD experiment
SWD_Mic_24hWD_tab = table(SWD24hWD$Gene %in% SWD_Mic$X)
SWD_Mic_24hWD_overlap = SWD24hWD$Gene[which(SWD24hWD$Gene
%in% SWD_Mic$X)]

# Two-way Sal/WD in NAc48hWD experiment vs Astrocytes48hWD experiment
SWD_Ast_48hWD_tab = table(SWD48hWD$Gene %in% SWD_Ast$X)
SWD_Ast_48hWD_overlap = SWD48hWD$Gene[which(SWD48hWD$Gene
%in% SWD_Ast$X)]

# Two-way Sal/WD in NAc48hWD experiment vs Microglia48hWD experiment
SWD_Mic_48hWD_tab = table(SWD48hWD$Gene %in% SWD_Mic$X)
```

```
SWD_Mic_48hWD_overlap = SWD48hWD$Gene[which(SWD48hWD$Gene %in% SWD_Mic$X)]
# Two-way Sal/WD in Astrocytes48hWD experiment vs Microglia48hWD experiment
SWD_Mic_Ast_tab = table(SWD_Ast$X %in% SWD_Mic$X)
SWD_Mic_Ast_overlap = SWD_Ast$X[which(SWD_Ast$X %in% SWD_Mic$X)]

######## NIC vs WD
# Two-way Nic/WD in NAc24hWD experiment vs NAc48hWD experiment
NWD_24h_48hWD_tab = table(NWD24hWD$Gene %in% NWD48hWD$Gene)
NWD_24h_48hWD_overlap = NWD24hWD$Gene[which(NWD24hWD$Gene %in% NWD48hWD$Gene)]

# Two-way Nic/WD in NAc24hWD experiment vs Astrocytes48hWD experiment
NWD_Ast_24hWD_tab = table(NWD24hWD$Gene %in% NWD_Ast$X)
NWD_Ast_24hWD_overlap = NWD24hWD$Gene[which(NWD24hWD$Gene %in% NWD_Ast$X)]

# Two-way Nic/WD in NAc24hWD experiment vs Microglia48hWD experiment
NWD_Mic_24hWD_tab = table(NWD24hWD$Gene %in% NWD_Mic$X)
NWD_Mic_24hWD_overlap = NWD24hWD$Gene[which(NWD24hWD$Gene %in% NWD_Mic$X)]
```

```
# Two-way Nic/WD in NAc48hWD experiment vs Astrocytes48hWD experiment
NWD_Ast_48hWD_tab = table(NWD48hWD$Gene %in% NWD_Ast$X)
NWD_Ast_48hWD_overlap = NWD48hWD$Gene[which(NWD48hWD$Gene %in% NWD_Ast$X)]

# Two-way Nic/WD in NAc48hWD experiment vs Microglia48hWD experiment
NWD_Mic_48hWD_tab = table(NWD48hWD$Gene %in% NWD_Mic$X)
NWD_Mic_48hWD_overlap = NWD48hWD$Gene[which(NWD48hWD$Gene %in% NWD_Mic$X)]

# Two-way Nic/WD in Astrocytes48hWD experiment vs Microglia48hWD experiment
NWD_Mic_Ast_tab = table(NWD_Ast$X %in% NWD_Mic$X)
NWD_Mic_Ast_overlap = NWD_Ast$X[which(NWD_Ast$X %in% SWD_Mic$X)]

#####################################################################
# Correlation analysis between samples
install.packages("corrplot")
library("corrplot")
col4 <- colorRampPalette(c("#053061","#053061","#053061","white","darkred"))

#For the withdrawal group from 24hWD and 48hWD experiments
twentyfour = dataframe of withdrawal group from 24hWD experiment
```

```
fortyeight = dataframe of withdrawal group from 24hWD experiment
vec = unique(rbind(twentyfour, fortyeight))
WD_cor = cor(vec[,c(8:10,18:20)], method = "spearman")
WD_cor1 = ((WD_cor) + 1)/2
head(WD_cor1)
corrplot(WD_cor1,method="shade",cl.lim=c(0,1),col=col4(20),cl.cex=1.3,addgrid.
col = "grey")

#For the cell type-specific (astrocytes and microglia) experiment
cell = dataframe of astrocytes and microglia samples combined
cell_cor = cor(cell, method = "spearman")
cell_co = ((cell_cor) + 1)/2
head(cell_co)

#Without clustering option
corrplot(cell_co,method="shade",cl.lim=c(0,1),col=col4(20),cl.cex=1.3,addgrid.col
= "grey")
#With hierarchical clustering option
corrplot(cell_co,method="shade",cl.lim=c(0,1),col=col4(20),cl.cex=1.3,addgrid.col
= "grey",order = "hclust", hclust.method = "median")
#Removing outliers and re-plotting
cell_cor1 = cell_co[-c(5,10),-c(5,10)]
```

```
corrplot(cell_cor1, method = "shade", cl.lim = c(0,1), col = col4(20) ,cl.cex = 1.3,addgrid.col = "grey")

######################################################################
# Validation of cell types using RNA seq expression data of classic cell markers
gene=c("Tmem119","P2ry12","Itgam","Csf1r","Cx3cr1","Gfap","S100B","Aldh1l1", "Slc1a3")

cellTPMZscore1 = Z-score dataframe for astrocytes and microglia samples
cell2 = cellTPMZscore1[rownames(cellTPMZscore1) %in% gene,]
head(cell2)
cell2a = cell2[,-c(5,10)]
cell3 = as.matrix(cell2a)
cell_annot = data.frame(Sample = factor(rep(c("Microglia","Astrocytes"),c(8,8))))
cell_ann = list(Sample = c(Microglia ="darkgreen", Astrocytes ="grey10"))
rownames(cell_annot) = colnames(cell3)
pheatmap(cell3,cluster_cols=FALSE,gaps_col=c(8),color=colorRampPalette(c("darkblue","white","brown"))(50),annotation_col = cell_annot, annotation_colors = cell_ann)
```